Neutrini in Cosmologia
Padova, 16-18 Maggio 2011

Primi risultati di Planck

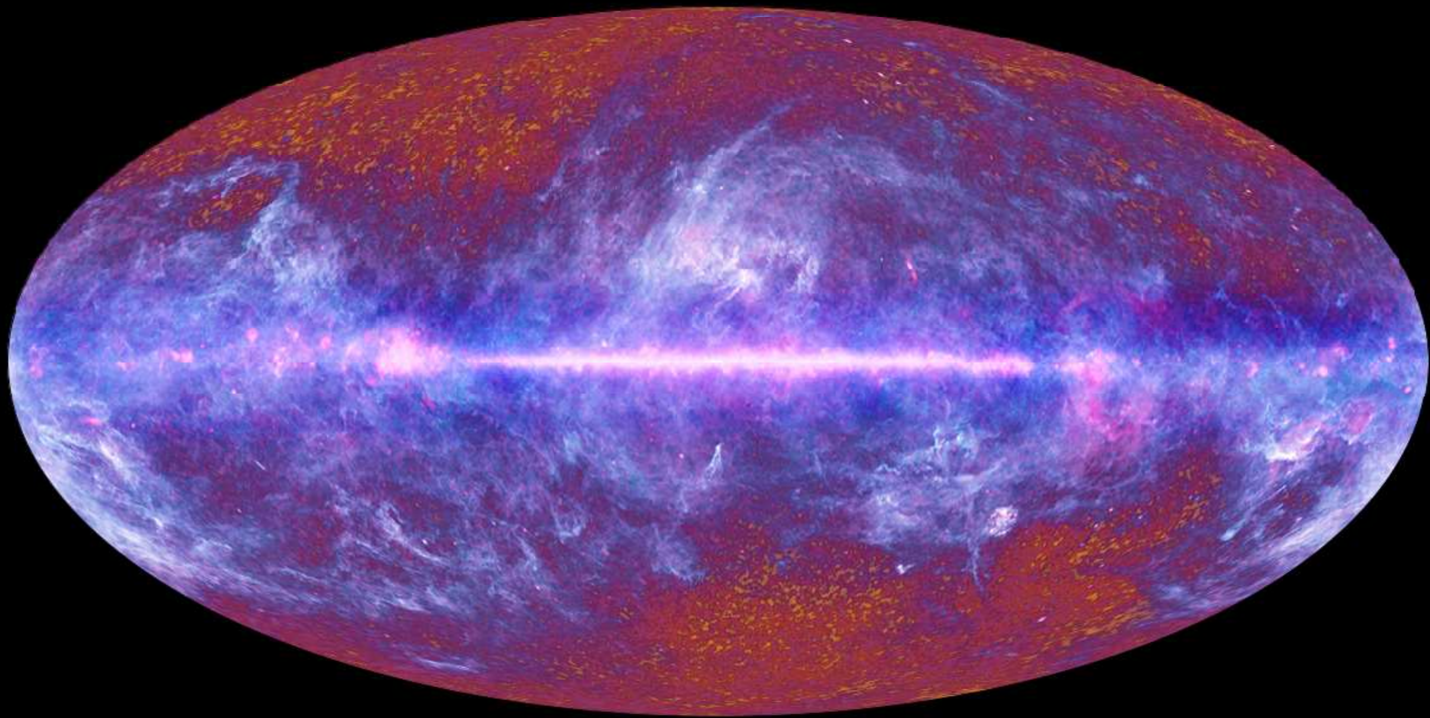

Marco Bersanelli
Dipartimento di Fisica, Università degli Studi di Milano
Planck-LFI Instrument Scientist

The Nobel Prize in Physics 2006

"For their discovery of the blackbody form and anisotropy of the cosmic microwave background radiation"

John C. Mather

George F. Smoot

COBE-FIRAS

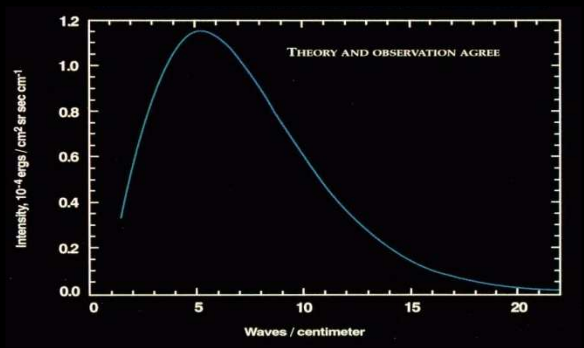

COBE-DMR

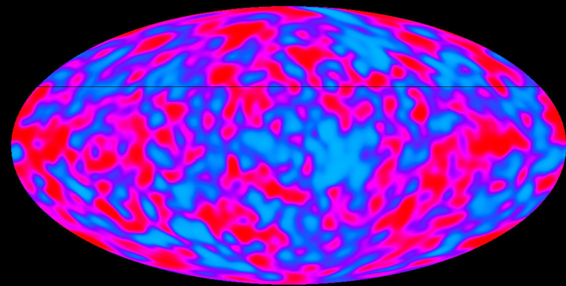

Cosmic Background Explorer

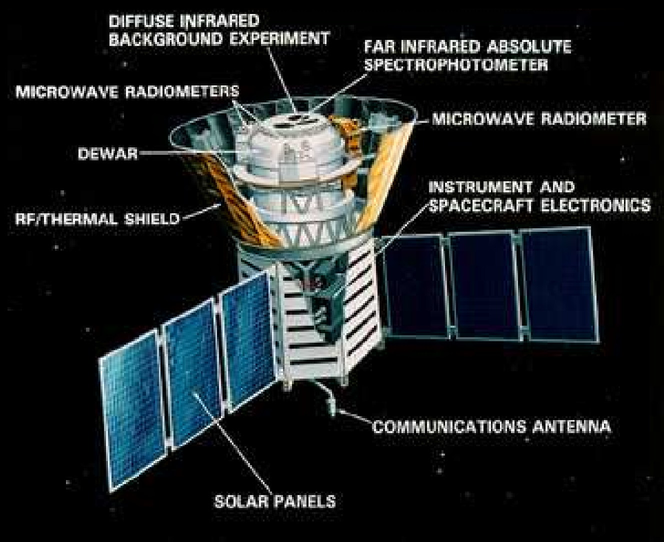

The CMB spectrum

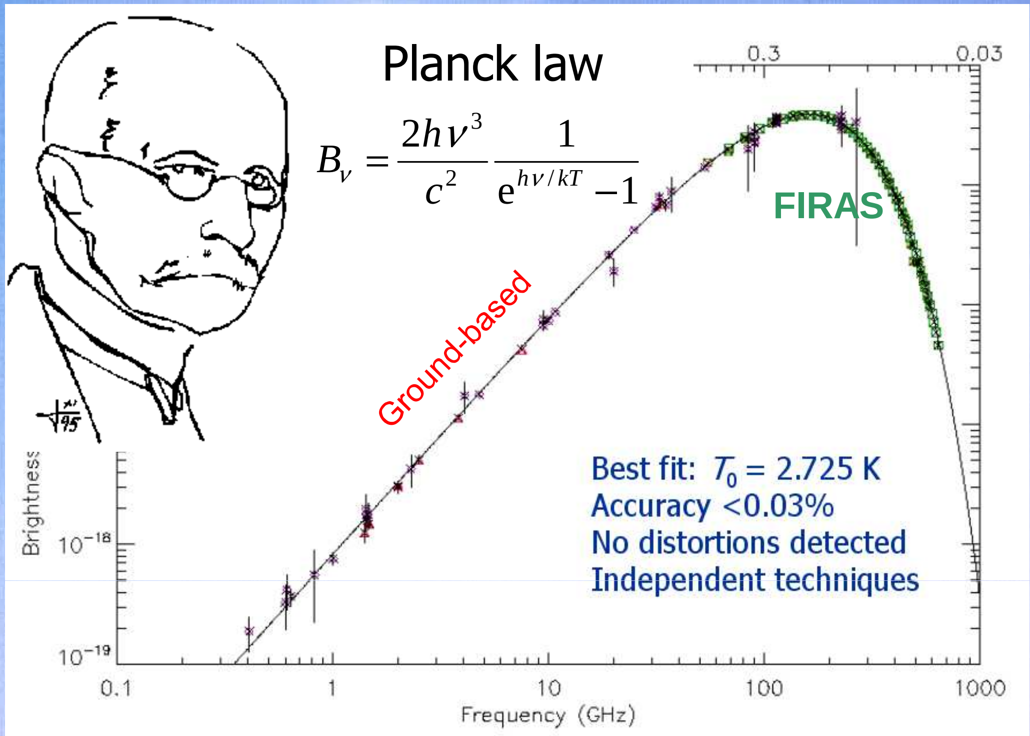

The CMB spectrum

$$T_0 = 2.725 \pm 0.002\ \mathrm{K}$$

High precision in cosmology!

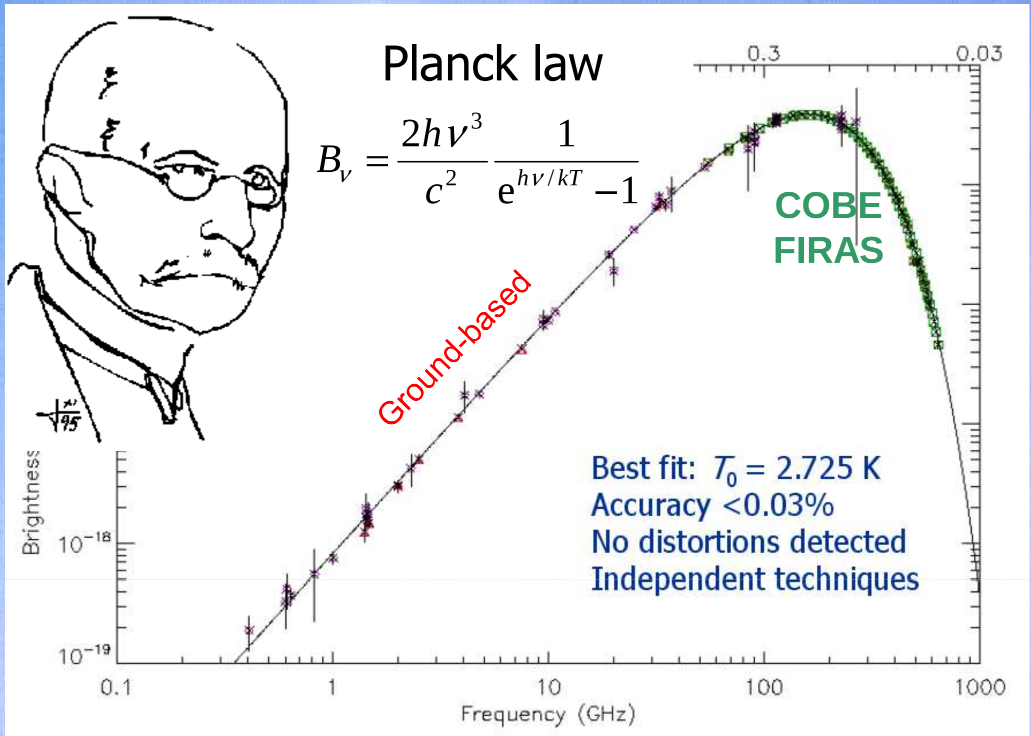

$$\rho_\gamma = \frac{4\pi}{c}\int B_\nu d\nu = \frac{8\pi h}{c^3}\int \frac{\nu^3}{e^{h\nu/kT}-1}d\nu$$

$$\Omega_\gamma = \frac{\rho_\gamma}{\rho_C} \approx 2.3\times10^{-5} h^{-2} \approx 4.6\times10^{-5}$$

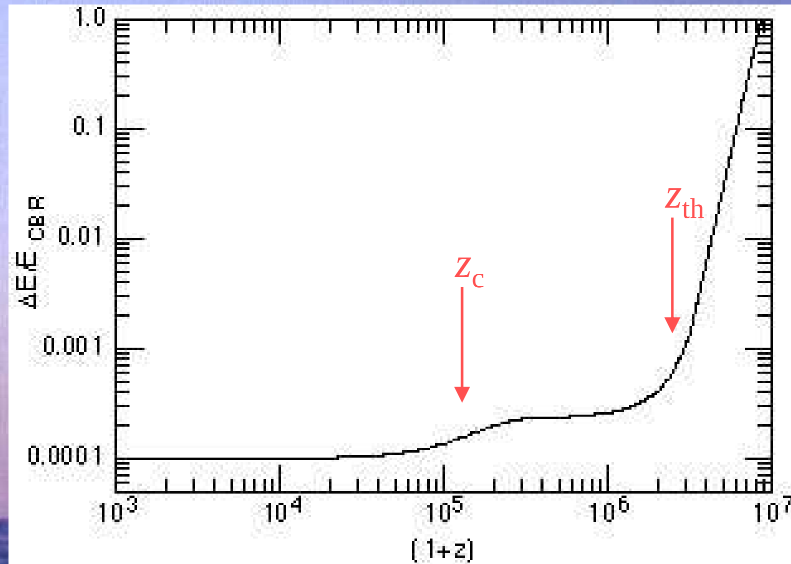

Constraints on distortions →

Tight limits on energy releases in the early universe

COBE – DMR full-sky map

Dipole-dominated map
$\Delta T \sim 3.5$ mK

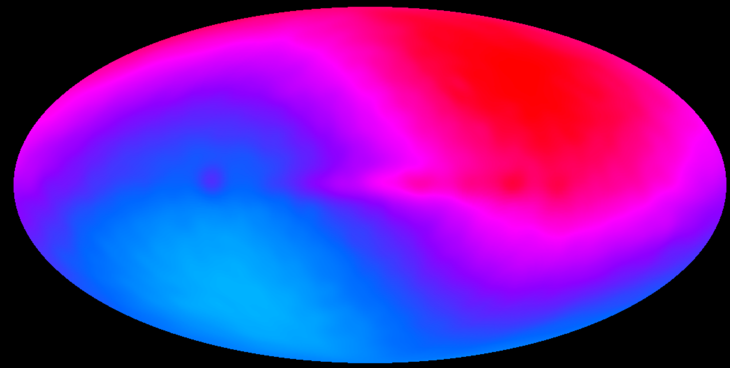

Fluctuations from Galaxy,
background and instrument noise
$\Delta T \sim 0.1$ mK

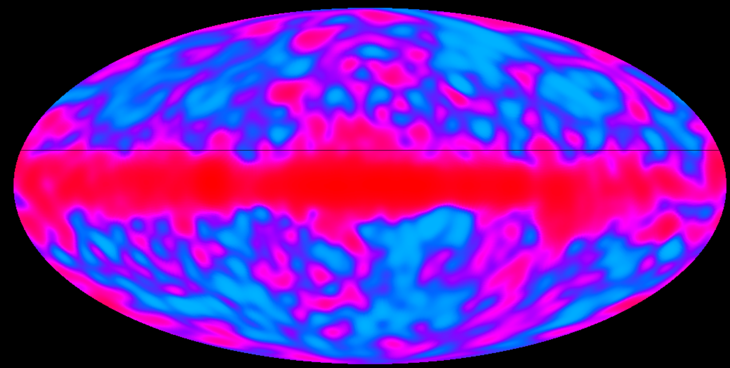

Fluctuations from CMB
(with instrument noise)
$\Delta T_{CMB} \sim 35$ μK

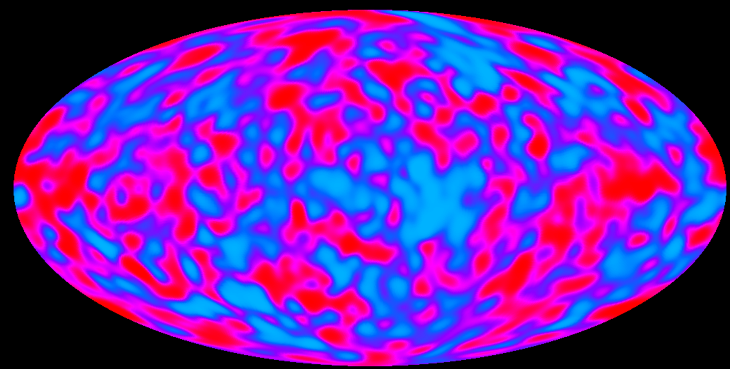

COBE-DMR full-sky map

$$\frac{\Delta T}{T} \approx \frac{\Delta\rho}{\rho} \approx 10^{-5}$$

$T \approx 2.7252$ K

$T \approx 2.7251$ K

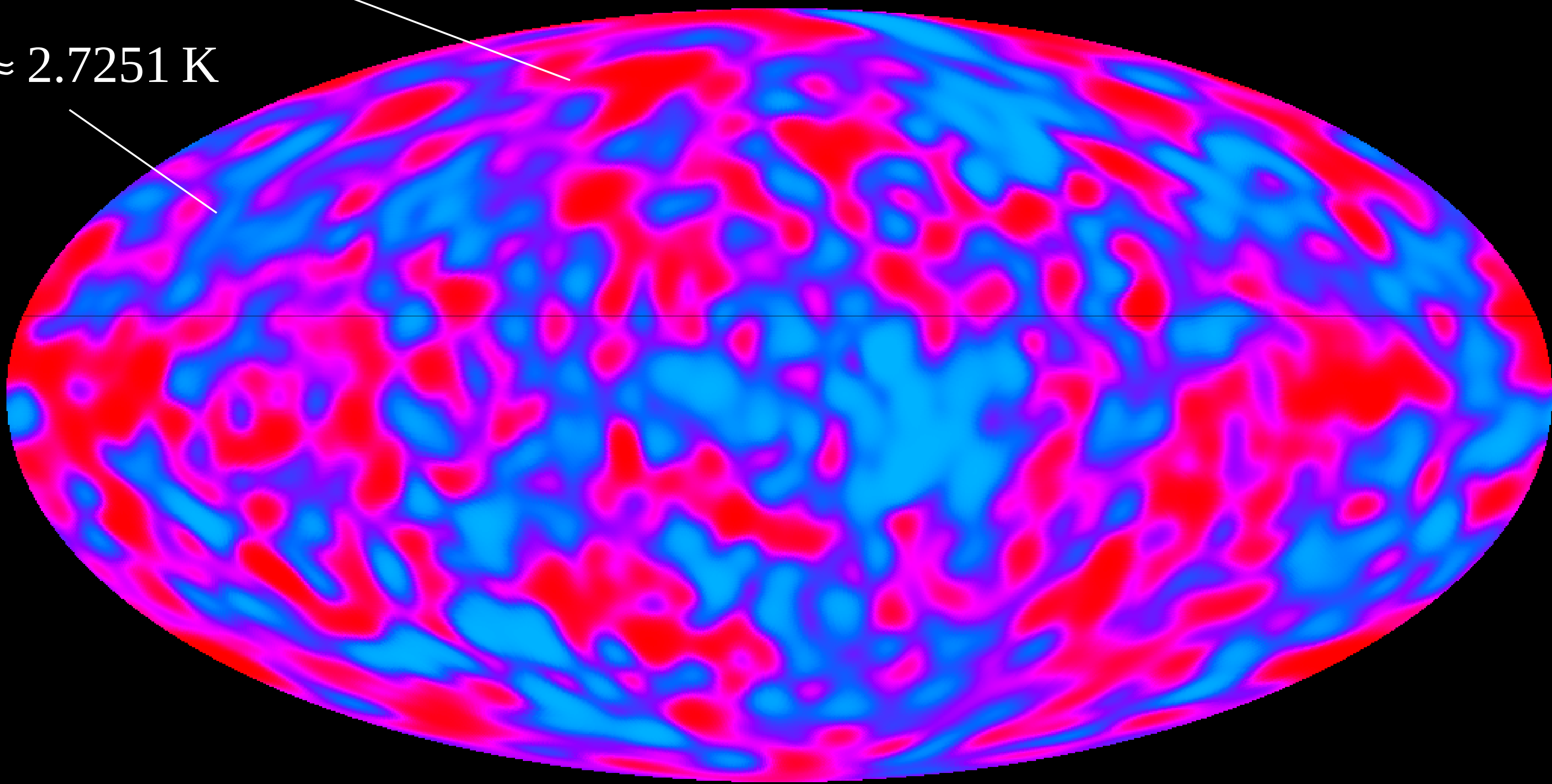

$$\theta_{FWHM} \approx 7^\circ$$

CMB Angular Power Spectrum

Spherical harmonics:

$$Y_{\ell m}(\vartheta,\varphi) \quad -\ell \le m \le \ell \qquad \ell \propto \frac{1}{\vartheta}$$

We represent the temperature distribution on the sky as:

$$\Delta T(\vartheta,\varphi) = \sum_{\ell m} a_{\ell m} Y_{\ell m}(\vartheta,\varphi)$$

The angular power spectrum is:

$$C_\ell = \left\langle \left| a_{\ell m} \right|^2 \right\rangle = \frac{1}{2\ell+1} \sum_{m=-\ell}^{\ell} a_{\ell m}^2$$

Qualitative shape of expected CMB power spectrum

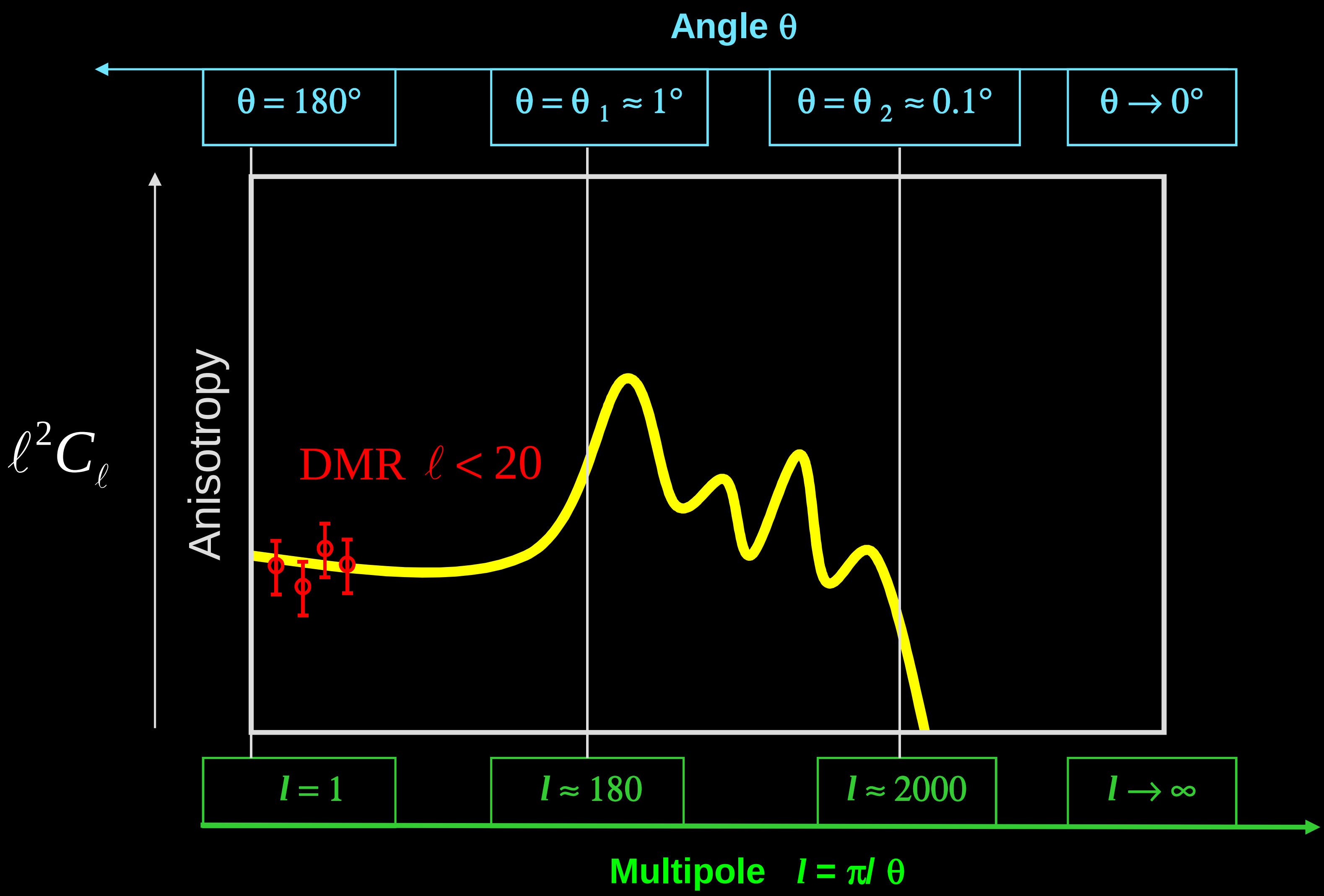

The details of the angular power spectrum depend on the value of the main cosmological parameters

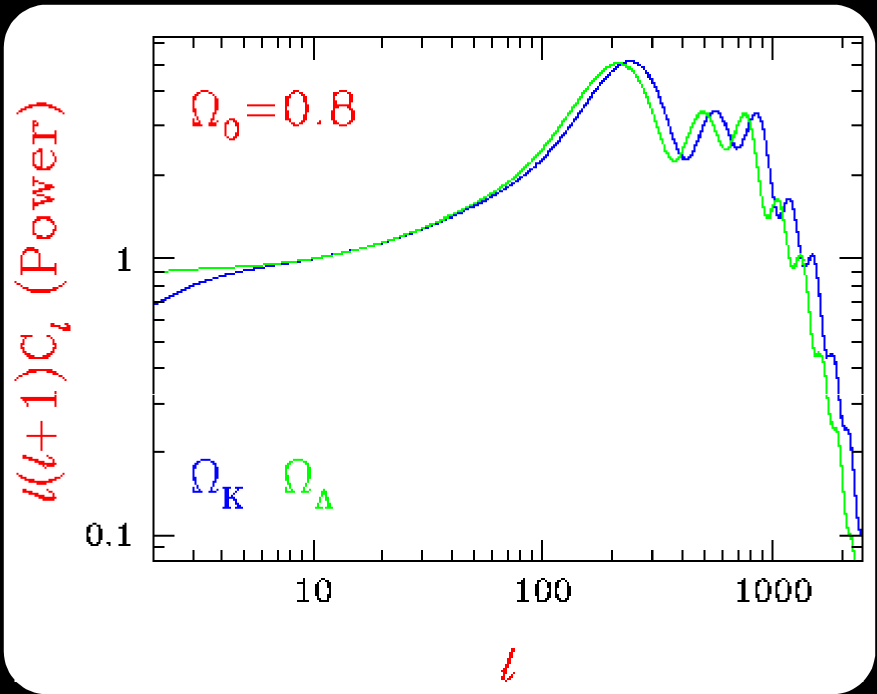

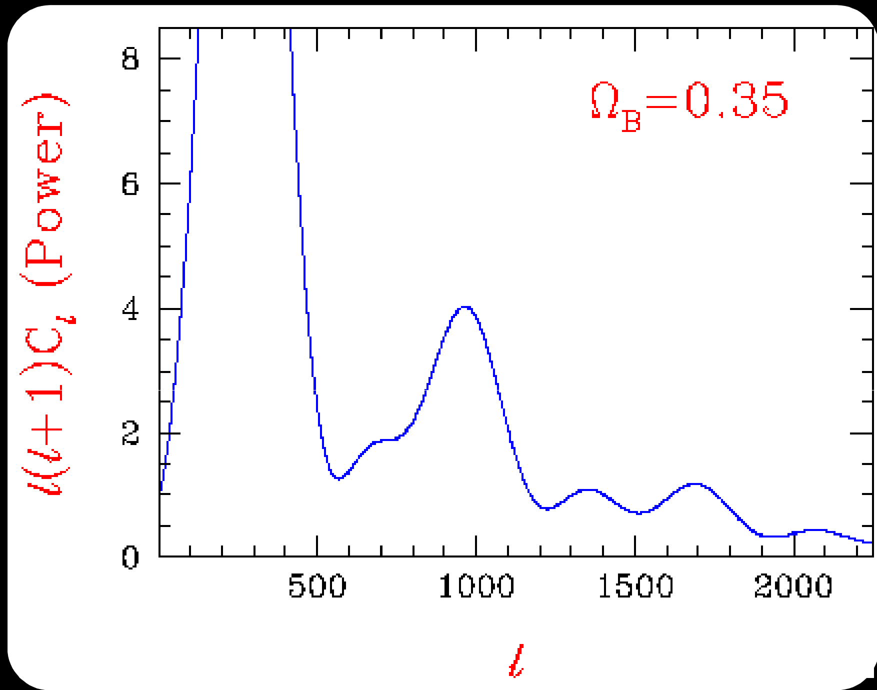

Accurate ***high resolution*** measurements of CMB anisotropies lead to *high precision* determination of parameters

$$\rightarrow H_0, \Omega_M, \Omega_\Lambda, \Omega_R, \Omega_0, \Omega_\nu h^2 \sim \sum m_\nu, N_\nu$$

Anisotropy experiments – 2002

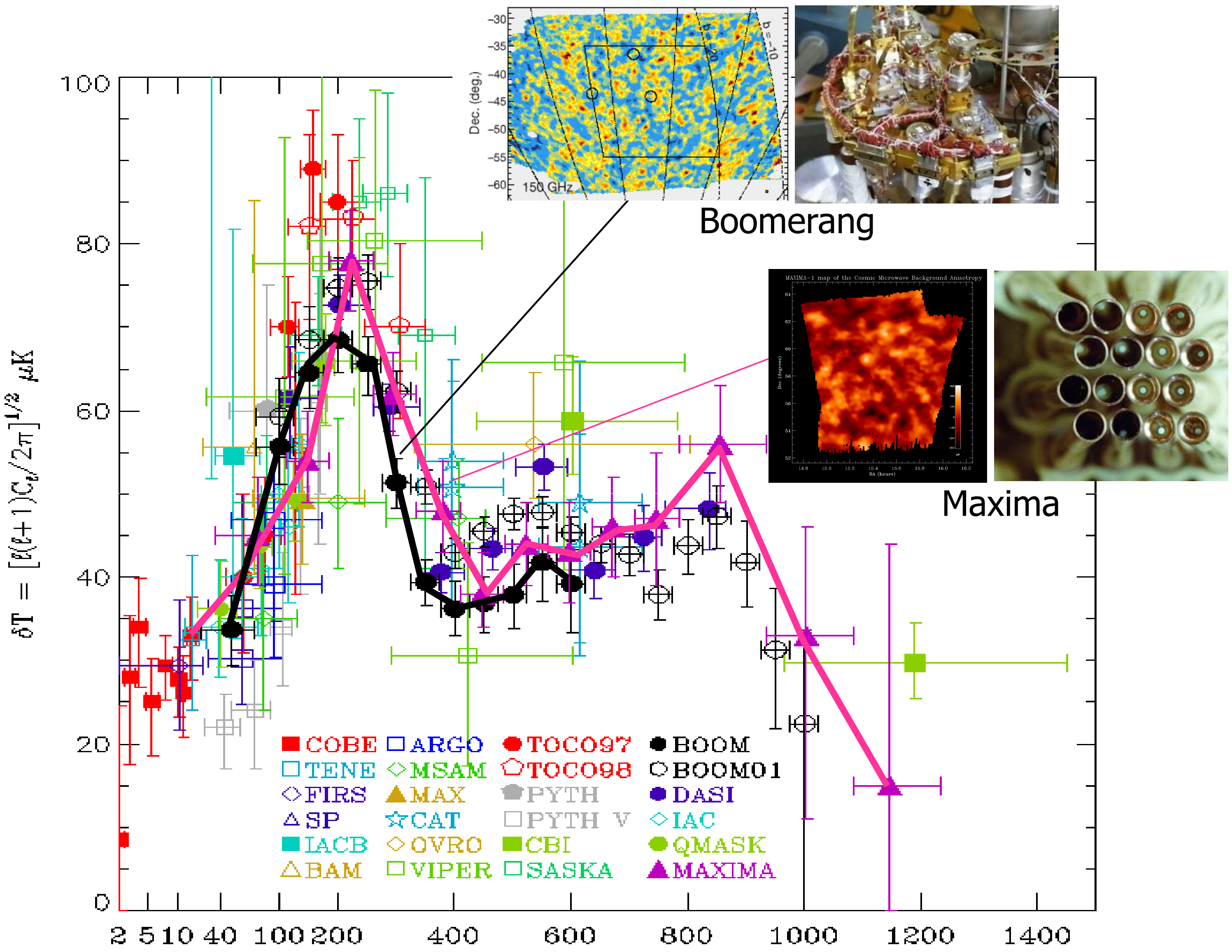

WMAP (launched 2001)

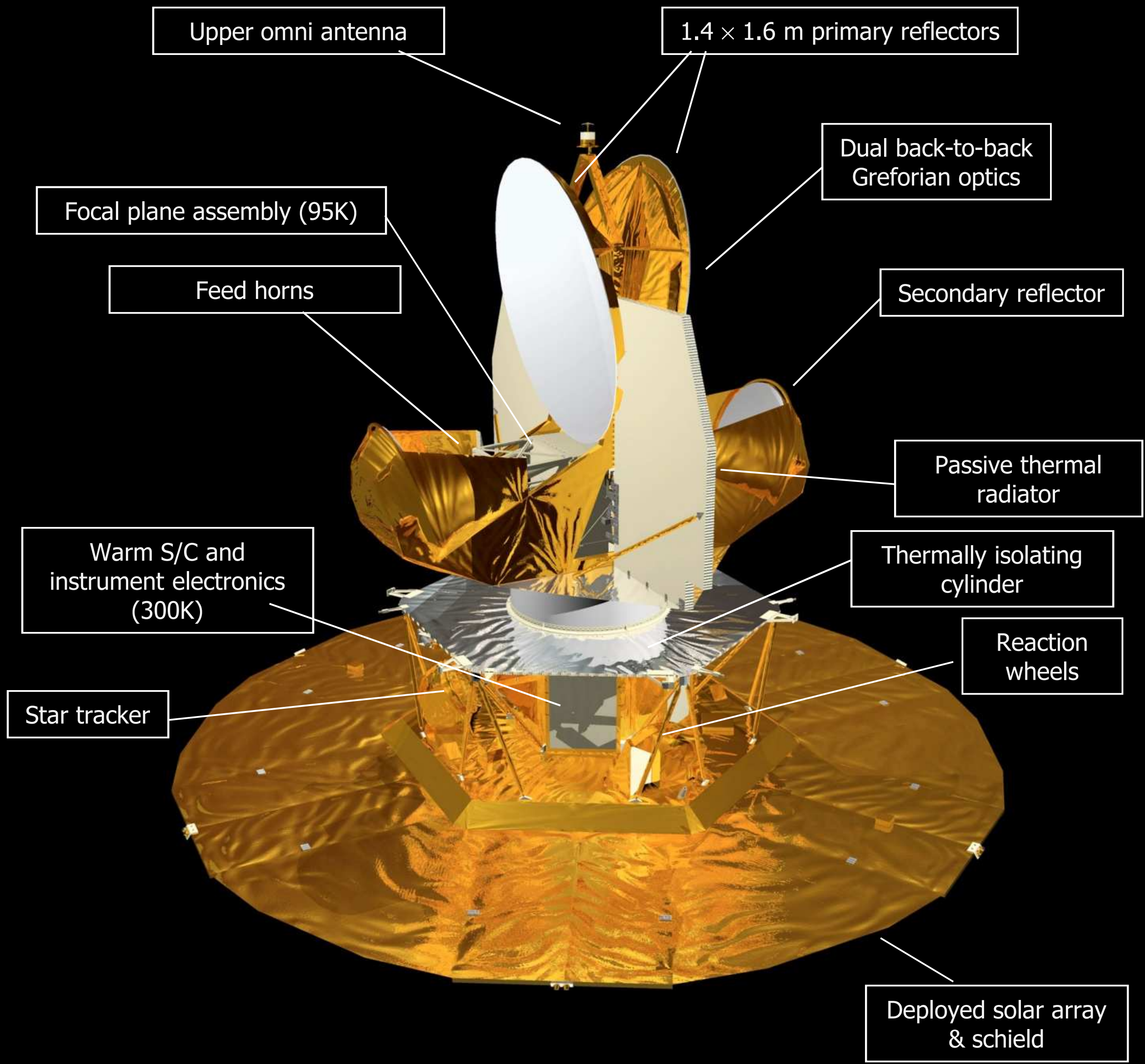

COBE-DMR full-sky map

$$\frac{\Delta T}{T} \approx \frac{\Delta \rho}{\rho} \approx 10^{-5}$$

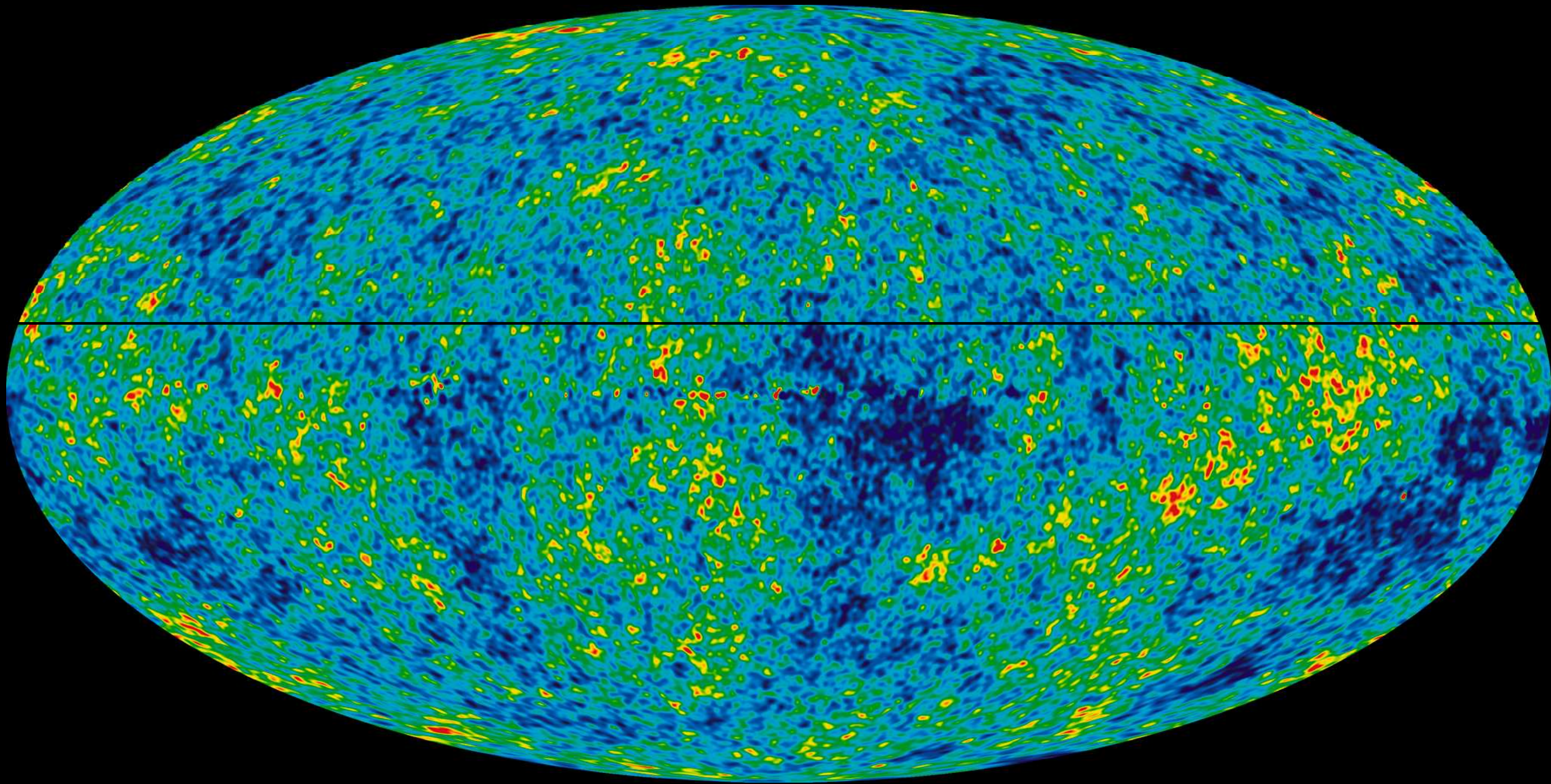

WMAP, 2007

Measuring cosmological parameters

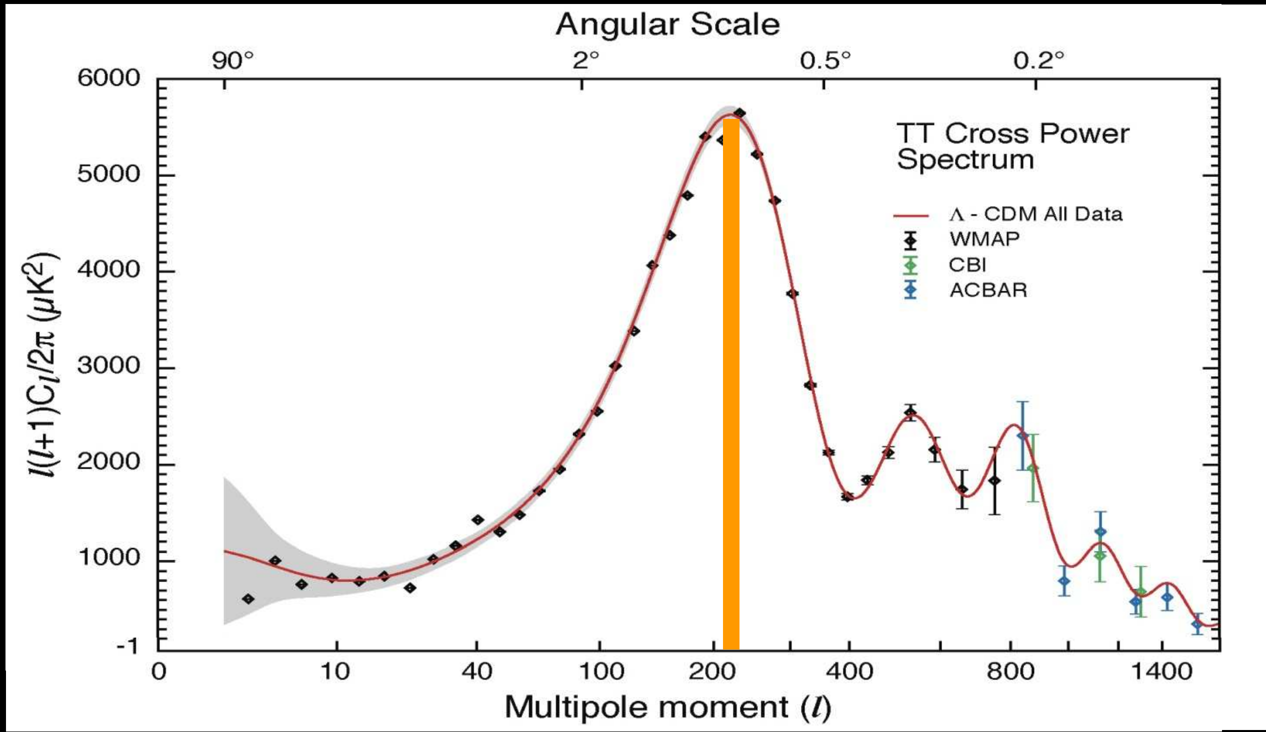

Hubble constant	$h \approx 0.72$	Cfr HST key project!!
Total density	$\Omega_0 \approx 1$	Consistent with inflation
Baryon density	$\Omega_B \approx 0.04$	
Dark matter density	$\Omega_{CDM} \approx 0.26$	We do not understand 96% of our universe!
Cosmological constant	$\Omega_\Lambda \approx 0.7$	Derived by difference
Radiation density	$\Omega_R \approx 10^{-4}$	

For details see: Komatsu et al. 2008

Accuracy in reconstruction of angular power spectrum

$$\frac{\delta C_\ell}{C_\ell} = f_{sky}^{-1/2}\sqrt{\frac{2}{2\ell+1}}\left[1+\frac{A\sigma_{pix}^2}{N_{pix}C_\ell W_\ell^2}\right]$$

"Cosmic variance"

Instrument

f_{sky} = fraction of observed sky

W_ℓ^2 = "Window function"

A = Sky area surveyed

N_{pix} = Number of pixels

σ_{pix} = Noise per pixels

Simulated T power spectrum

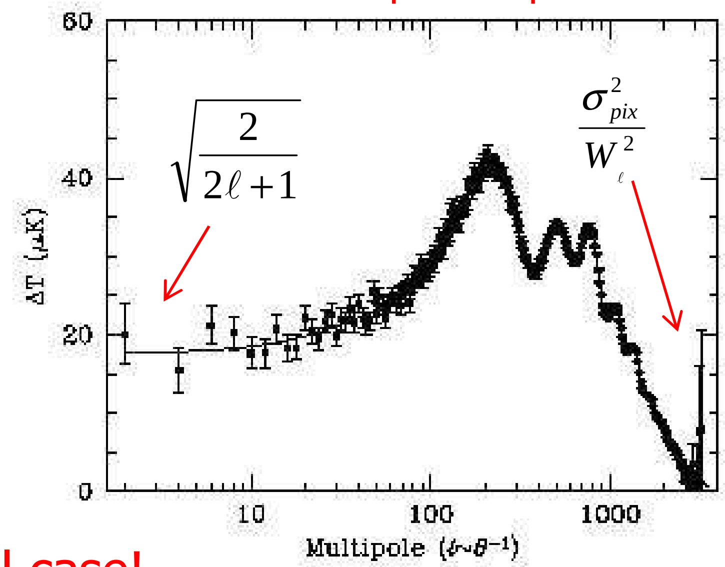

This is still an ideal case!

→ "Ideal instrument" (systematic effects are neglected)

→ "Ideal sky" (astrophysical foregrounds not considered)

Sensitivity

$$\frac{\delta C_\ell}{C_\ell} = f_{sky}^{-1/2}\sqrt{\frac{2}{2\ell+1}}\left[1+\frac{A\sigma_{pix}^2}{N_{pix}C_\ell W_\ell^2}\right]$$

$$\sigma_{pix} = k_R \frac{T_{sys}+T_{sky}}{\sqrt{(n_{det}\tau)\Delta\nu}}$$

$k_R \approx 1$ receiver constant

T_{sys} = System temperature

T_{sky} = Sky (input) brightness temperature

n_{det} = Number of detectors

τ = Integration time

$\Delta\nu$ = Bandwidth

Noise temperature is function of physical temperature and frequency

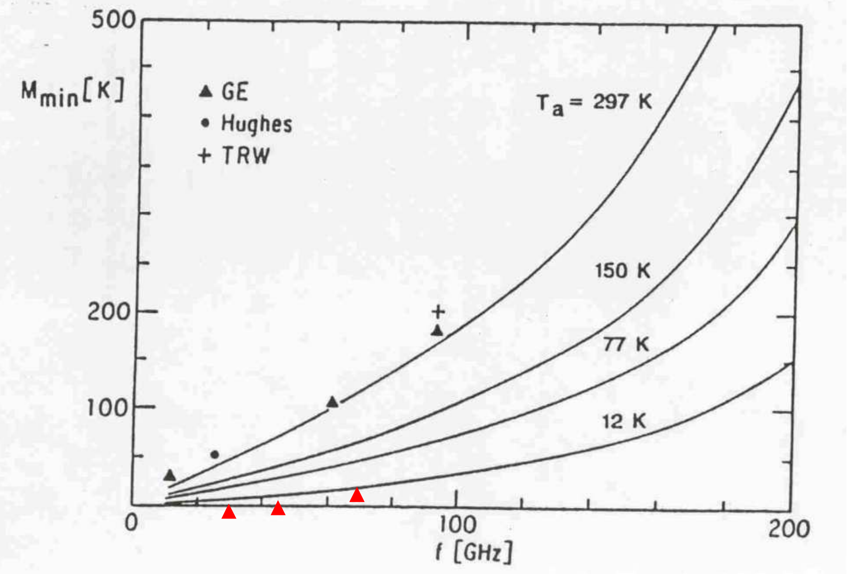

Planck (20K)

30 GHz	12K	
44GHz	18K	$\Delta\nu/\nu$~20%
70GHz	30K	

Window function

$$\frac{\delta C_\ell}{C_\ell} = f_{sky}^{-1/2}\sqrt{\frac{2}{2\ell+1}}\left[1+\frac{A\sigma_{pix}^2}{N_{pix}C_\ell W_\ell^2}\right]$$

For a Gaussian beam scan

$$W_\ell^2 = \exp\left[-\ell(\ell+1)\sigma_B^2\right]$$

$$\sigma_B = \frac{\theta_{HPBW}}{\sqrt{8\ln 2}} = (1.235\times 10^{-4})\theta_{HPBW}\,[\text{arcmin}]$$

Measured power spectrum:

$$C_{\ell-MEAS} = C_\ell W_\ell^2$$

$$C_\ell = \frac{C_{\ell-MEAS}}{W_\ell^2} = C_{\ell-MEAS}\exp\left[\ell(\ell+1)\sigma_B^2\right]$$

Requirement: precise a-priori knowledge of σ_B

Telescope and beam pattern

$$\vartheta_{FWHM}[rad] \approx \frac{\lambda}{D}$$

CMB instruments: Double reflector off-axis

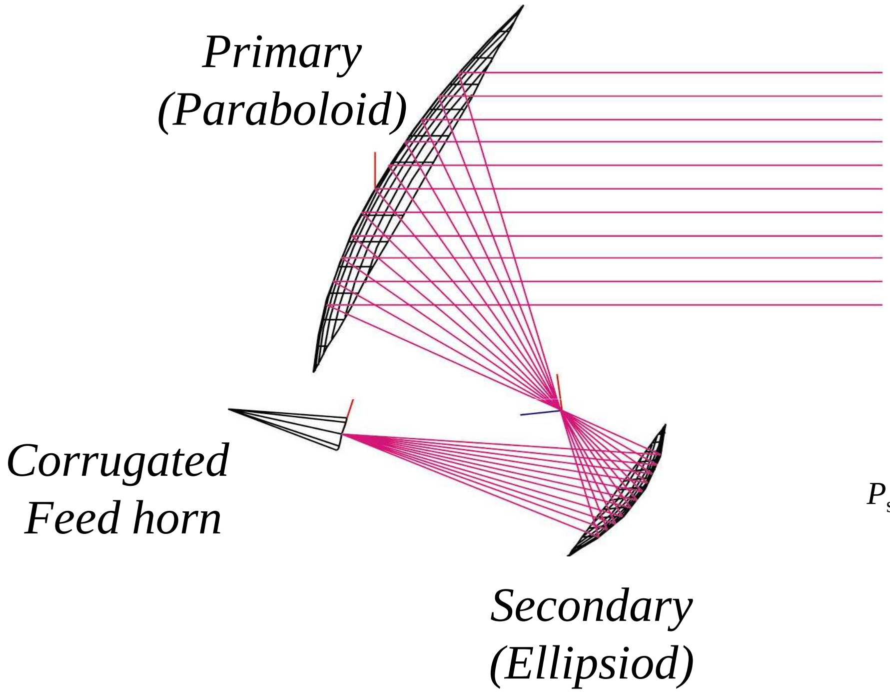

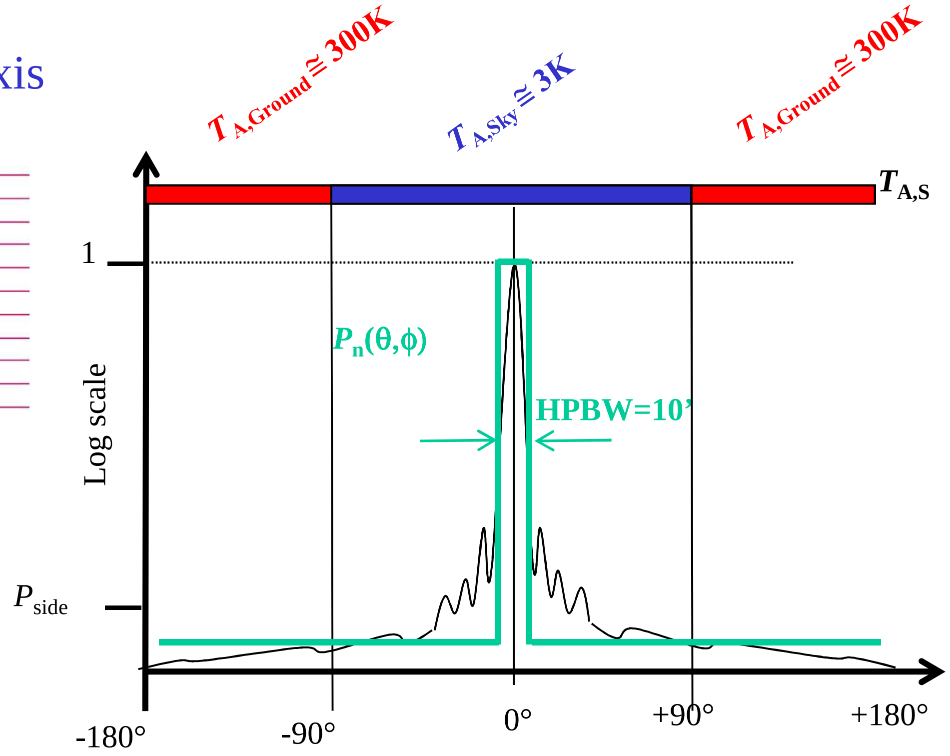

→ Antenna temperature

→ No diffraction from secondary mirror
→ Can be optimised for aberration effects

$$T_A(\theta_0,\phi_0) = \frac{\iint_{4\pi} T_{B,S}(\theta,\phi)P_n(\theta,\phi)d\Omega}{\iint_{4\pi} P_n(\theta,\phi)d\Omega}$$

PLANCK

PLANCK

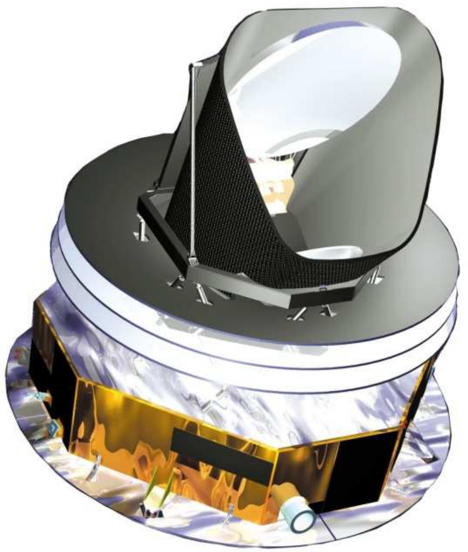

Design goals

- Angular resolution: ~7’
- Sensitivity per pixel: < 10 μK
- Full frequency range: 30-900 GHz
- Polarisation sensitive in CMB channels
- Sky coverage: 100%
- High control of systematic effects

SUMMARY OF PLANCK INSTRUMENT CHARACTERISTICS

Instrument Characteristic	LFI			HFI					
Detector Technology	HEMT arrays			Bolometer arrays					
Center Frequency [GHz]	30	44	70	100	143	217	353	545	857
Bandwidth ($\Delta\nu/\nu$)	0.2	0.2	0.2	0.33	0.33	0.33	0.33	0.33	0.33
Angular Resolution (arcmin)	33	24	14	10	7.1	5.0	5.0	5.0	5.0
$\Delta T/T$ per pixel (Stokes I)[a]	2.0	2.7	4.7	2.5	2.2	4.8	14.7	147	6700
$\Delta T/T$ per pixel (Stokes Q & U)[a]	2.8	3.9	6.7	4.0	4.2	9.8	29.8	...	...

[a] Goal (in μK/K) for 14 months integration, 1σ, for square pixels whose sides are given in the row “Angular Resolution”

GOAL values from Planck Scientific Programme, ESA-SCI(2005)1 (“Blue book”)

PLANCK

Looking back to the dawn of time

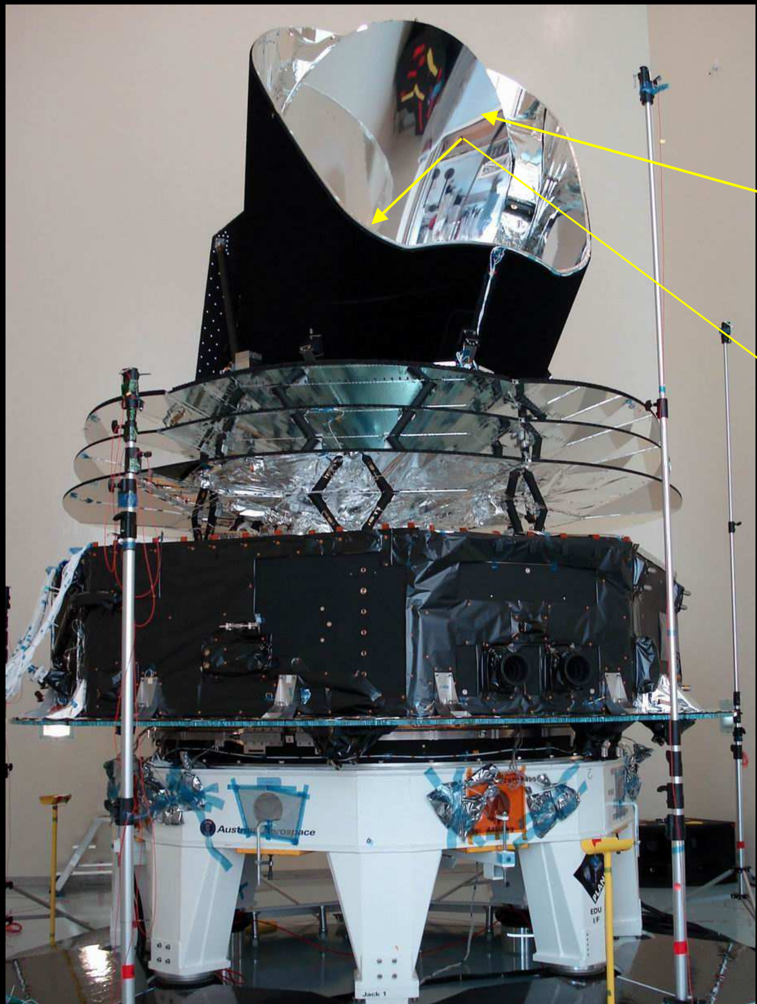

Planck Telescope
1.5x1.9m off-axis
Gregorian
T = 50 K

LFI Radiometers
27-77 GHz, T = 20 K

HFI Bolometers
100-850 GHz, T = 0.1 K

Precision cosmology with the CMB

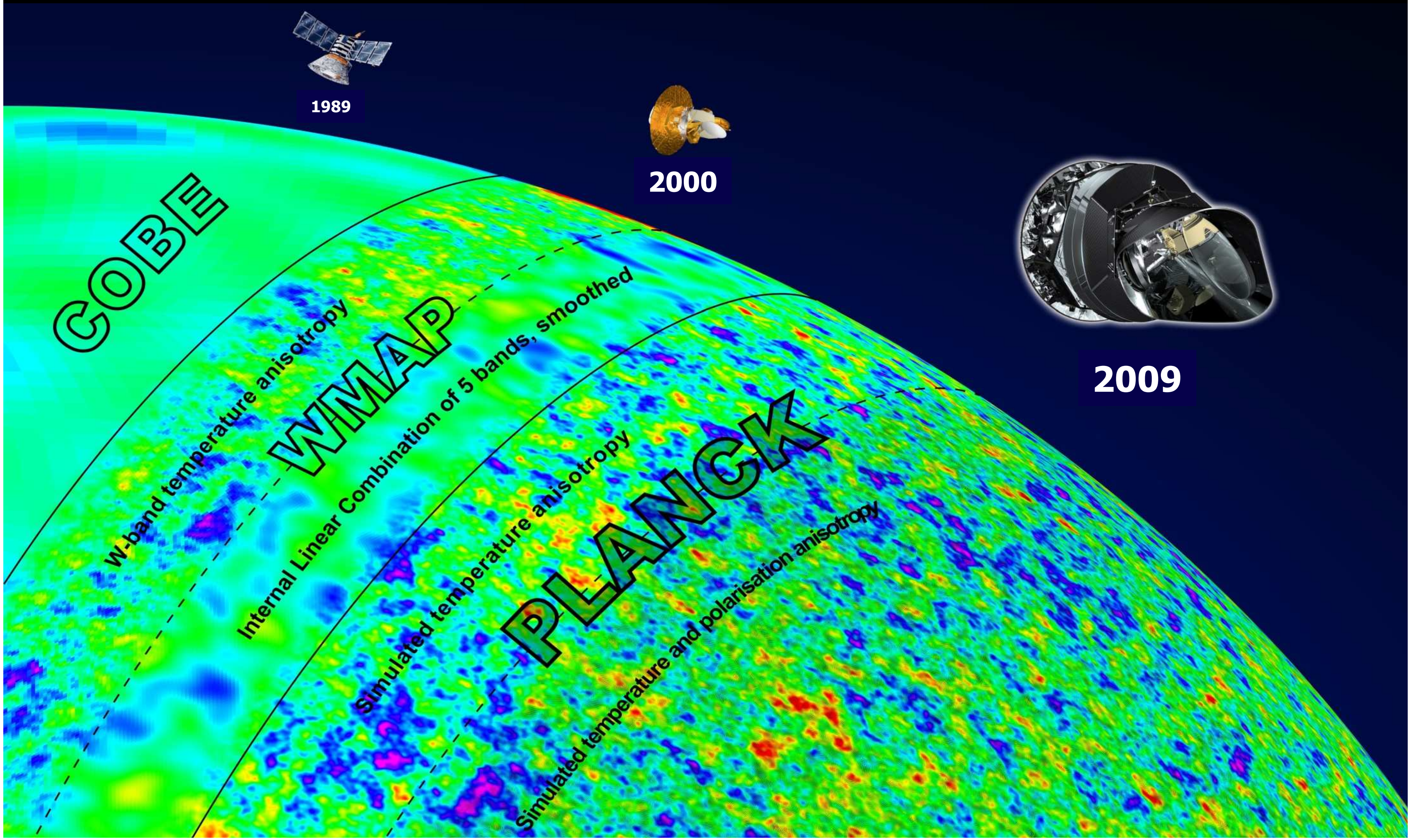

CMB angular power spectrum

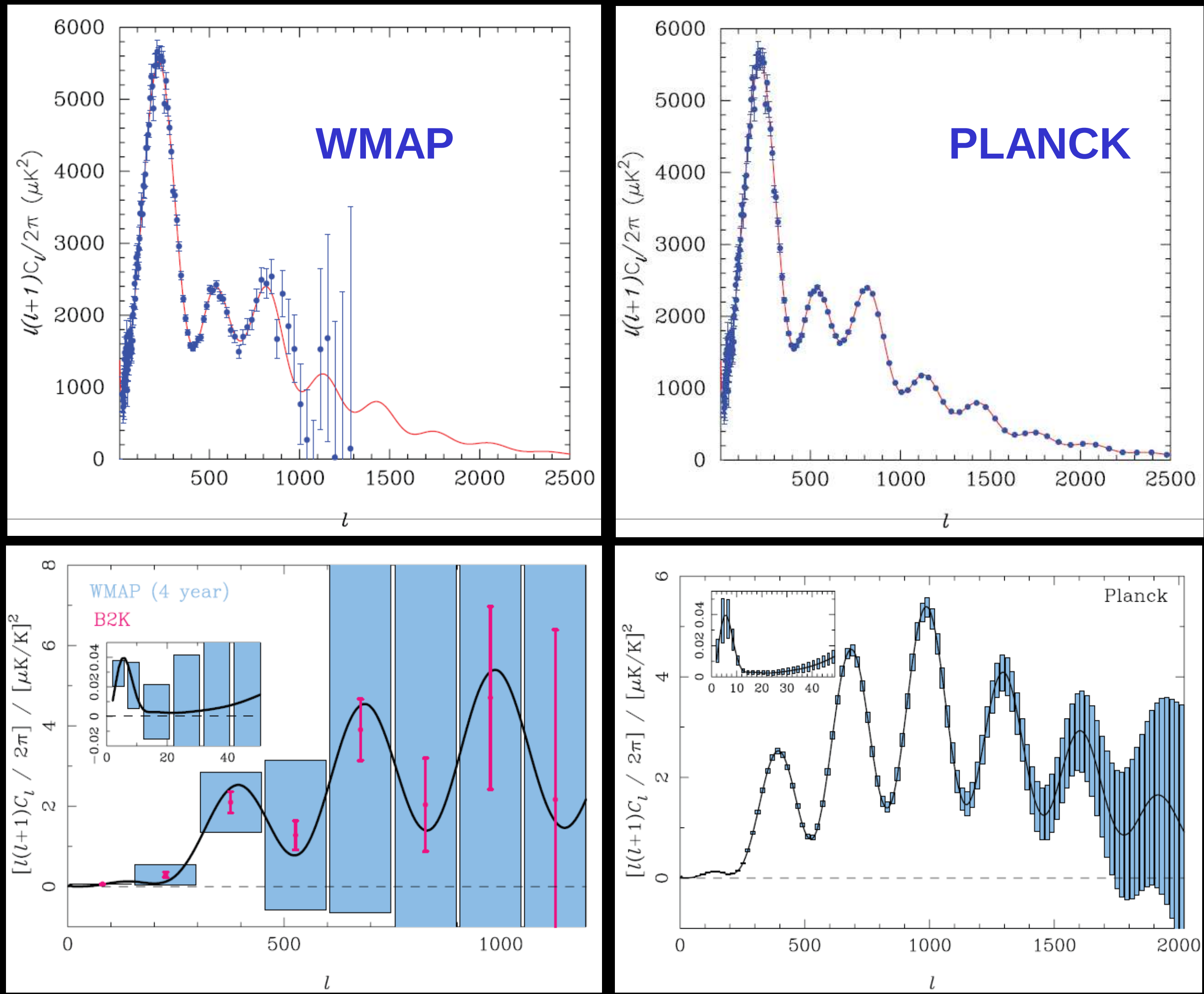

$$\rightarrow H_0, \Omega_M, \Omega_\Lambda, \Omega_R, \Omega_0$$

Composition, geometry and dynamics of the universe

CMB angular power spectrum

$$C_\ell = \left\langle |a_{\ell m}|^2 \right\rangle = \frac{1}{2\ell+1} \sum_{m=-\ell}^{\ell} a_{\ell m}^2$$

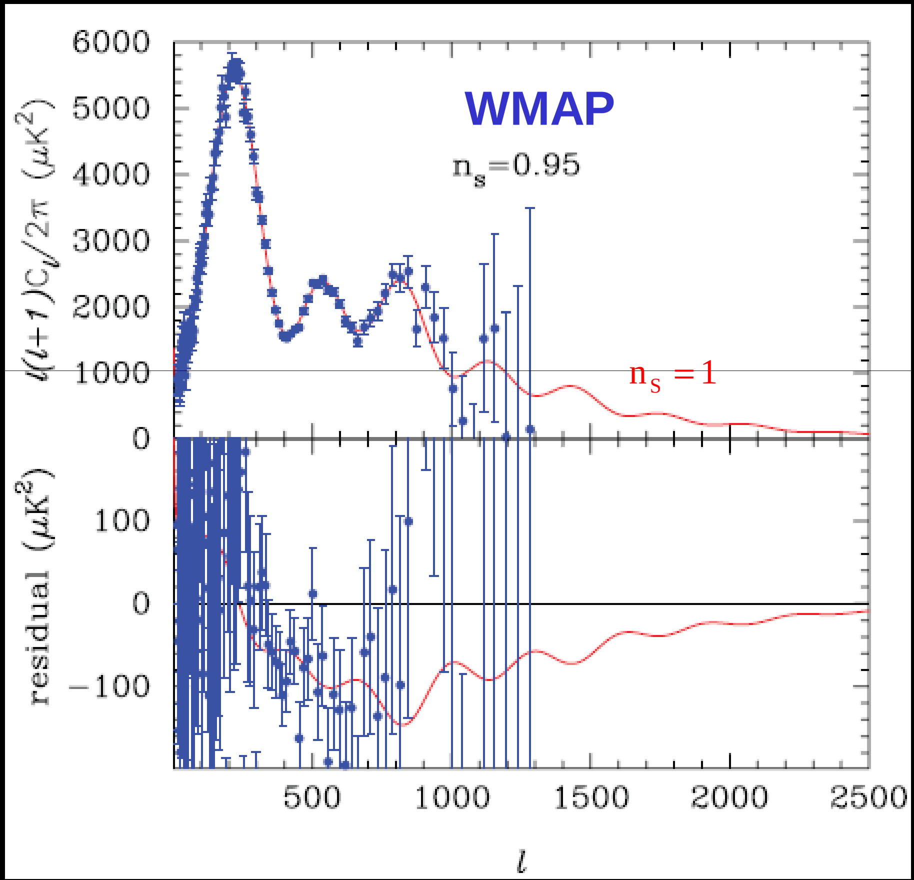

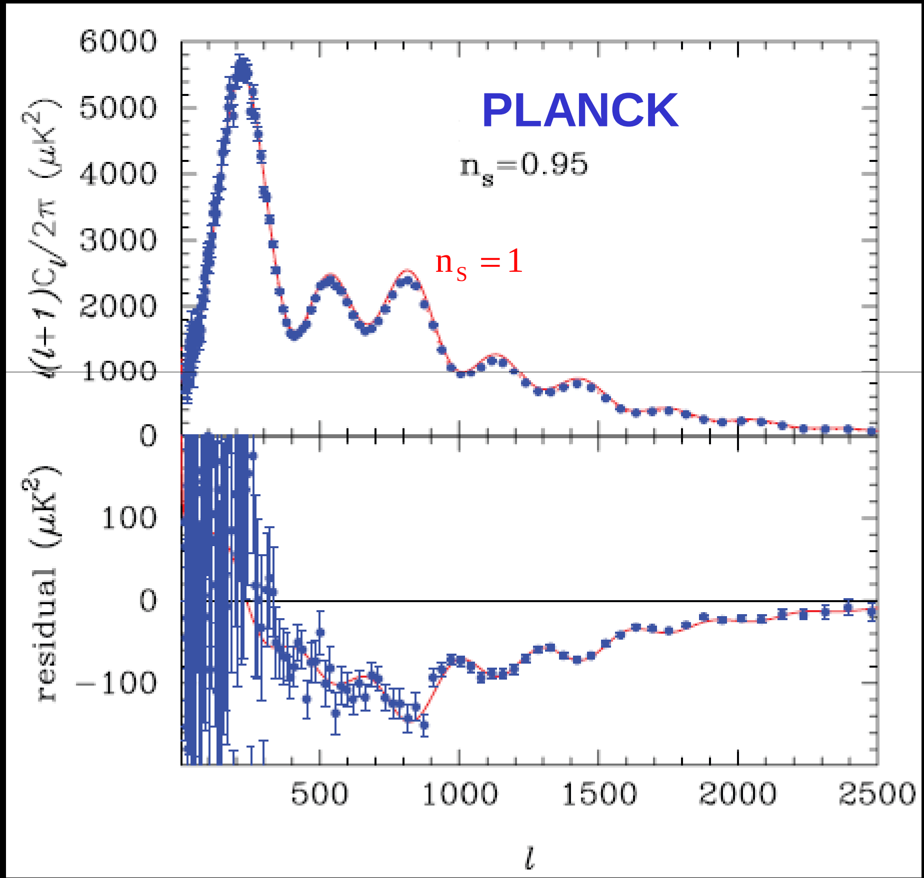

Probing inflation with CMB polarisation

WMAP data

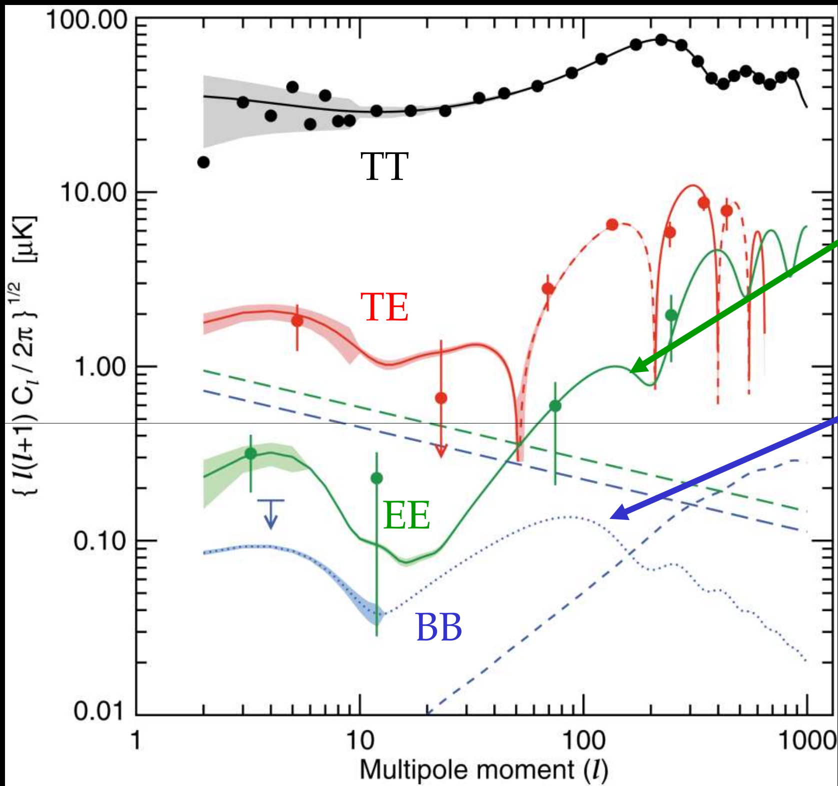

PLANCK simulations

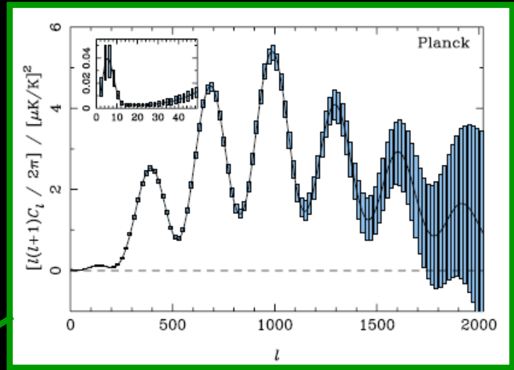

"E-mode" from last scattering surface

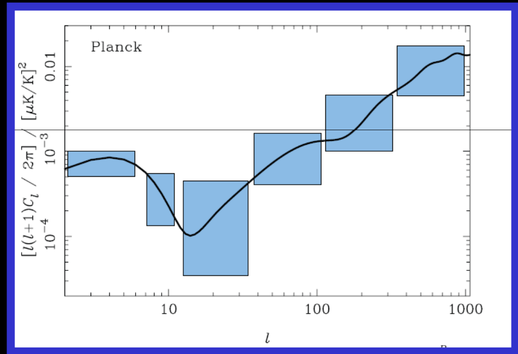

"B-mode" polarisation from primordial gravitational waves

If detected:
- strong confirmation of inflation scenario
- estimate energy scale of inflation

Extremely difficult experimentally
Theoretically poorly bound (several orders of magnitude range!)
→ Post-Planck mission?

Precision cosmology with Planck

Planck Bluebook (2005)

Temperature and Polarisation power spectra

Cosmological parameters

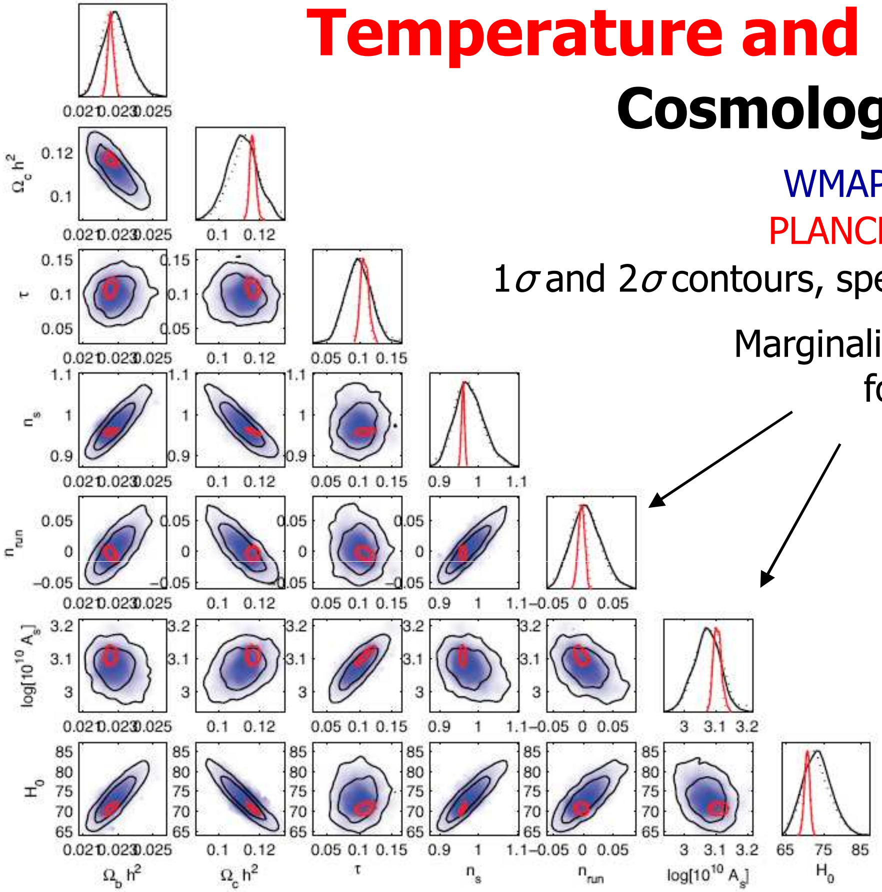

WMAP, 4yr observation

PLANCK, 1yr observation

1σ and 2σ contours, spectral index allowed to run

Marginalized posterior distributions for each parameter

Neutrino physics

Planck alone	$\delta\left(\sum m_\nu\right) \approx 0.26$ eV
Planck + SDSS	$\delta\left(\sum m_\nu\right) \approx 0.2$ eV
Planck alone (indep. BBN)	$\delta\left(N_\nu\right) \approx 0.24$

Imaging

Beyond the power spectrum

Non-Gaussianity

Astrophysical studies

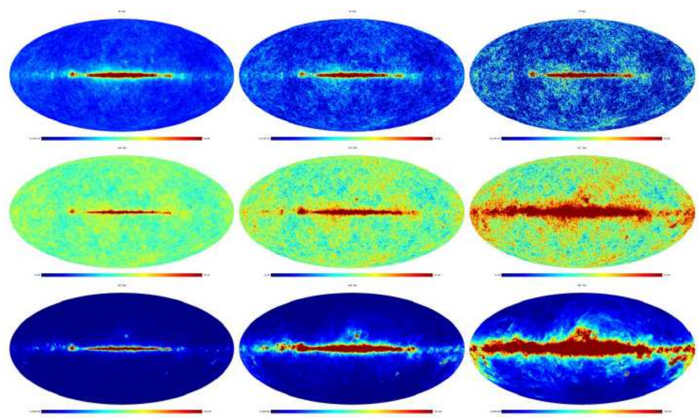

Foregrounds: more work, more science

Multifrequency observations are needed to disentangle non-cosmological contributions

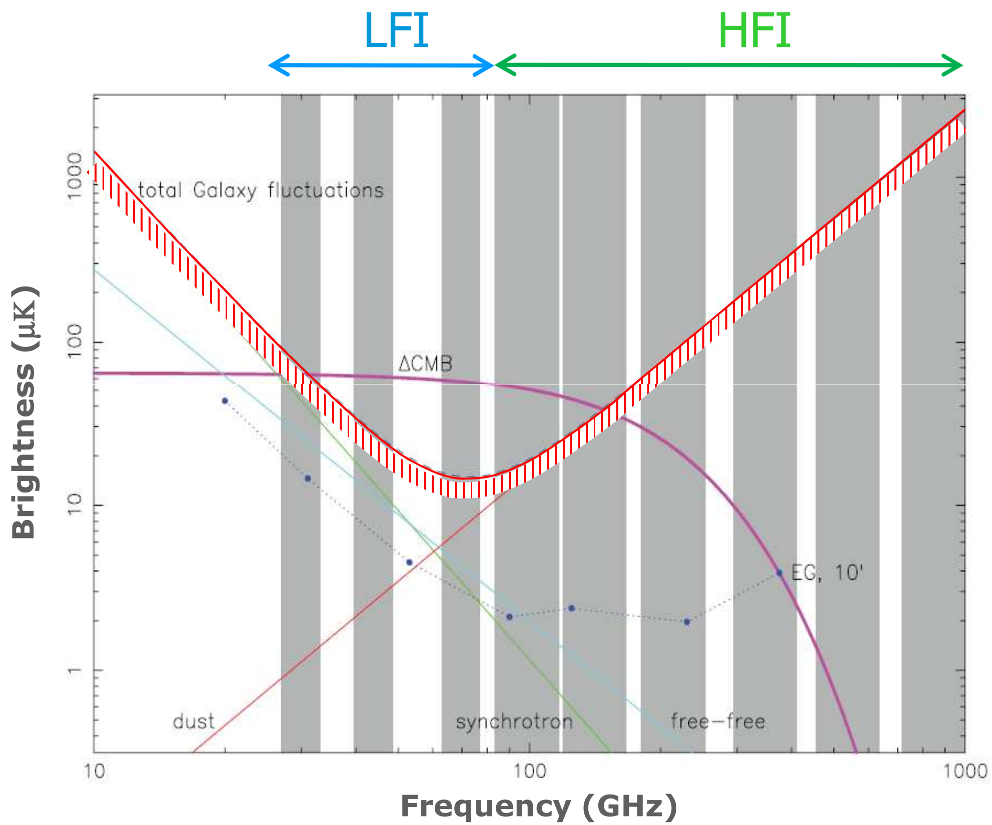

- Galactic diffuse emission (synchrotron, free-free, dust)
- Extragalactic point sources

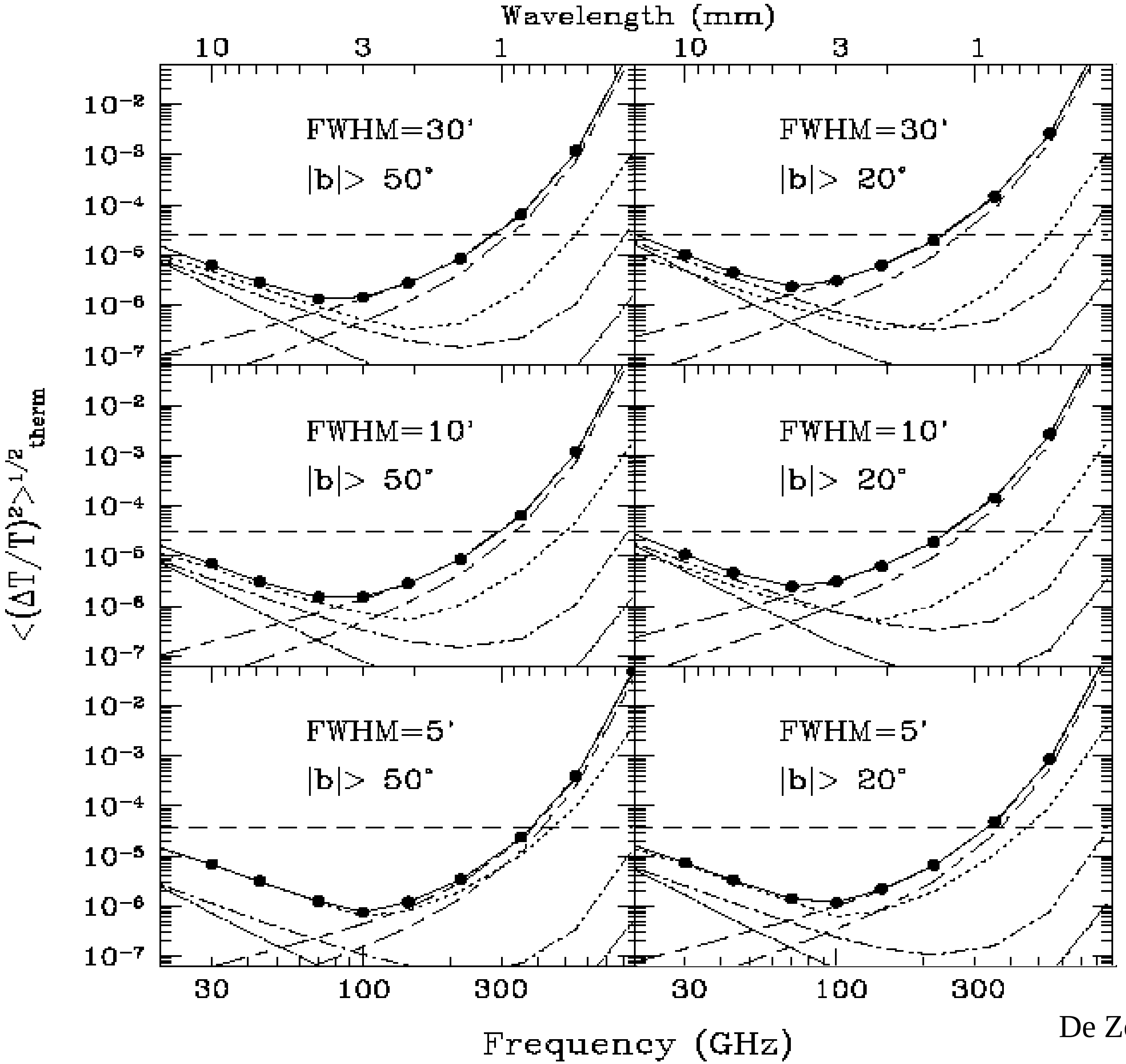

De Zotti et al 2005

Minimum of foregrounds near 70GHz

PLANCK

Università di MIlano

PLANCK

COBRAS/SAMBA Redbook (1996)

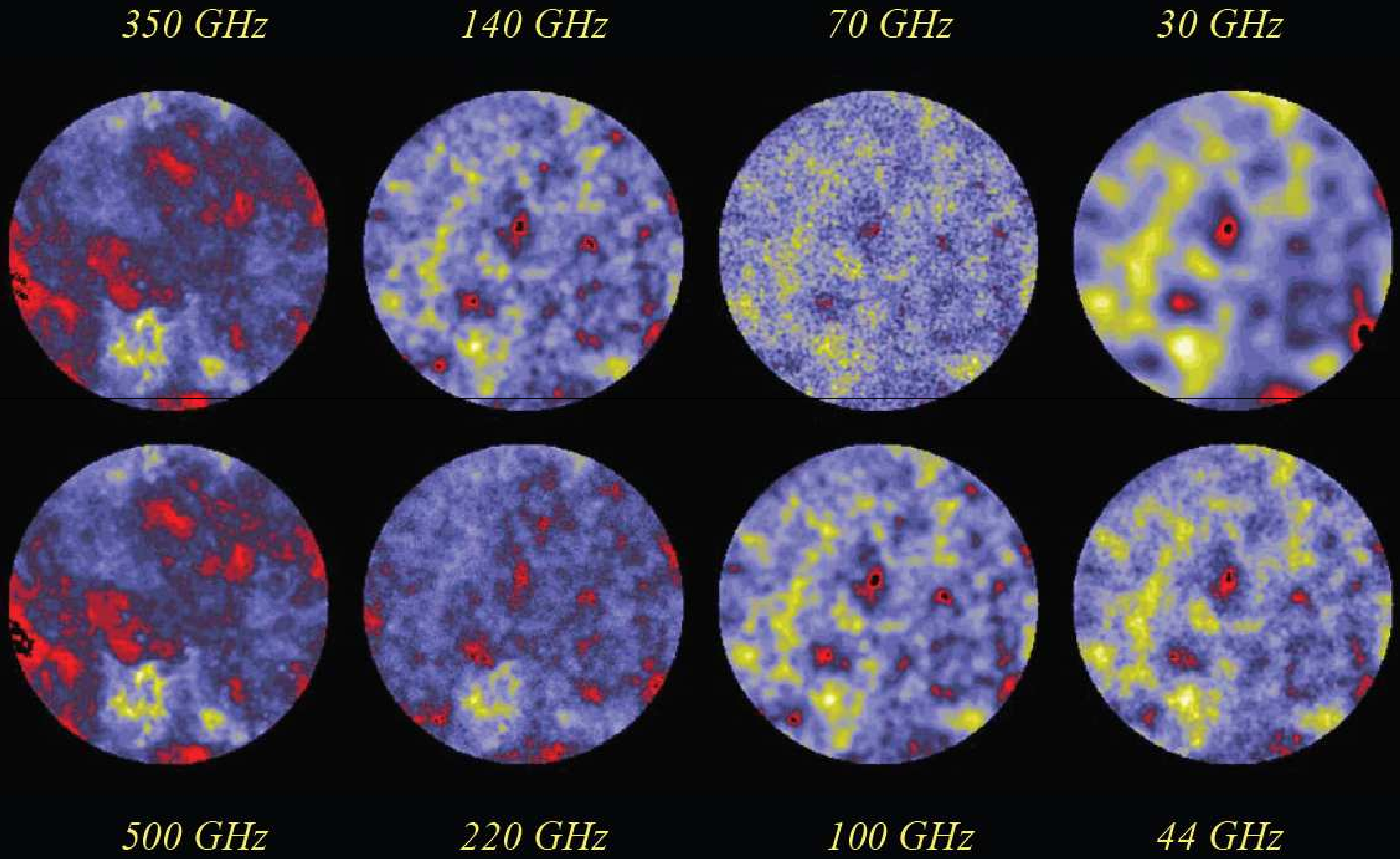

PLANCK

COBRAS/SAMBA Redbook (1996)

CMB Input *CMB Recovered*

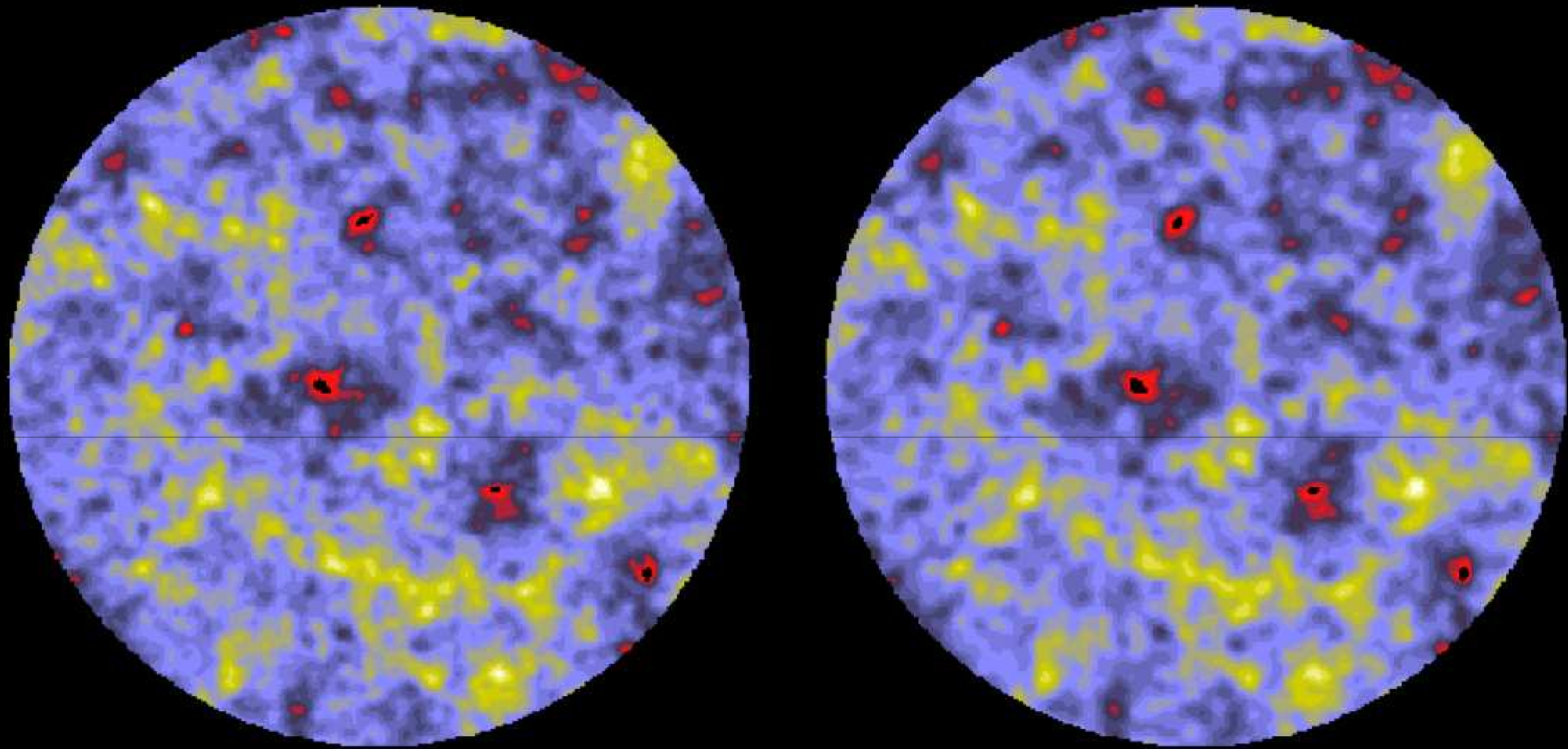

Not only statistical measure, but high singal-to-noise imaging

PLANCK

Planck Instrument Calibration Plan

	Unit	Assembly	Instrument	Satellite	In-flight
LFI		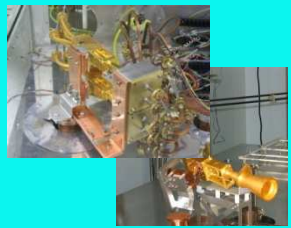		**CSL Campaign** 	 **CPV & FLS**
HFI	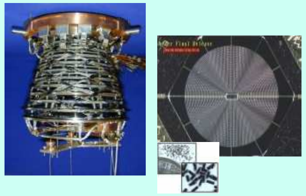		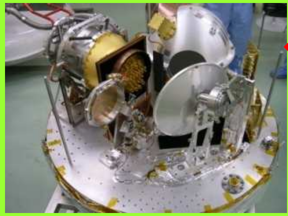		
Qualification Model (QM)	***Completed***	***Completed***	***Completed***	***Completed***	
Flight Model (FM)	***Completed***	***Completed***	***Completed***	***Completed***	***Completed***

Supported by Data Processing Centers

LFI FM cryo testing

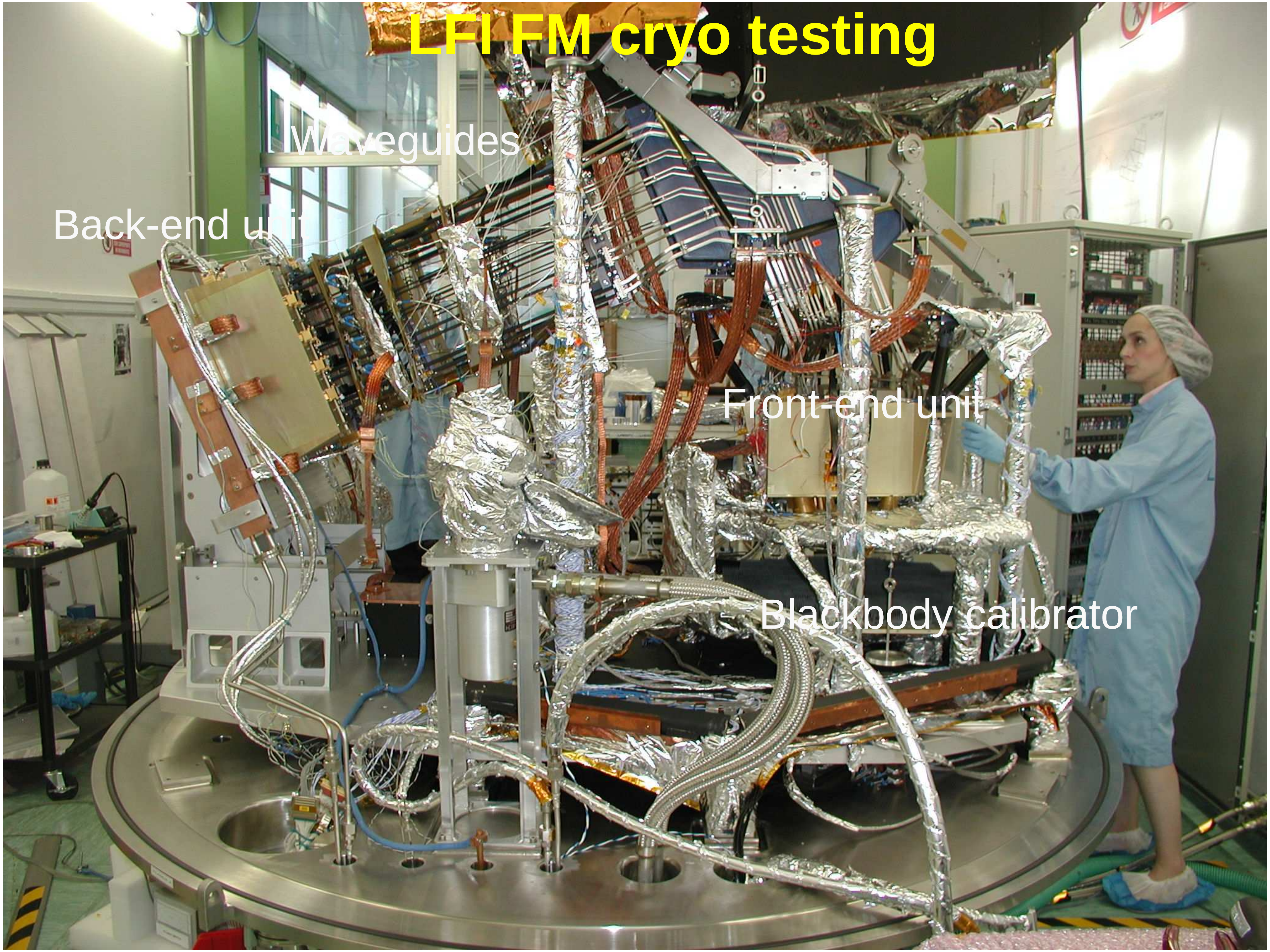

Planck-LFI design

Bersanelli et al 2010

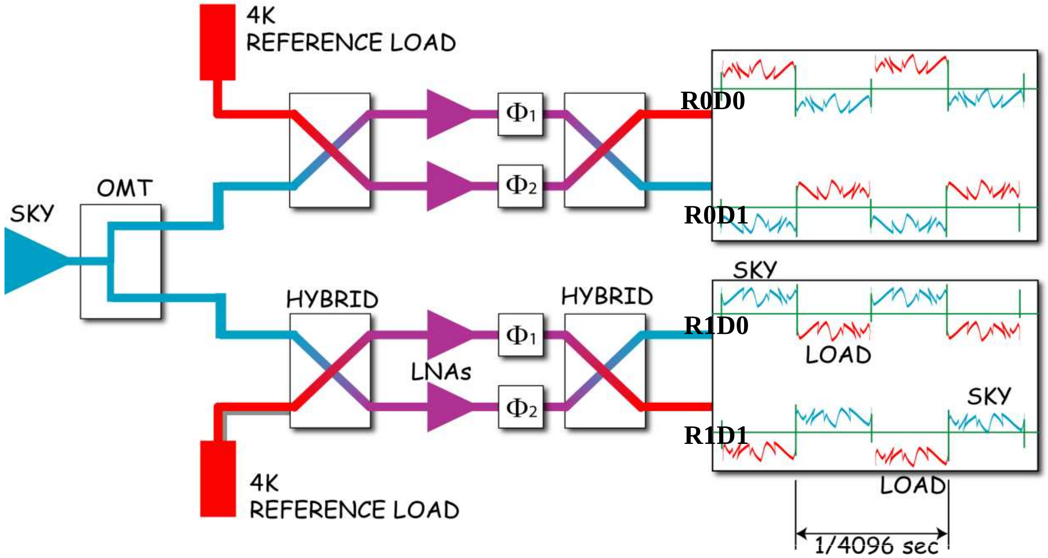

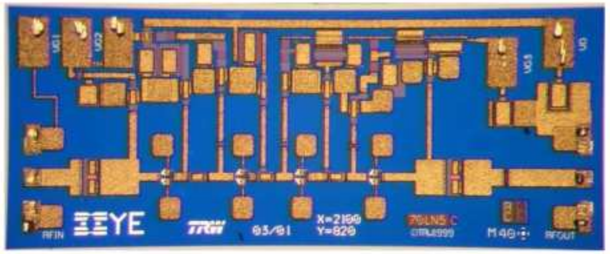

70 GHz MMIC HEMT

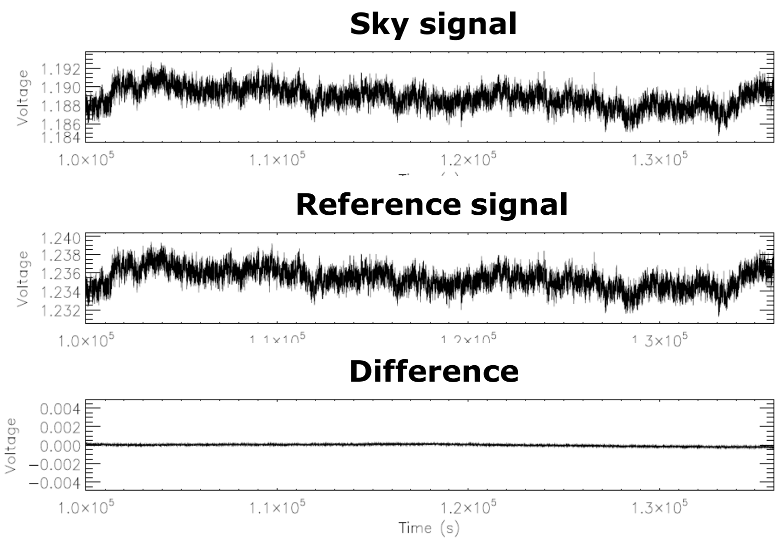

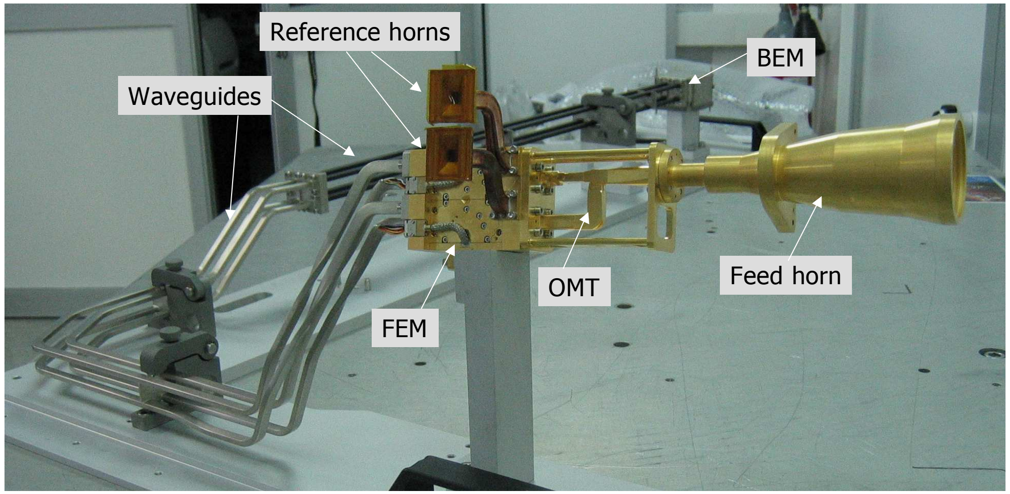

30 GHz FM RCA

HFI FM cryo testing

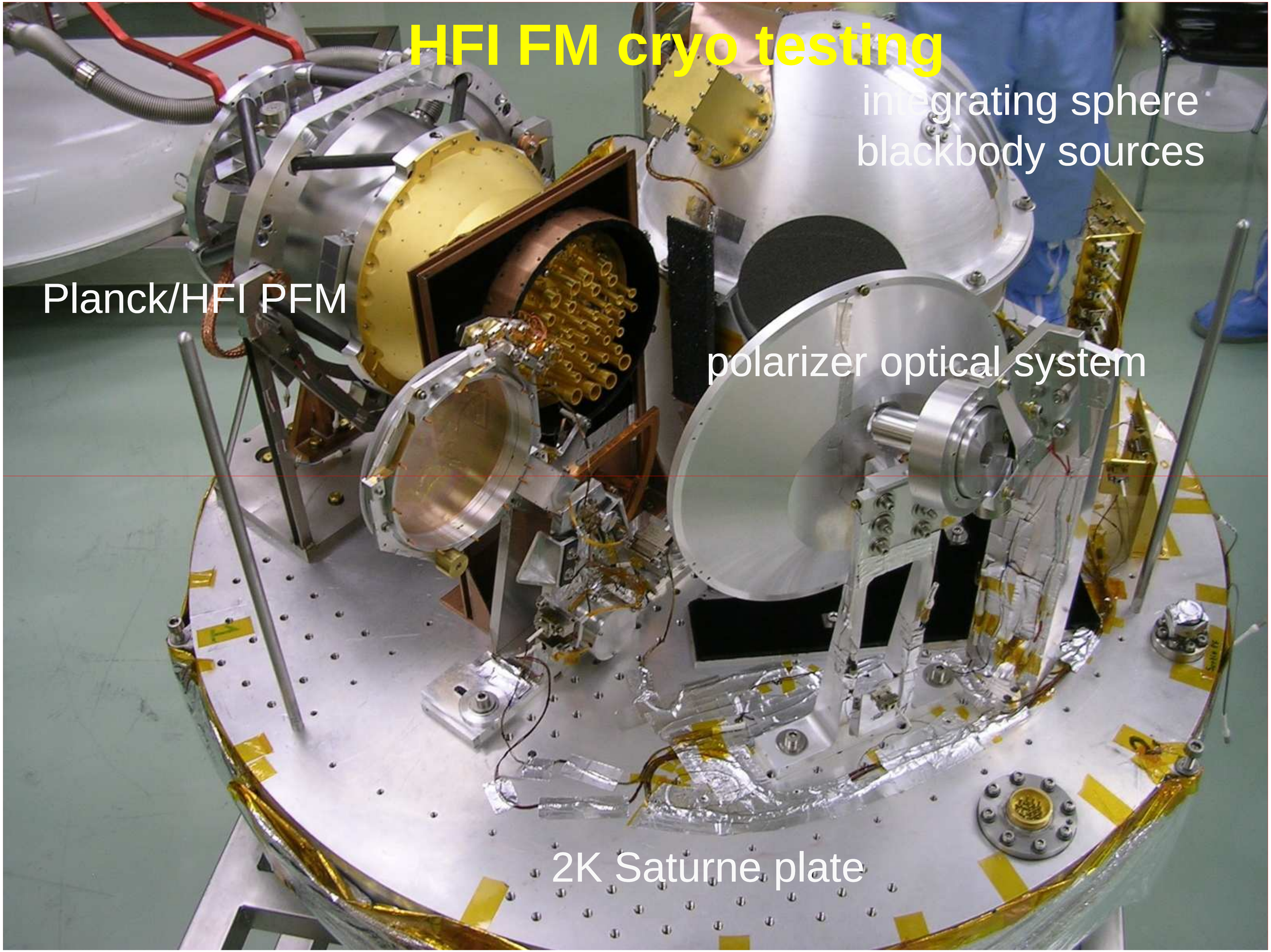

Planck-HFI design

Lamarre et al 2010

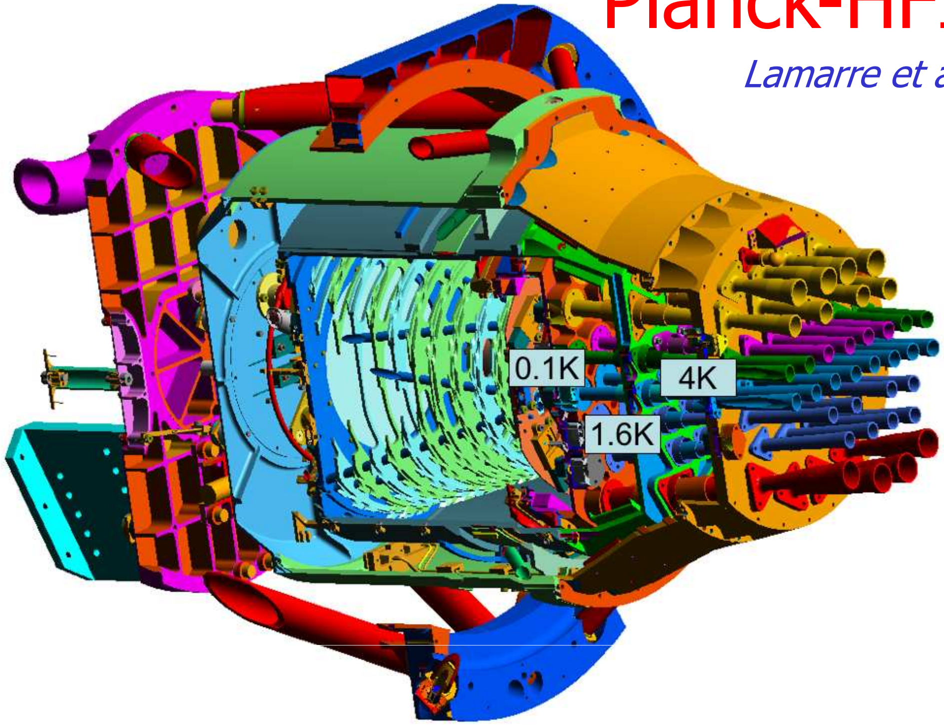

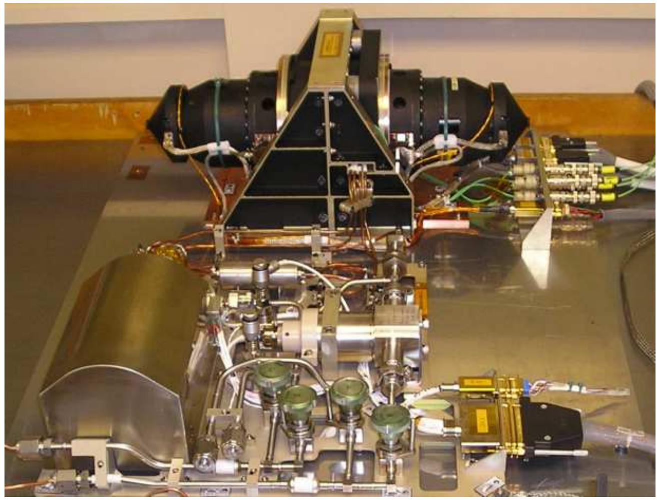

4K Stirling cooler

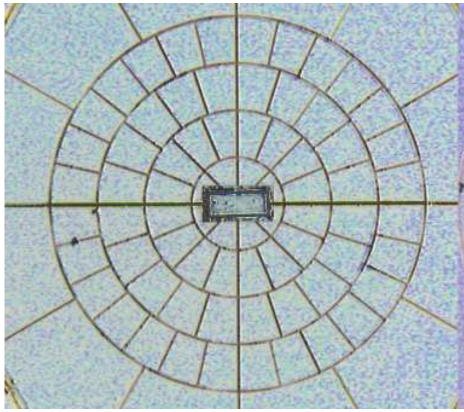

Spider-web Bolometer

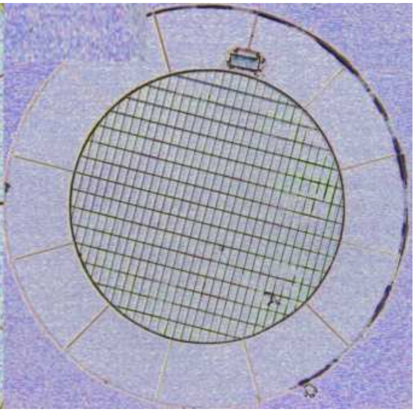

Polarisation Sensitive Bolometer

Heat exchanger of the dilution cooler (1.6 – 0.1 K)

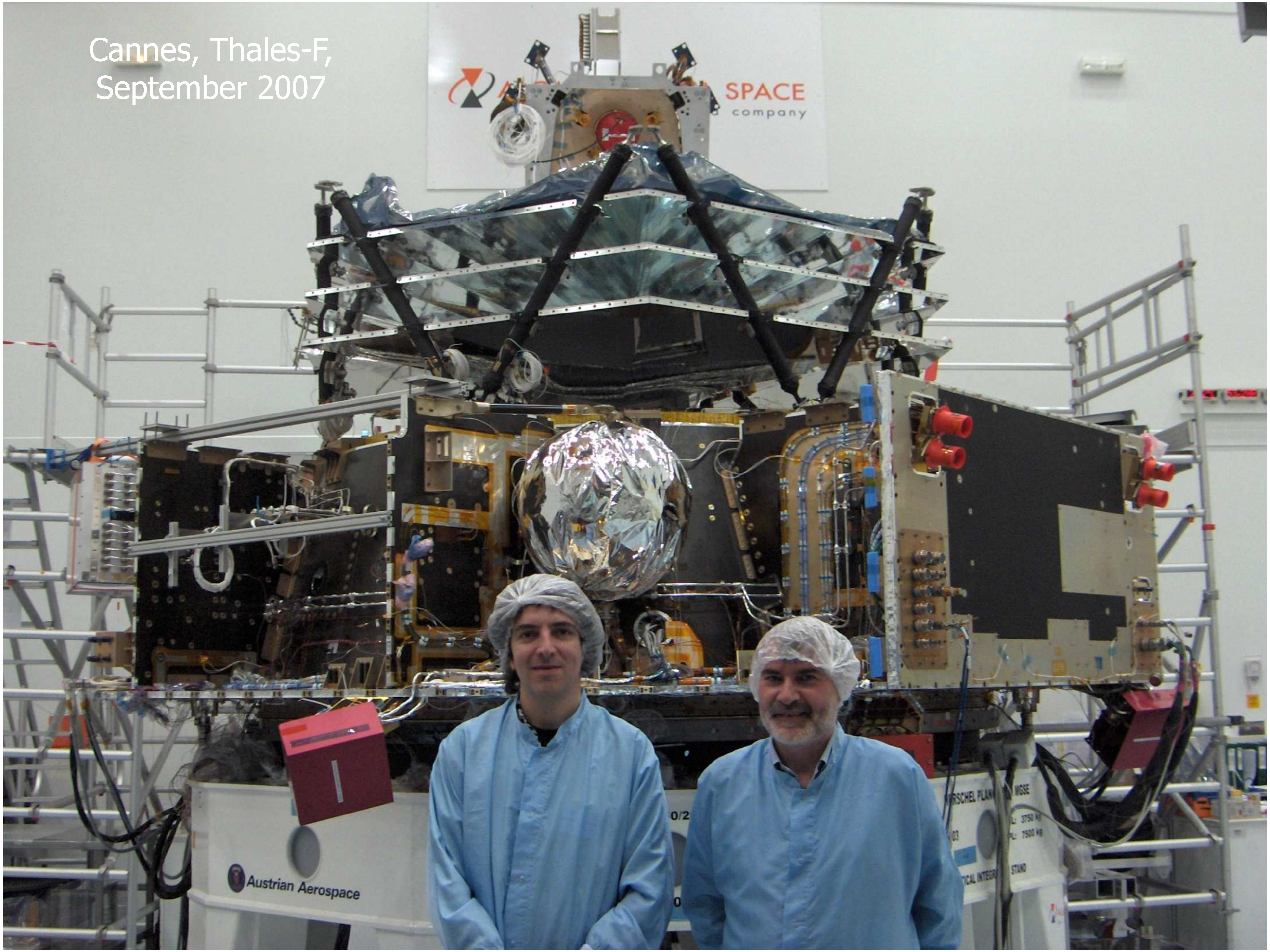
Cannes, Thales-F,
September 2007
SPACE
company
Austrian Aerospace

PLANCK Optical verification

RFQM campaign:

- QM mirrors and representative FPU and limited number of frequencies
- At room temperature

Videogrammetry test on cold telescope

Software models

GRASP9 simulations:

–Main beams

–Intermediate beams

–Full sky beams

Main beams

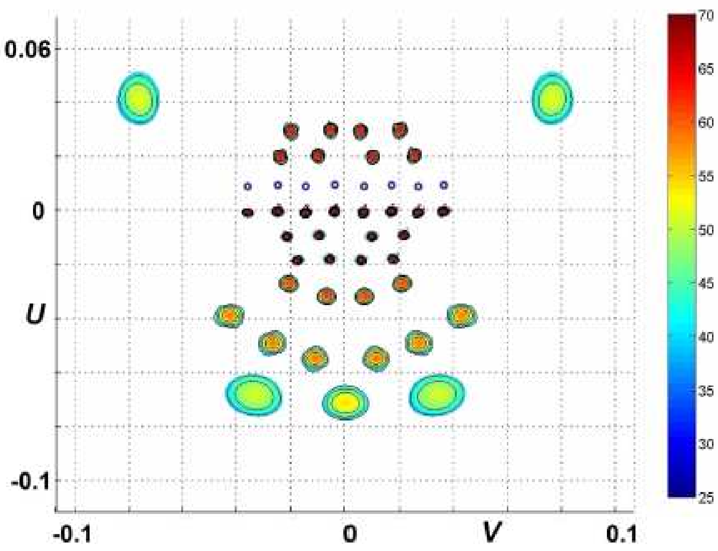

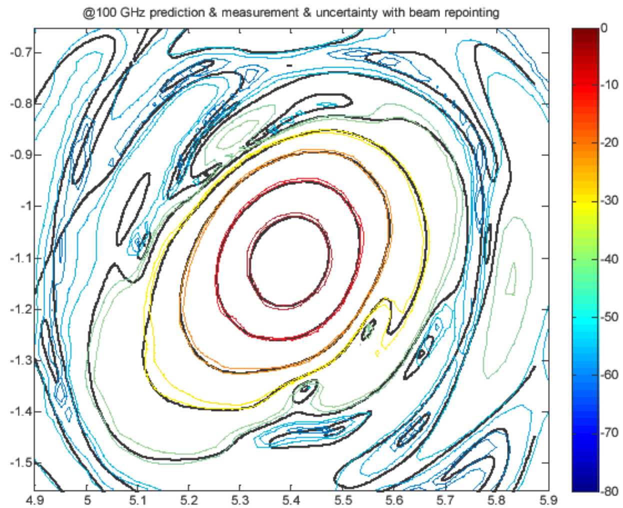

Uncertainty in the main beam shape after ground test campaign (integrated power, in percent of total) as a function of angular radius from peak.
(70 GHz: horn 23); 100 GHz: horn 1; 353 GHz: horn 6).

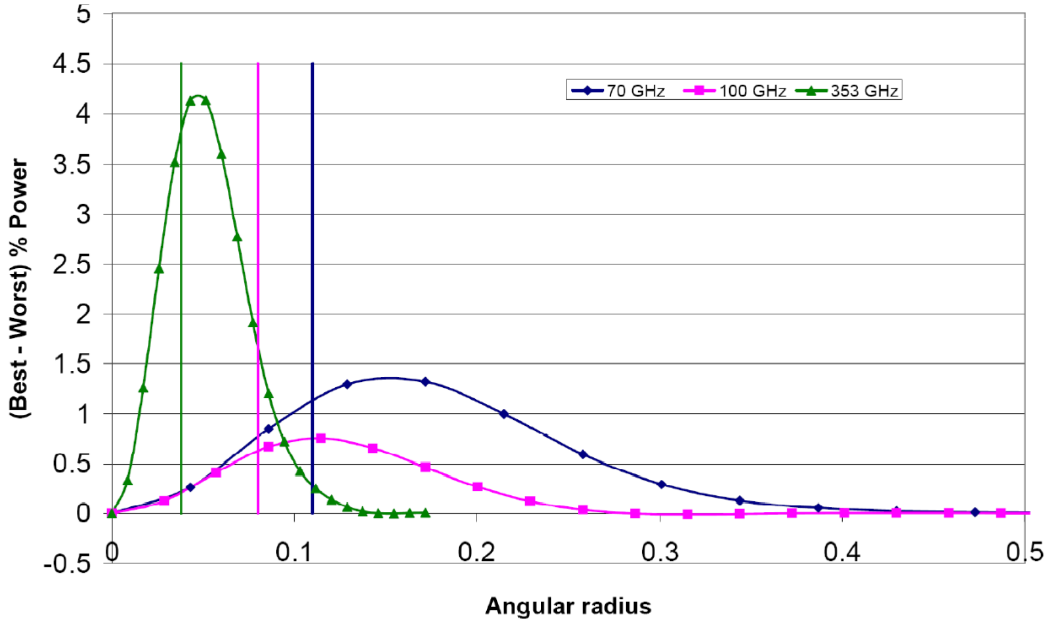

Straylight and far-sidelobes

30 GHz

Predicted Measured

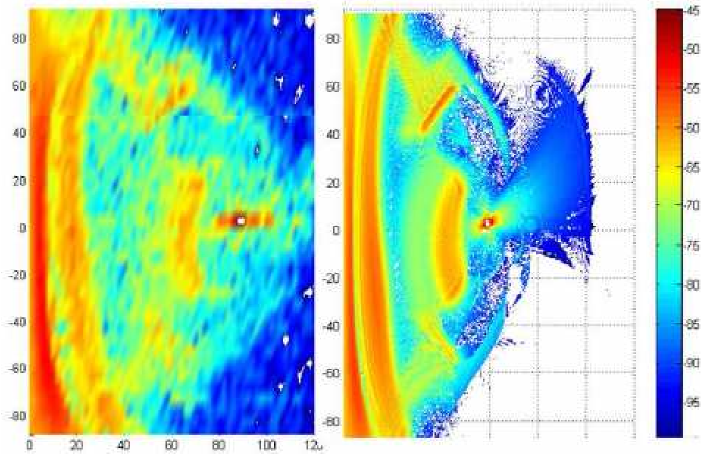

100 GHz

Predicted Measured

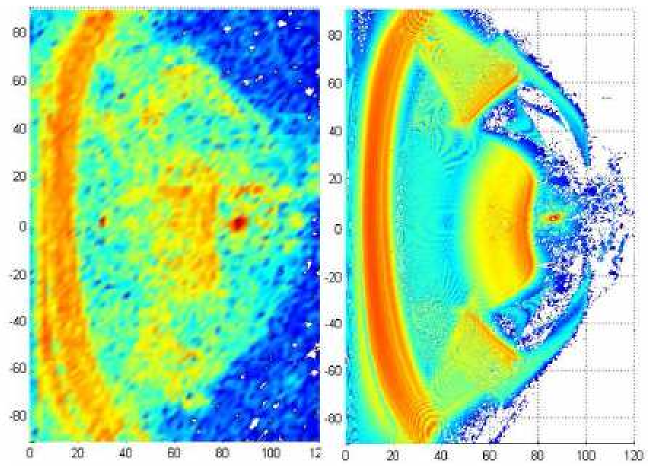

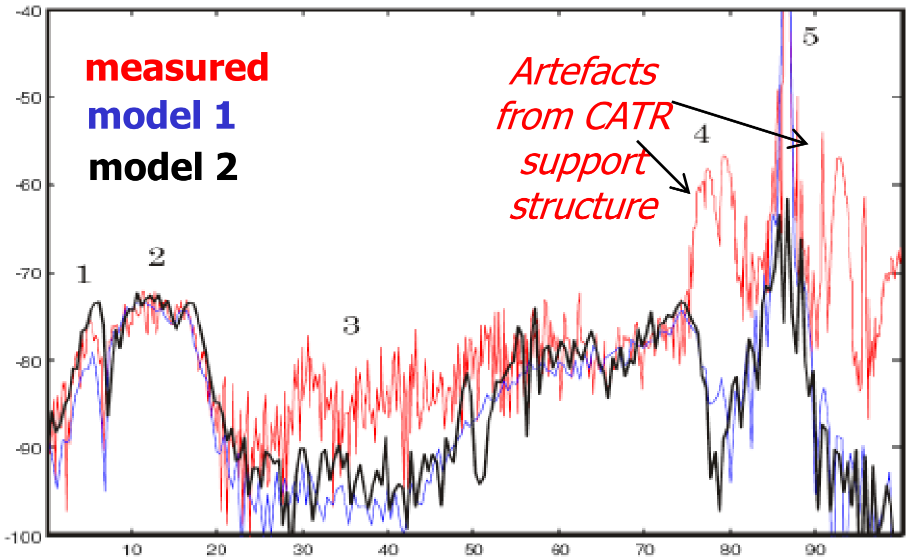

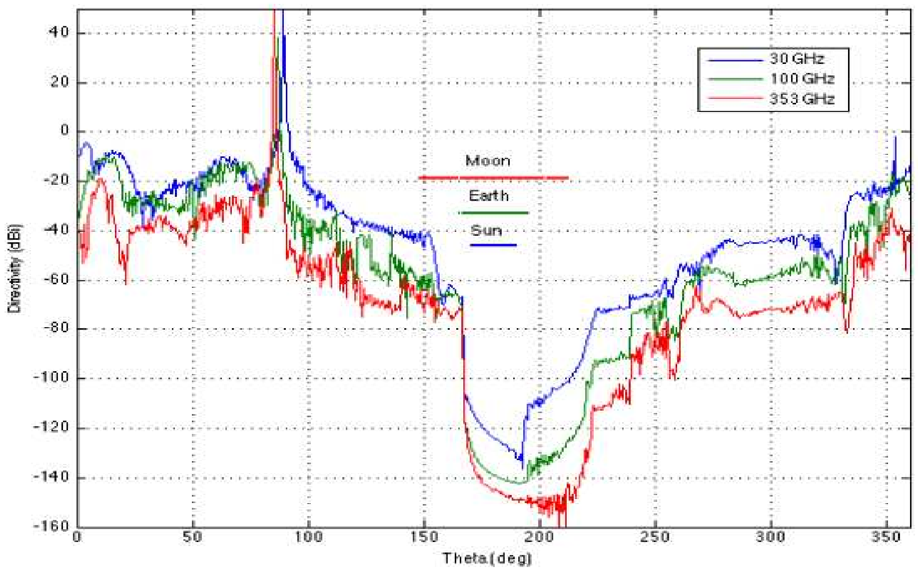

Planck Collaboration: ~400 scientists!

PLANCK SCIENCE TEAM: J. TAUBER (ESA), M. BERSANELLI, F. R. BOUCHET, G. EFSTATHIOU, J.-M. LAMARRE, C. R. LAWRENCE, N. MANDOLESI, H. U. NØRGAARD-NIELSEN, J.-L. PUGET, A. ZACCHEI

Planck Core Team

PLANCK COLLABORATION:

P. A. R. ADE, N. AGHANIM, B. AJA, E. ALIPPI, L. ALOY, P. ARMAND, M. ARNAUD, A. ARONDEL, A. ARREOLA-VILLANUEVA, E. ARTAL, E. ARTINA, A. ARTS, M. ASHDOWN, J. AUMONT, M. AZZARO, A. BACCHETTA, C. BACCIGALUPI, M. BAKER, M. BALASINI, A. BALBI, A. J. BANDAY, G. BARBIER, R. B. BARREIRO, M. BARTELMANN, P. BATTAGLIA, E. BATTANER, K. BENABED, J.-L. BENEY, R. BENEYTON, K. BENNETT, A. BENOIT, J.-P. BERNARD, P. BHANDARI, R. BHATIA, M. BIGGI, R. BIGGINS, G. BILLIG, Y. BLANC, H. BLAVOT, J. J. BOCK, A. BONALDI, R. BOND, J. BONIS, J. BORDERS, J. BORRILL, L. BOSCHINI, F. BOULANGER, J. BOUVIER, M. BOUZIT, R. BOWMAN, E. BRELLE, T. BRADSHAW, M. BRAGHIN, M. BREMER, D. BRIENZA, D. BROSZKIEWICZ, C. BURIGANA, M. BURKHALTER, P. CABELLA, T. CAERTY, M. CAIROLA, S. CAMINADE, P. CAMUS, C. M. CANTALUPO, B. CAPPELLINI, J.-F. CARDOSO, R. CARR, A. CATALANO, L. CAYON, M. CESA, M. CHAIGNEAU, A. CHALLINOR, A. CHAMBALLU, J. P. CHAMBELLAND, M. CHARRA, L.-Y. CHIANG, G. CHLEWICKI, P. R. CHRISTENSEN, S. CHURCH, E. CIANCIETTA, M. CIBRARIO, R. CIZERON, D. CLEMENTS, B. COLLAUDIN, J.-M. COLLEY, S. COLOMBI, A. COLOMBO, F. COLOMBO, O. CORRE, F. COUCHOT, B. COUGRAND, A. COULAIS, P. COUZIN, B. CRANE, B. CRILL, M. CROOK, D. CRUMB, F. CUTTAIA, U. D¨ORL, P. DA SILVA, R. DADDATO, C. DAMASIO, L. DANESE, G. D'AQUINO, O. D'ARCANGELO, K. DASSAS, R. D. DAVIES, W. DAVIES, R. J. DAVIS, P. DE BERNARDIS, D. DE CHAMBURE, G. DE GASPERIS, M. L. DE LA FUENTA, P. DE PACO, A. DE ROSA, G. DE TROIA, G. DE ZOTTI, M. DEHAMME, J. DELABROUILLE, J.-M. DELOUIS, F.-X. D´ESERT, G. DI GIROLAMO, C. DICKINSON, E. DOELLING, K. DOLAG, I. DOMKEN, M. DOUSPIS, D. DOYLE, S. DU, D. DUBRUEL, C. DUFOUR, C. DUMESNIL, X. DUPAC, P. DURET, C. EDER, A. ELFVING, T. A. ENßLIN, P. ENG, K. ENGLISH, H. K. ERIKSEN, P. ESTARIA, M. C. FALVELLA, F. FERRARI, F. FINELLI, A. FISHMAN, S. FOGLIANI, S. FOLEY, A. FONSECA, G. FORMA, O. FORNI1, P. FOSALBA, J.-J. FOURMOND, M. FRAILIS, E. FRANCESCHI, S. FRANOIS, M. FRERKING, M. F. GOMEZ-RENASCO, K. M. GORSKI, T. C. GAIER, S. GALEOTTA, J. GALLEGOS, K. GANGA, J. GARCIA LAZARO, A. GARNICA, M. GASPARD, E. GAVILA, M. GIARD1, G. GIARDINO, G. GIENGER, Y. GIRAUD-HERAUD, J.-M. GLORIAN, M. GRIN, A. GRUPPUSO, L. GUGLIELMI, D. GUICHON, B. GUILLAUME, P. GUILLOUET, J. HAISSINSKI, F. K. HANSEN, J. HARDY, D. HARRISON, A. HAZELL, M. HECHLER, V. HECKENAUER, D. HEINZER, R. HELL, S. HENROT-VERSILLE, C. HERNANDEZ-MONTEAGUDO, D. HERRANZ, J. M. HERREROS, V. HERVIER, A. HESKE, A. HEURTEL, S. R. HILDEBRANDT, R. HILLS, E. HIVON, M. HOBSON, D. HOLLERT, W. HOLMES, A. HORNSTRUP, W. HOVEST, R. J. HOYLAND, G. HUEY, K. M. HUENBERGER, N. HUGHES, U. ISRAELSSON, B. JACKSON, A. JAE, T. R. JAE, T. JAGEMANN, N. C. JESSEN, J. JEWELL, W. JONES, M. JUVELA, J. KAPLAN, P. KARLMAN, F. KECK, E. KEIHANEN, M. KING, T. S. KISNER, P. KLETZKINE, R. KNEISSL, J. KNOCHE, L. KNOX, T. KOCH, M. KRASSENBURG, H. KURKI-SUONIO, A. LAHTEENMAKI, G. LAGACHE, E. LAGORIO, P. LAMI, J. LANDE, A. LANGE, F. LANGLET, R. LAPINI, M. LAPOLLA, A. LASENBY, M. LE JEUNE, J. P. LEAHY, M. LEFEBVRE, F. LEGRAND, G. LEMEUR, R. LEONARDI, B. LERICHE, C. LEROY, P. LEUTENEGGER, S. M. LEVIN, P. B. LILJE, C. LINDENSMITH, M. LINDEN-VØRNLE, A. LOC, Y. LONGVAL, P. M. LUBIN, T. LUCHIK, I. LUTHOLD, J. F. MACIAS-PEREZ, T. MACIASZEK, C. MACTAVISH, S. MADDEN, B. MAEI, C. MAGNEVILE, D. MAINO, A. MAMBRETTI, B. MANSOUX, D. MARCHIORO, M. MARIS, F. MARLIANI, J.-C. MARRUCHO, J. MARTI-CANALES, E. MARTINEZ-GONZALEZ, A. MARTIN-POLEGRE, P. MARTIN, C. MARTY, W. MARTY, S. MASI, M. MASSARDI, S. MATARRESE, F. MATTHAI, P. MAZZOTTA, A. MCDONALD, P. MCGRATH, A. MEDIAVILLA, P. R. MEINHOLD, J.-B. MELIN, F. MELOT, L. MENDES, A. MENNELLA, C. MERVIER, L. MESLIER, M. MICCOLIS, M.-A. MIVILLE-DESCHENES, A. MONETI, D. MONTET, L. MONTIER, J. MORA, G. MORGANTE, G. MORIGI, G. MORINAUD, N. MORISSET, D. MORTLOCK, S. MOTTET, J. MULDER, D. MUNSHI, A. MURPHY, P. MURPHY, P. MUSI, J. NARBONNE, P. NASELSKY, A. NASH, F. NATI, P. NATOLI, B. NETTERFIELD, J. NEWELL, M. NEXON, C. NICOLAS, P. H. NIELSEN, N. NINANE, F. NOVIELLO, D. NOVIKOV, I. NOVIKOV, I. J. O'DWYER, P. OLDEMAN, P. OLIVIER, L. OUCHET, C. A. OXBORROW, L. PEREZ-CUEVAS, L. PAGAN, C. PAINE, F. PAJOT, R. PALADINI, F. PANCHER, J. PANH, G. PARKS, P. PARNAUDEAU, B. PARTRIDGE, B. PARVIN, J. P. PASCUAL, F. PASIAN, D. P. PEARSON, T. PEARSON, M. PECORA, O. PERDEREAU, L. PEROTTO, F. PERROTTA, F. PIACENTINI, M. PIAT, E. PIERPAOLI, O. PIERSANTI, E. PLAIGE, S. PLASZCZYNSKI, P. PLATANIA, E. POINTECOUTEAU, G. POLENTA1, N. PONTHIEU, L. POPA, G. POULLEAU, T. POUTANEN, G. PREZEAU, L. PRADELL, M. PRINA, S. PRUNET, J. P. RACHEN, D. RAMBAUD, F. RAME, I. RASMUSSEN, J. RAUTAKOSKI, W. T. REACH, R. REBOLO, M. REINECKE, J. REITER, C. RENAULT, S. RICCIARDI, P. RIDEAU, T. RILLER, I. RISTORCELLI, J. B. RITI, G. ROCHA, Y. ROCHE, R. ROGER PONS, R. ROHLFS, D. ROMERO, S. ROOSE, C. ROSSET, S. ROUBEROL, M. ROWAN-ROBINSON, J. A. RUBINO-MARTIN, P. RUSCONI, B. RUSHOLME, M. SALAMA, E. SALERNO, M. SANDRI, D. SANTOS, J. L. SANZ, L. SAUTER, F. SAUVAGE, G. SAVINI, M. SCHMELZEL, A. SCHNORHK, W. SCHWARZ, D. SCOTT, M. D. SEIERT, P. SHELLARD, C. SHIH, M. SIAS, J. I. SILK, R. SILVESTRI, R. SIPPE, G. F. SMOOT, J.-L. STARCK, P. STASSI, J. STERNBERG, F. STIVOLI, V. STOLYAROV, R. STOMPOR, L. STRINGHETTI, D. STROMMEN, T. STUTE, R. SUDIWALA, R. SUGIMURA, R. SUNYAEV, J.-F. SYGNET, M. TURLER, E. TADDEI, J. TALLON, C. TAMIATTO, M. TAURIGNA, D. TAYLOR, L. TERENZI, S. THUEREY, J. TILLIS, G. TOFANI, L. TOOLATTI, E. TOMMASI, M. TOMMASI, E. TONAZZINI, J.-P. TORRE, S. TOSTI, F. TOUZE, M. TRISTRAM, J. TUOVINEN, M. TUTTLEBEE, G. UMANA, L. VALENZIANO, D. VALLEE, M. VAN DER VLIS, F. VAN LEEUWEN, J.-C. VANEL, B. VANTENT, J. VARIS, E. VASSALLO, C. VESCOVI, F. VEZZU, D. VIBERT, P. VIELVA, J. VIERRA, F. VILLA, N. VITTORIO, C. VUERLI, L. A. WADE, A. R. WALKER, B. D. WANDELT, C. WATSON, D. WERNER, M. WHITE, S. D. M. WHITE, A. WILKINSON, P. WILSON, A. WOODCRAFT, B. YOO, M. YUN, V. YURCHENKO, D. YVON, B. ZHANG, O. ZIMMERMANN, A. ZONCA, AND D. ZORITA

Planck in Italy

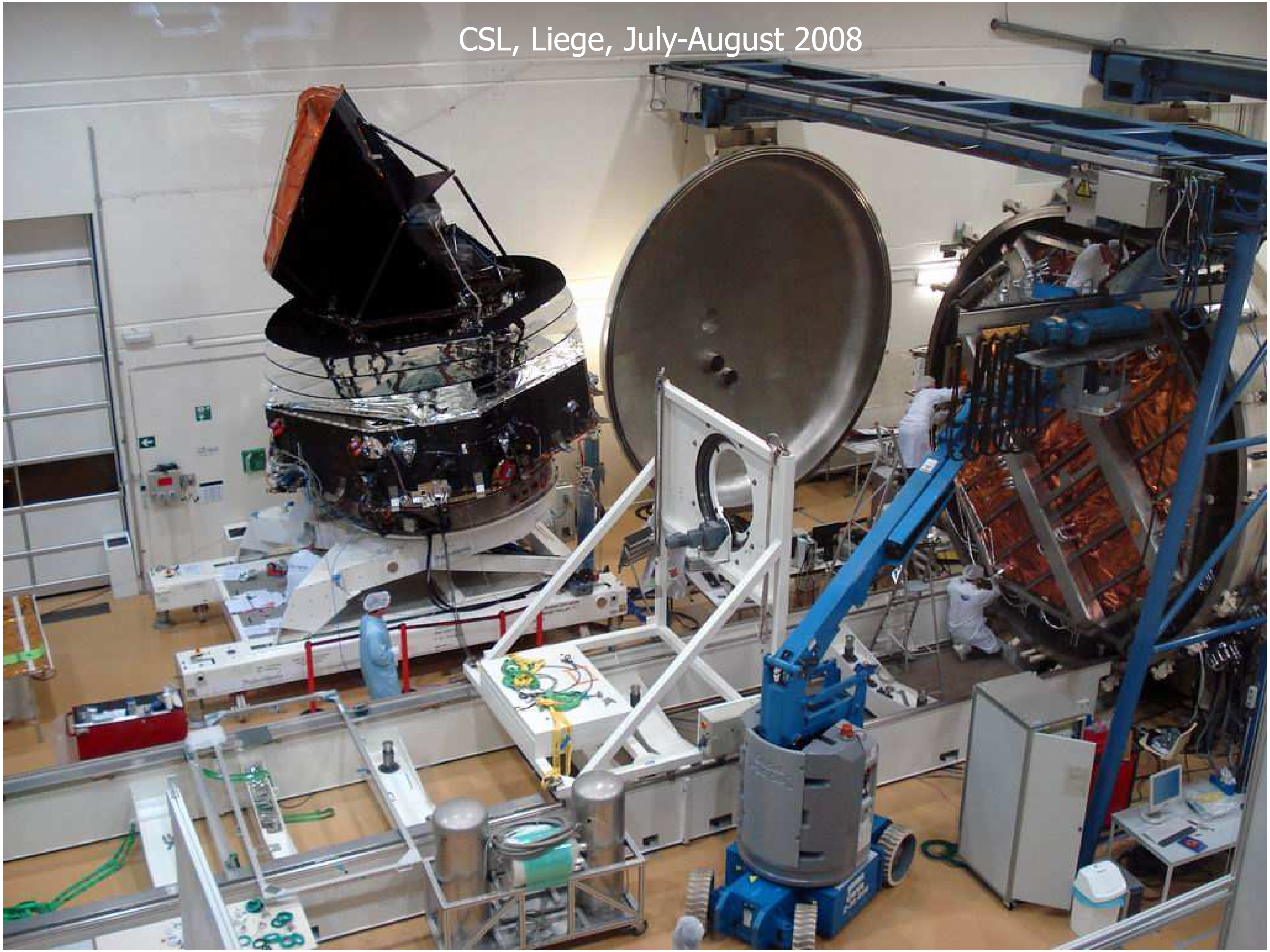
CSL, Liege, July-August 2008


CSL, Liege, July-August 2008
18
Thales


CSL, Liege, July-August 2008

CSL, Liege, July-August 2008

(by Stuart Lowe)

Kourou (Franch Guyana), February 2009


Kourou, March 2009

Kourou, French Guyana, 14 May 2009, h 10:12

Planck in volo

Lancio "perfetto" (attitudine <0.1°, semiasse maggiore <1,6%)

Planck: Universo appena nato (fondo cosmico di microonde)
Herschel: Universo giovane (galassie ad alto redsift)

Traiettoria di trasferimento (~2 mesi)
Orbita finale (Sun-Earth L2), 1.5 milioni di km dalla Terra
Calibrazione: "accordatura" degli strumenti

Cooldown

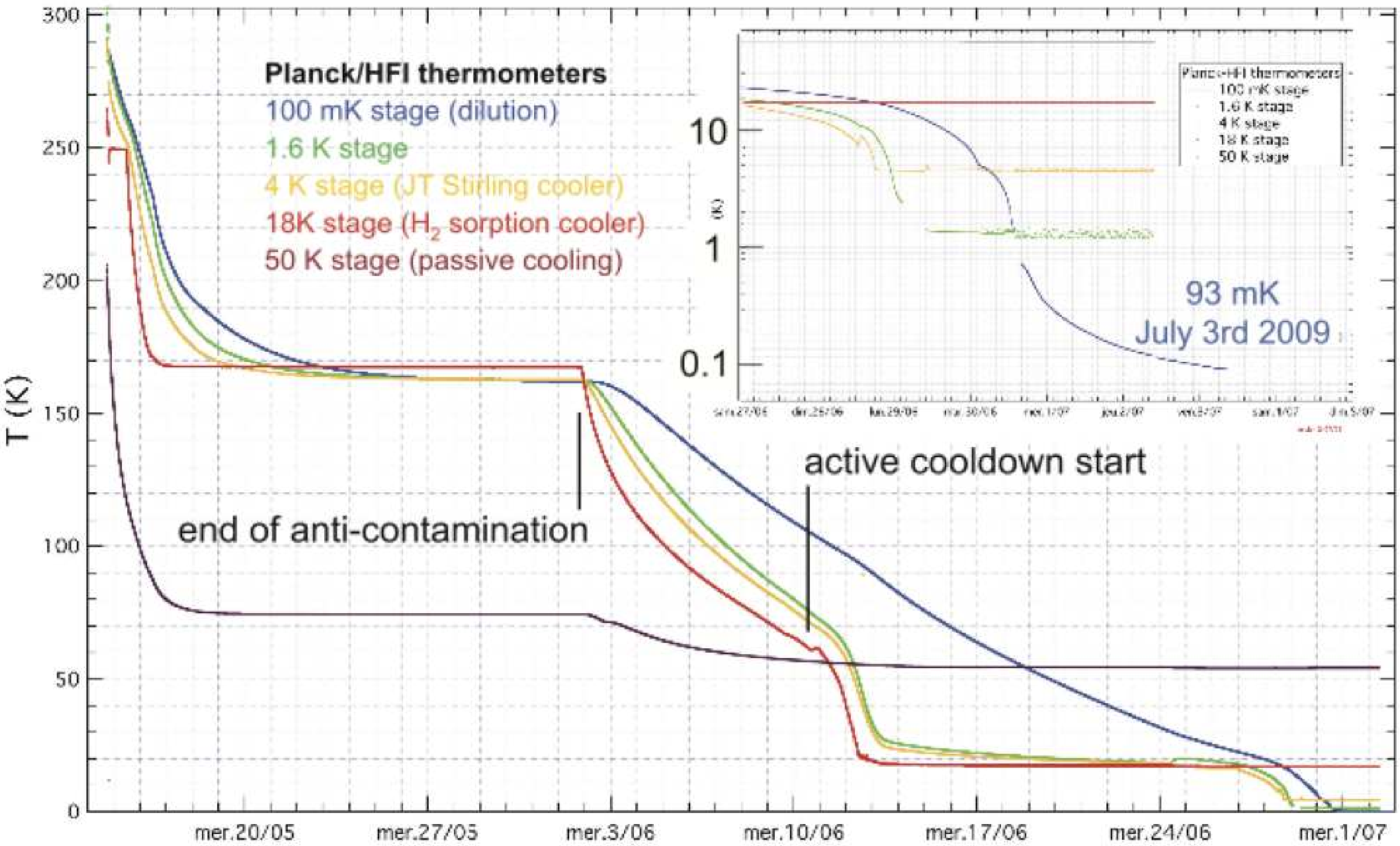
Planck/HFI thermometers
100 mK stage (dilution)
1.6 K stage
4 K stage (JT Stirling cooler)
18K stage (H2 sorption cooler)
50 K stage (passive cooling)
T (K)
300
250
200
150
100
50
0
mer.20/05
mer.27/05
mer.3/06
mer.10/06
mer.17/06
mer.24/06
mer.1/07
end of anti-contamination
active cooldown start
10
1
0.1
93 mK
July 3rd 2009

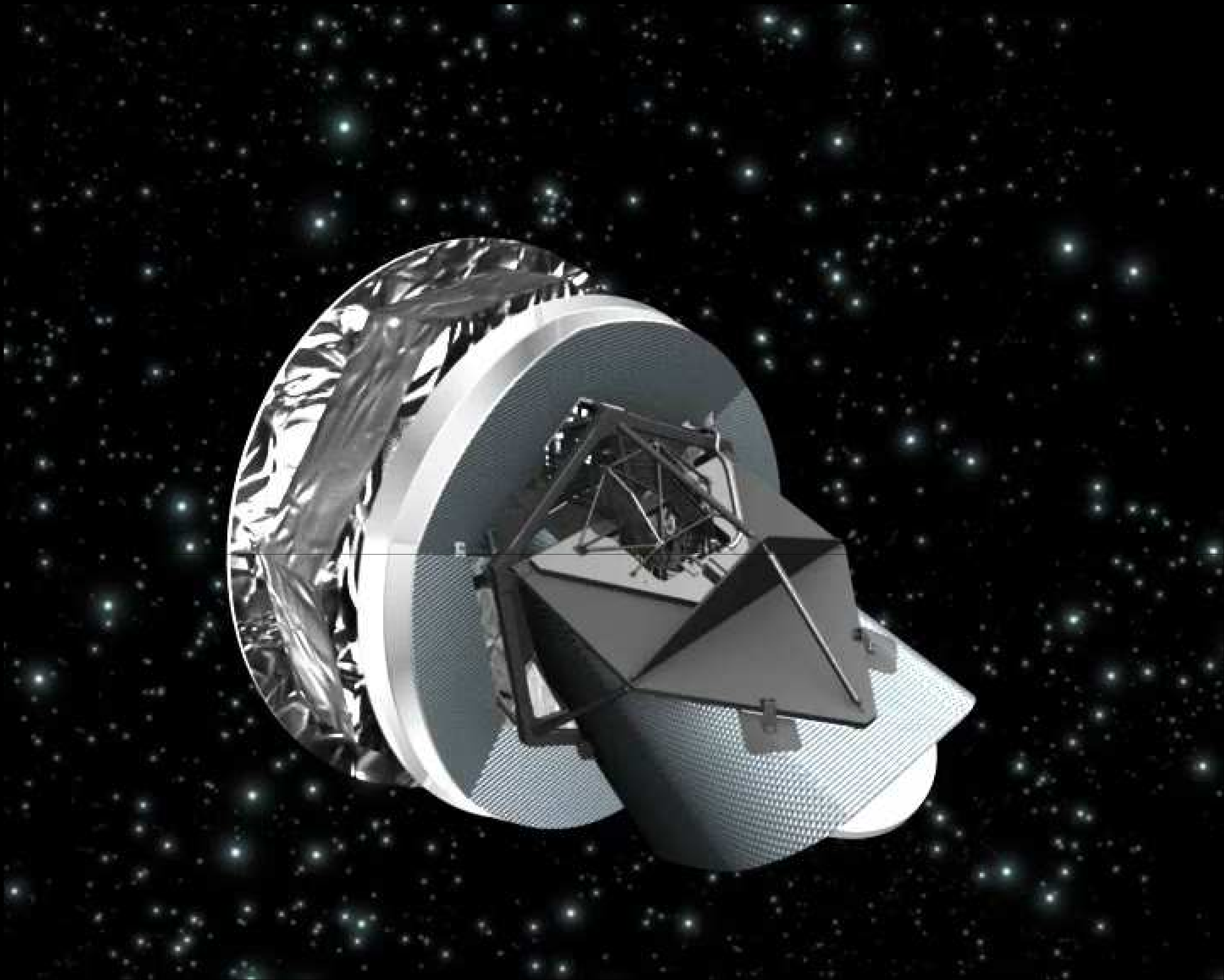

Planck-LFI: i dati “grezzi”

10min of flight data – 1/44 LFI detectors

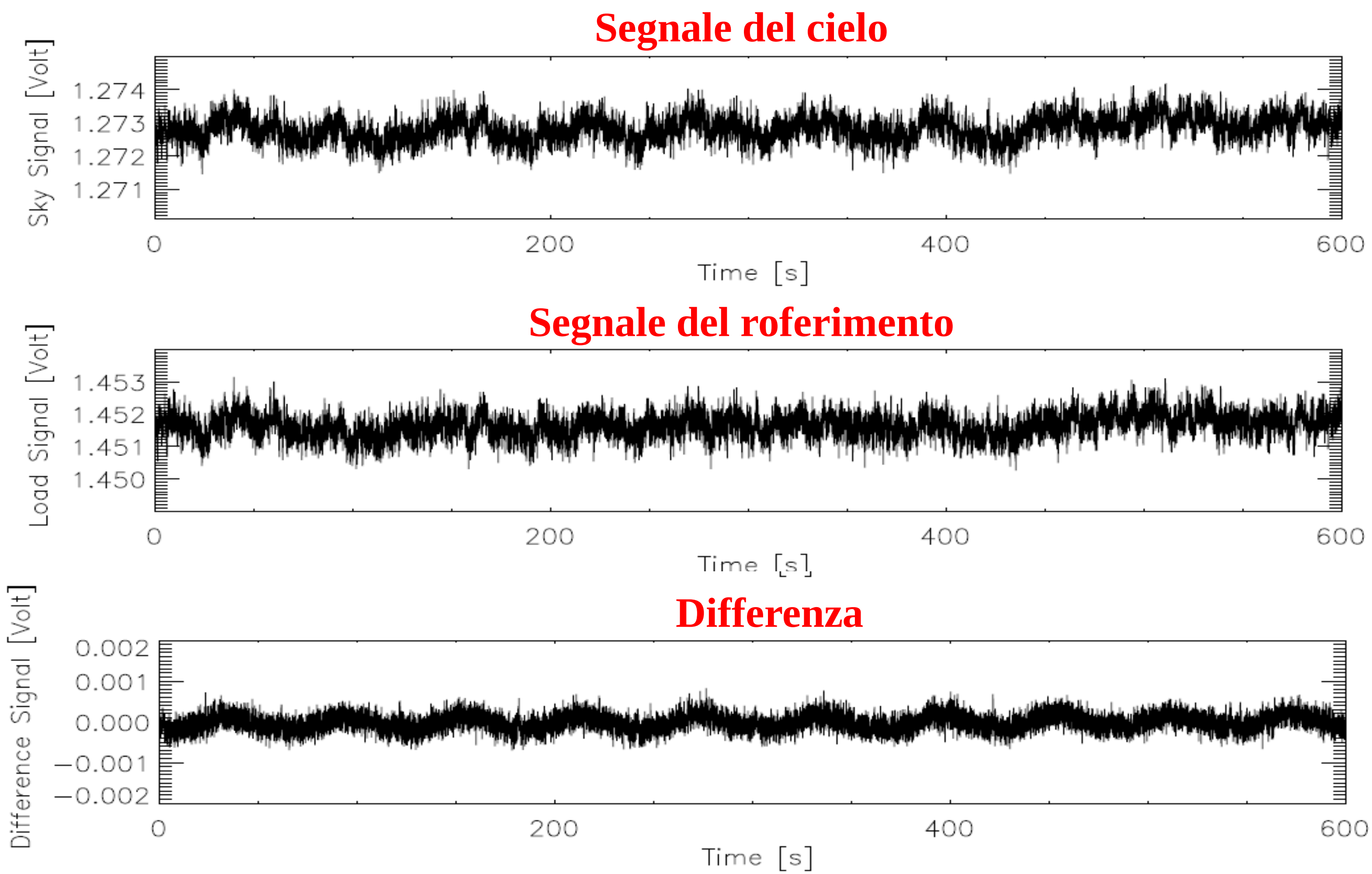

"First light"

Data from 14 Jun 09 (2 months before start of survey, NO tuning)

Sky

Ref

Diff

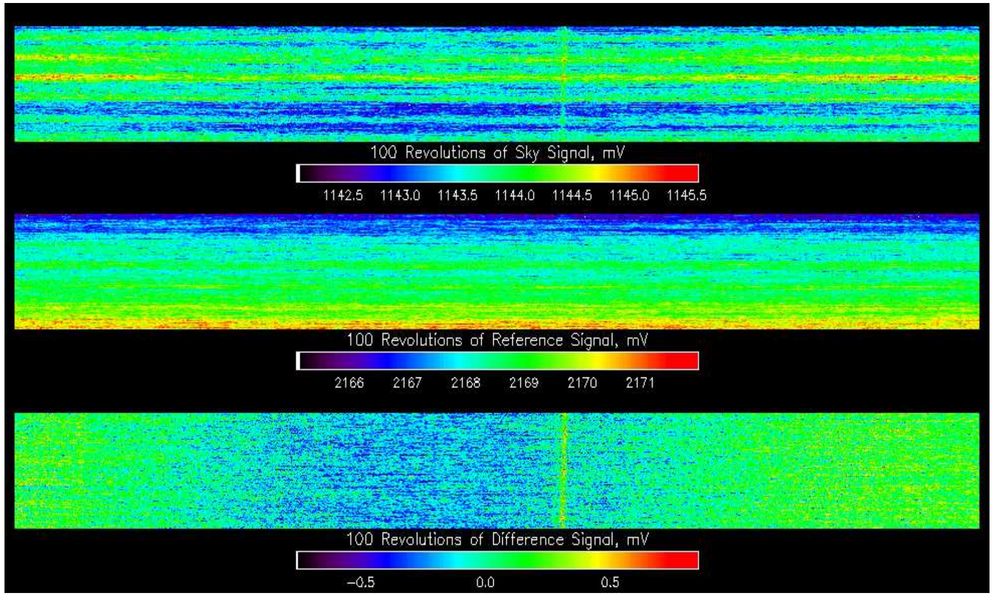

- Preliminary Dipole Calibration

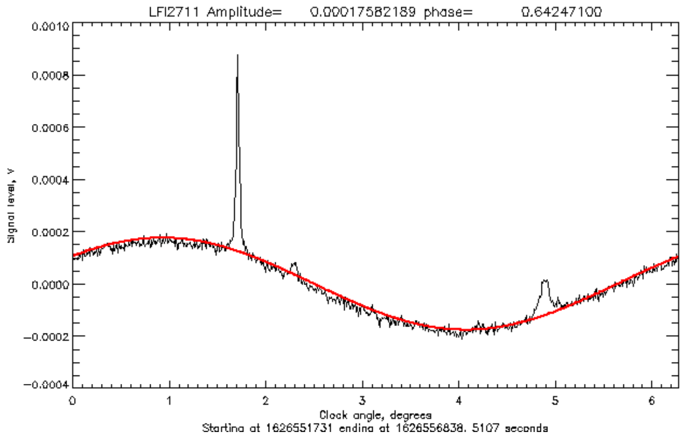

In-flight tuning

(Jun-Jul 09)

(Cuttaia et al 2009, Gregorio et al 2011)

- Functionality tests …

  → all 44 LFI detectors OK!

- Optimisation of bias for LNAs, Phase switches

  Exploit cool-down of HFI 4K stage (LFI loads)

LFI cooldown

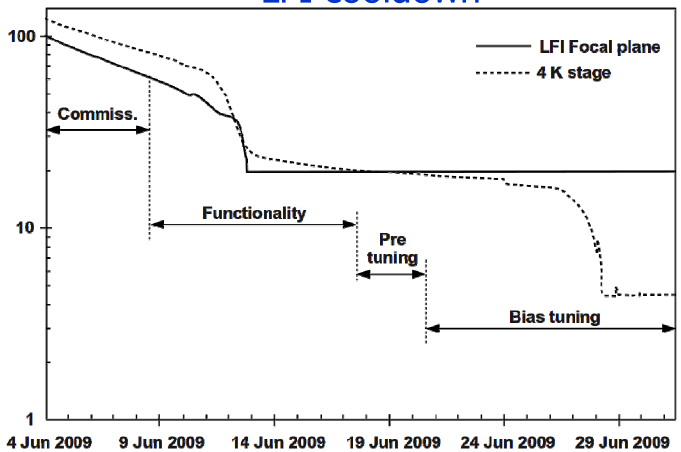

Planck-HFI: i dati "grezzi"

3min of flight data – 1/54 HFI detectors

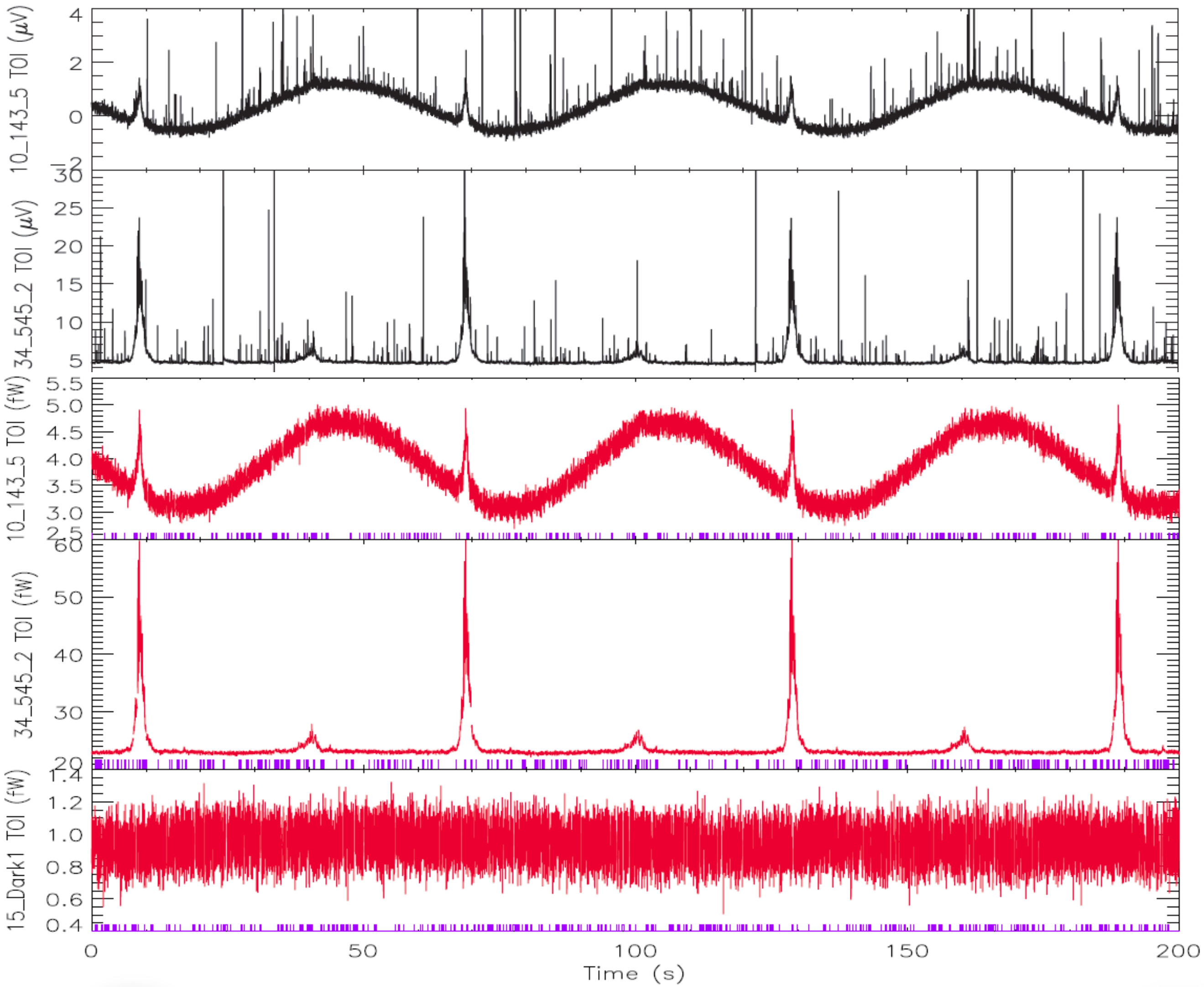

Planck-HFI: Cosmic rays

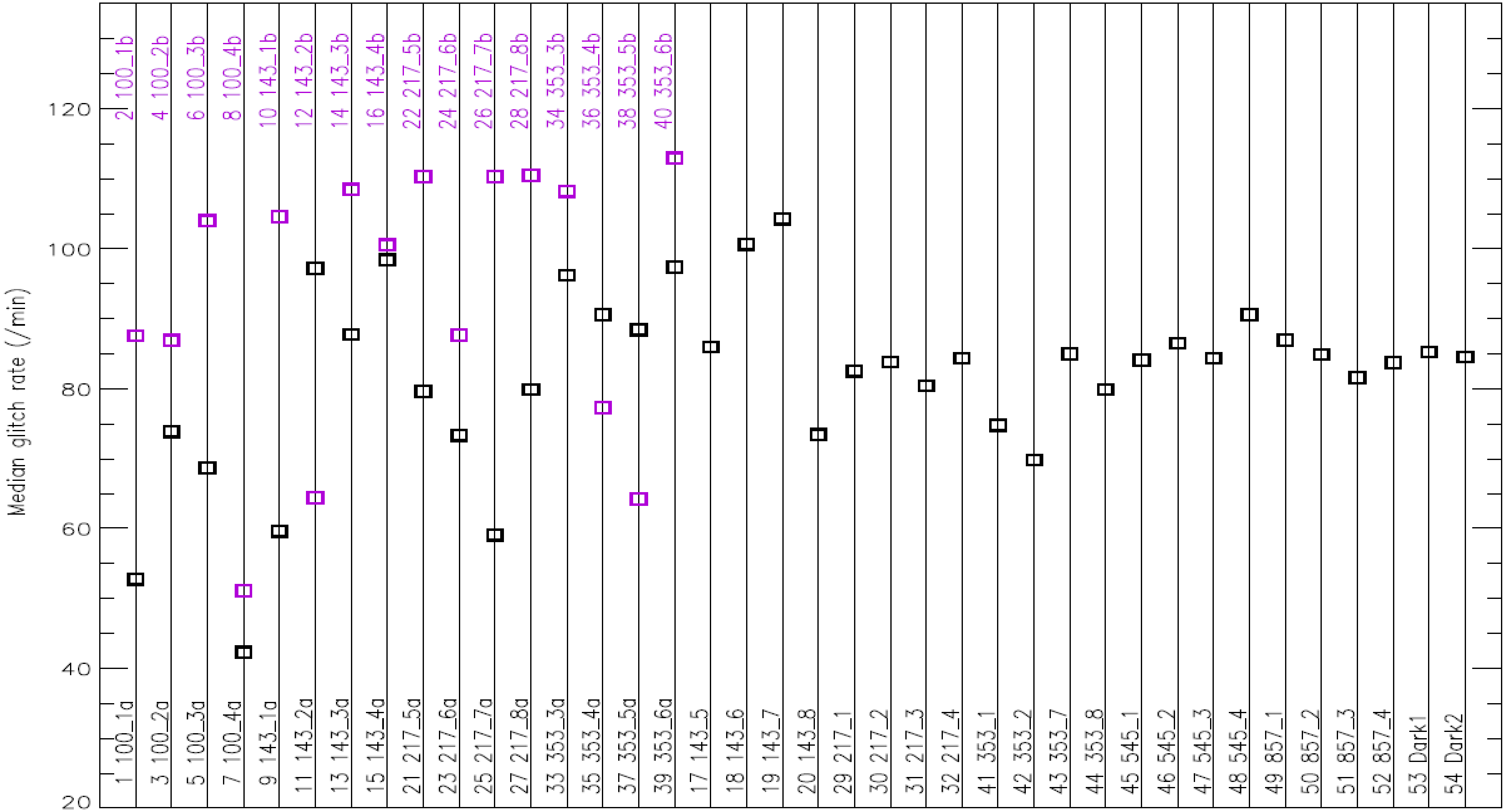

Figure 19. Glitch rate of all HFI bolometers. An average over the first sky survey has been performed. The asymmetry between PSB bolometers sharing the same horn is an effect of detection threshold and asymmetric time constant properties between PSB a and b.

Planck-HFI: Bandpasses and CO lines

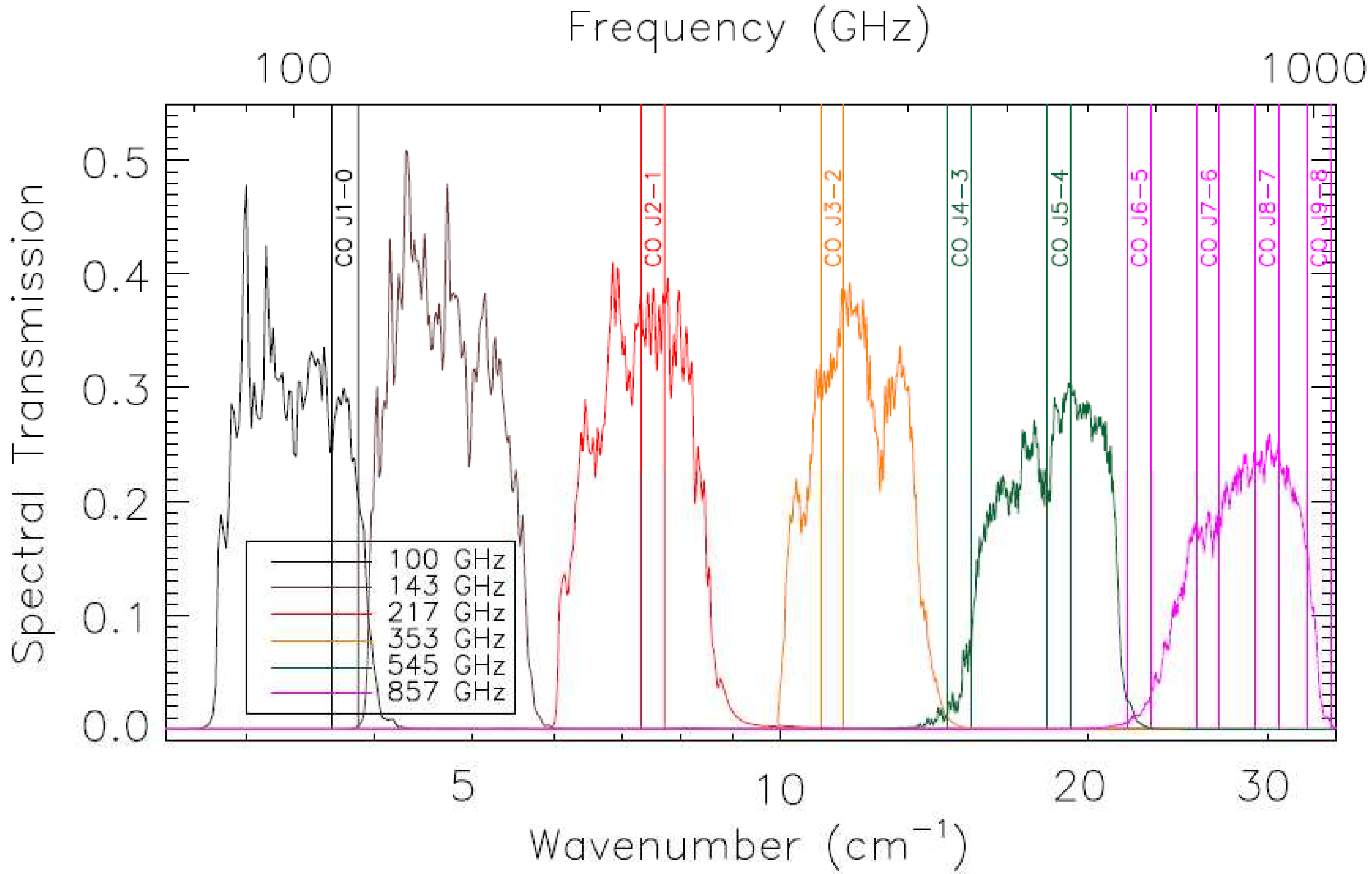

Figure 44. The average spectral response for each of the HFI frequency bands. The vertical bars represent the spectral regions of CO transitions and are interpolated by a factor of ~ 10.

Planck-LFI beams

Simulation

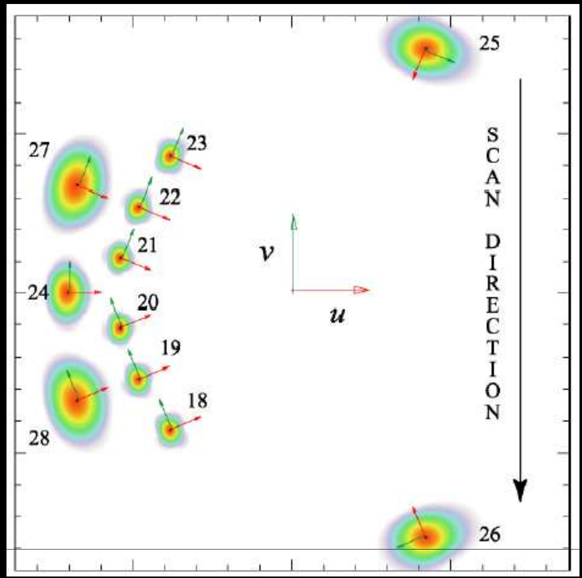

Measurement

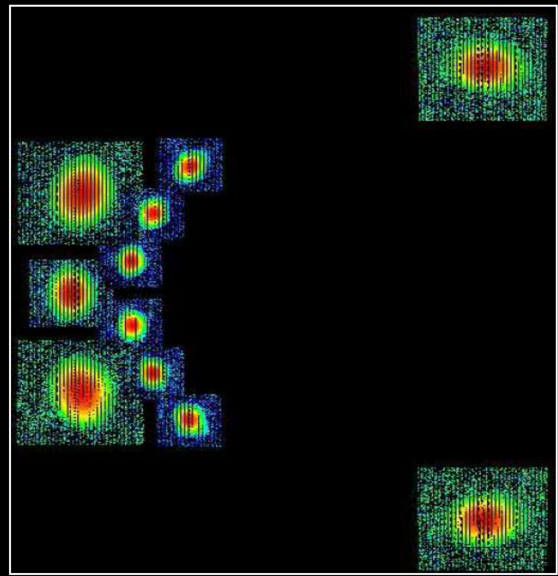

• Jupiter is by far best beam calibrator for LFI
(in LFI beams: 24 Oct – 1 Nov, 2009)

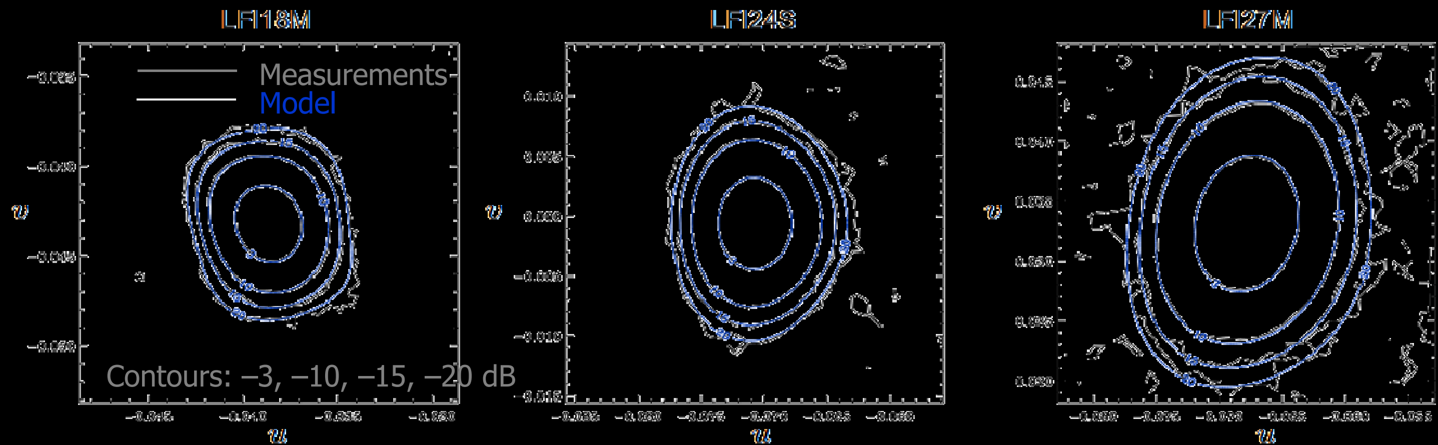

Model computation: GRASP9, PO/PTD on primary and sub-reflector

HFI Beams

(Bouchet et al 2011)

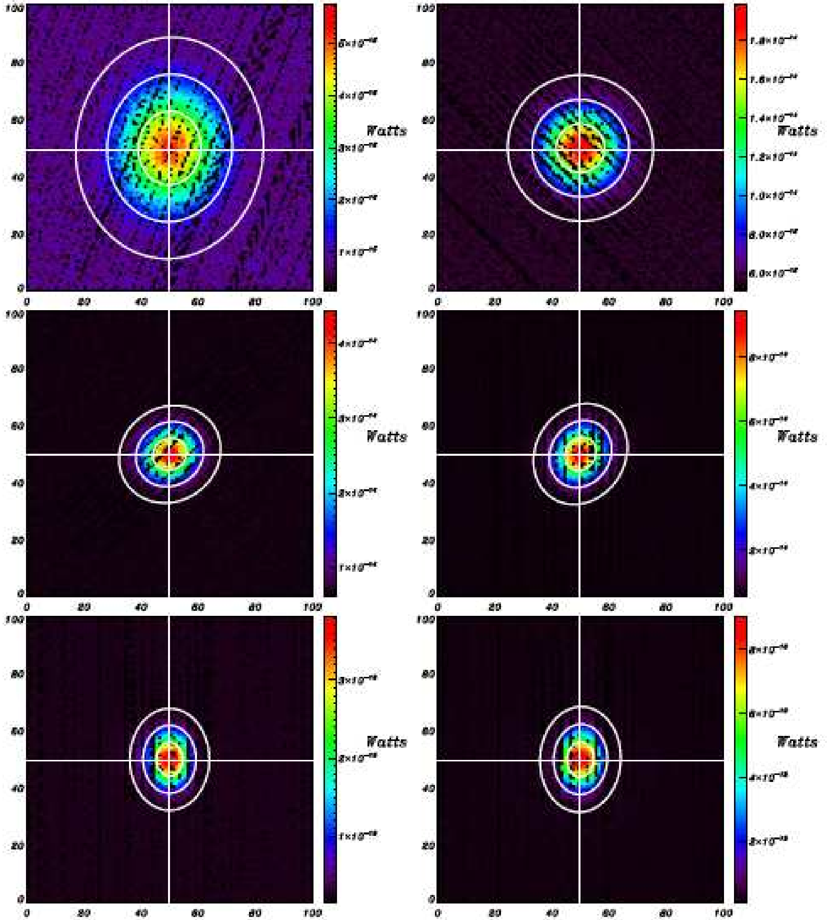

Figure 23. Maps of Mars, for the 100-4a, 143-2a, 217-6b, 353-1, 545-2 and 857-1 detectors, along with the best-fit Gaussian beam. Note that the motion of Mars is taken into account. The stripes visible here are due to the spacing between successive rings, which is a significant fraction of the FWHM of the beam.

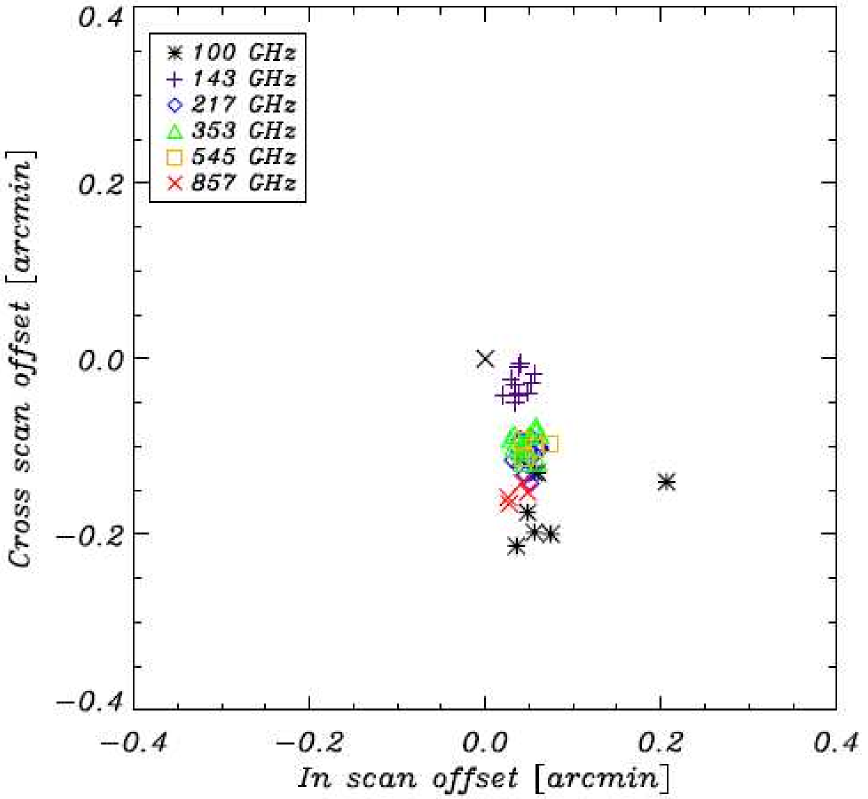

Figure 25. Detector positions on the HFI Focal Plane for the second observation of Mars with respect to the first observation of Mars.

Calibration
Current model (1% accuracy)

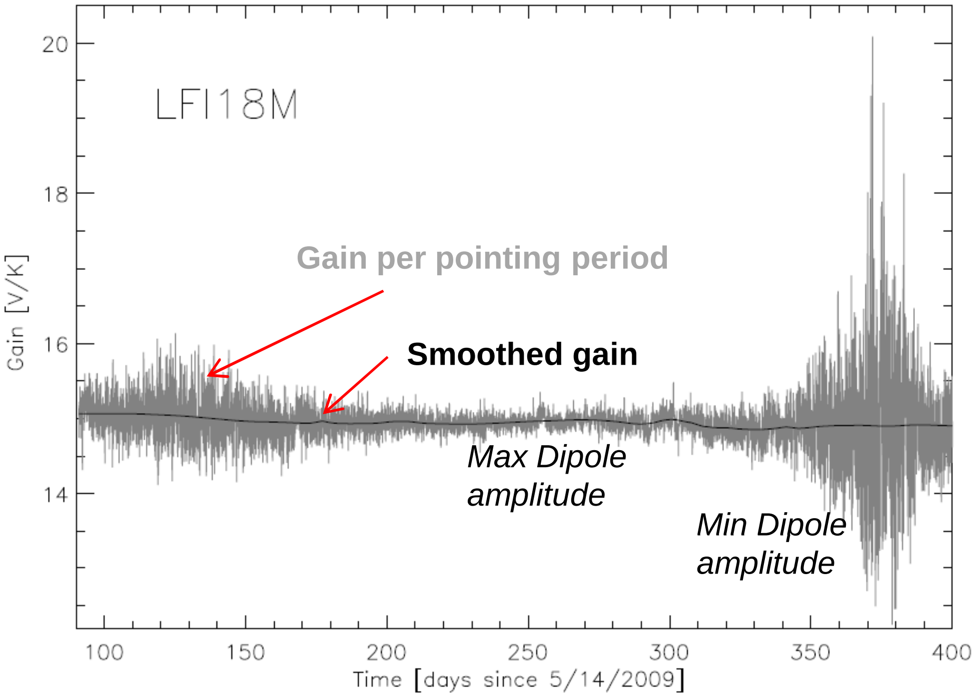

Instrument stable <0.5% in several weeks!

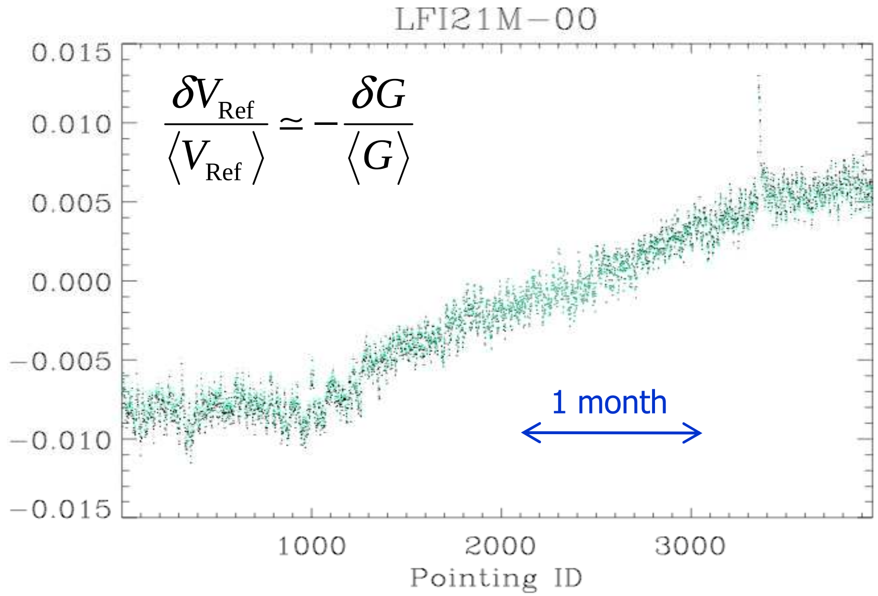

→ Running average (5 to 30 OD's)
→ Further smoothing (wavelets)

Calibration Accuracy

Absolute calibration
per frequency map: ~1% (conservative)

Relative calibration
per radiometer: ~0.3 –0.4% (typical)
per frequency map:
30 GHz: ~0.05%
44 GHz: ~0.07%
70 GHz: ~0.12%

Calibration

The next step: 0.1% accuracy

$$G(t) = G_0\left(1+\frac{\delta G(t)}{G_0}\right)$$

Absolute calibration → G_0 Relative calibration → $\frac{\delta G(t)}{G_0}$

Absolute calibration

$$\frac{\sigma_{G_0}}{G_0} = \frac{1}{<\Delta T_D + \Delta T_v>}\sqrt{\sigma^2_{\Delta T_D} + \sigma^2_{\Delta T_v} + (G_0\sigma_{\Delta V})^2} \longrightarrow \sigma_{\Delta T_v} << \sigma_{\Delta T_D} = 0.4\%$$

(FIRAS)

Use only orbital component

Relative calibration

1. Total power voltage (ref load)

$$\frac{\delta V_{\mathrm{Ref}}}{\langle V_{\mathrm{Ref}}\rangle} = \sqrt{\left(\frac{\delta(1/G)}{\langle 1/G\rangle}\right)^2 + \left(\frac{\delta T_{\mathrm{Ref}}}{\langle T_{\mathrm{Ref}} + T_{\mathrm{Noise}}\rangle}\right)^2 + \left(\frac{\delta T_{\mathrm{Noise}}}{\langle T_{\mathrm{Ref}} + T_{\mathrm{Noise}}\rangle}\right)^2}$$

$< 2\times10^{-4}$ Worst case 44GHz $< 10^{-3}$ Thermal

2. Gain model $$\frac{\delta G}{\langle G\rangle} = \eta_{BE}\,\delta T_{BE}(t) + \eta_{FE}\,\delta T_{FE}(t) + \ldots$$

3. White noise $$\frac{\delta G}{\langle G\rangle} = \frac{\delta(wn)}{\langle wn\rangle}$$

4. Multiple component model

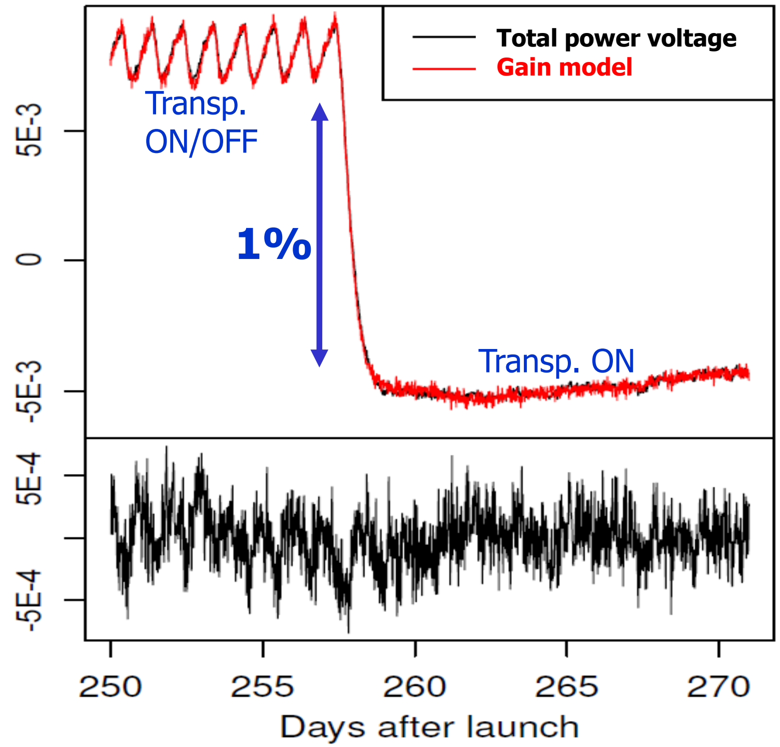

→ Optimise for polarisation analysis

Noise properties: LFI

- Noise spectra well described by 2-component (3-parameter) model (of all 22 LFI radiometers)

$$P(f) = \sigma_{\mathrm{WN}}^2 \left[1 + \left(\frac{f}{f_{\mathrm{knee}}} \right)^{\alpha} \right]$$

with slope: $\alpha \approx -1$

- Fit to noise power spectra
  (Natoli et al. 2001)
  (de Gasperis et al. 2005)

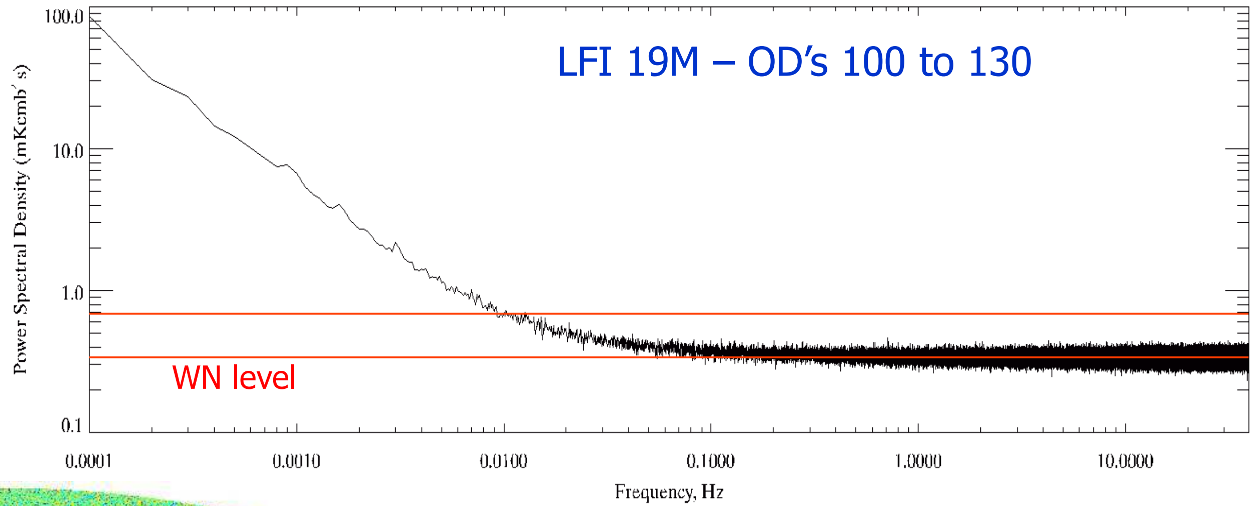

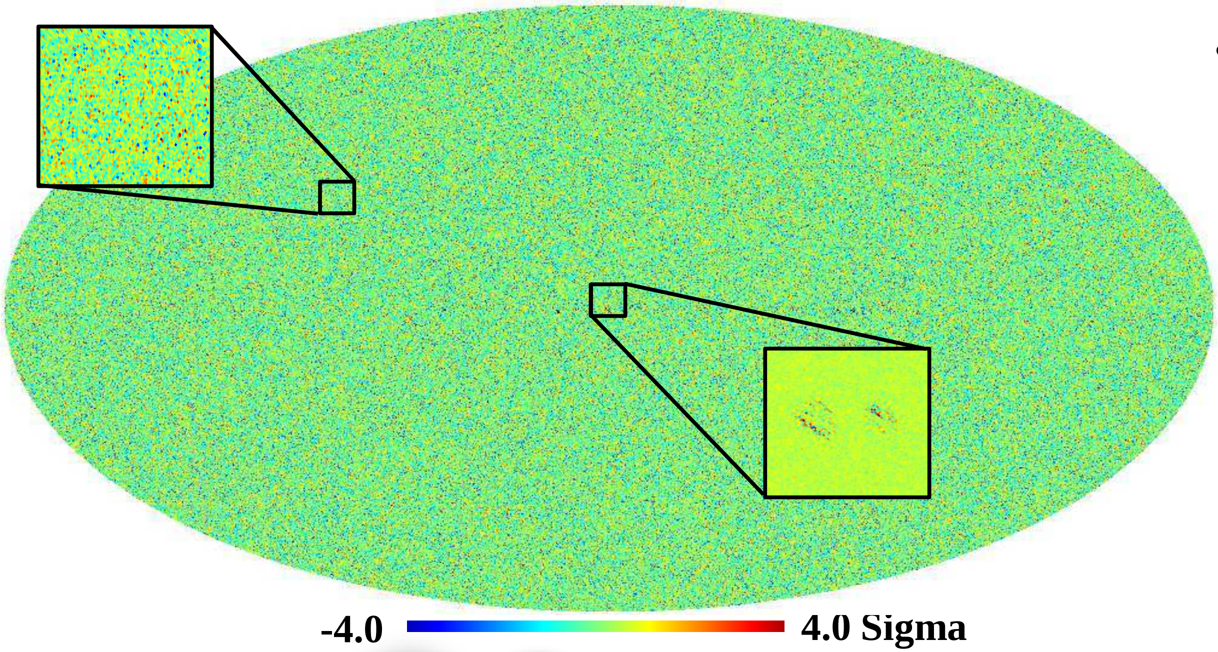

- Map from Jack-knife timelines:
  1st – 2nd half of each pointing period
  - Structure-less map
  - Small residuals on galactic plane due to beam ellipticity

Contribution of residual 1/f to white noise:
4.0% at 30 GHz
1.6% at 44 GHz
0.2% at 70 GHz

Requirement: < 12%

Noise properties: HFI

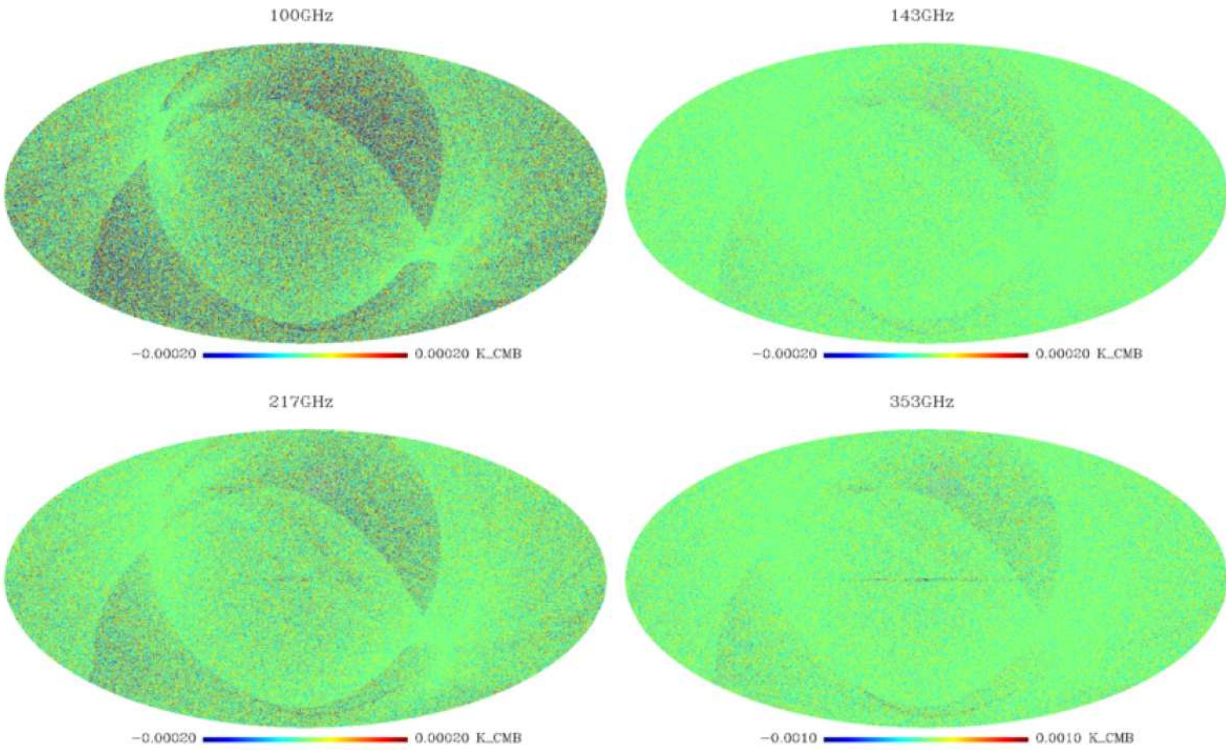

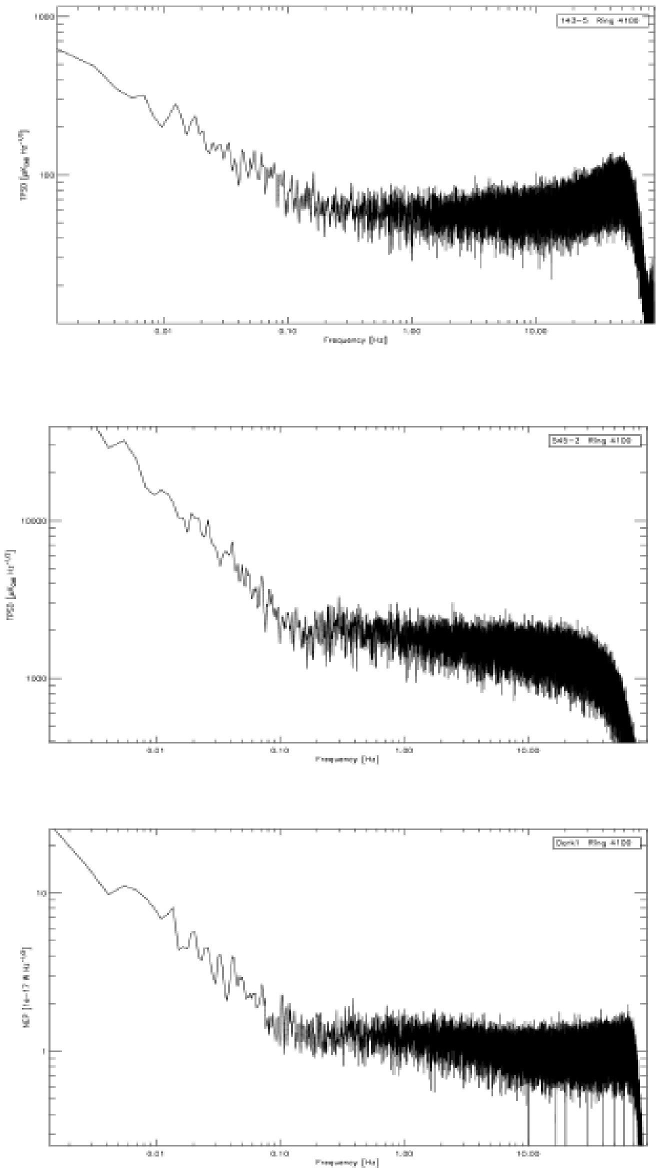

Figure 21. Examples of noise power spectra for the bolometers 143-5 (top), 545-2 (middle), and Dark1 (bottom). The first two have been calibrated in CMB temperature units, by using the calibration coefficients derived during the map making step. The last spectrum is in Watts. The central region shows a nearly white noise plateau, with a low frequency '1/f' component, and a high frequency cut-off due to the filtering of frequencies above the sampling frequency. At 143 GHz, the upturn due to the deconvolution of the (bolometer dependent) temporal transfer function is clearly seen (see details in Sect. 4.6).

Noise properties: wn component

Calibrated WN from flight data, compared to ground tests

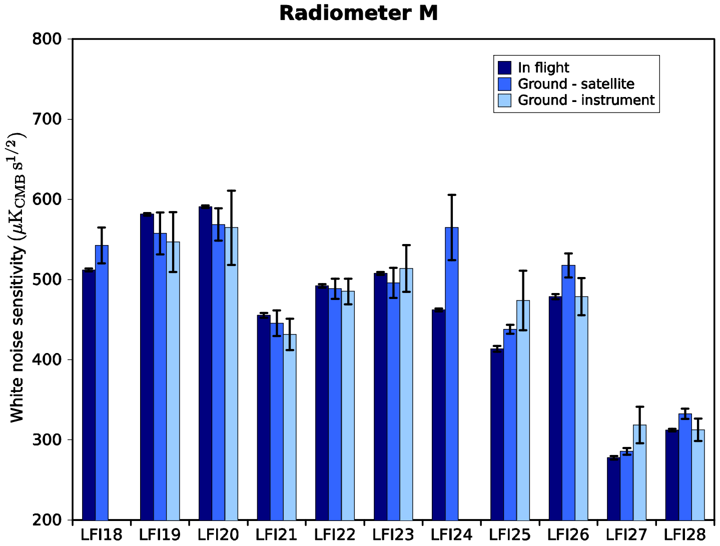

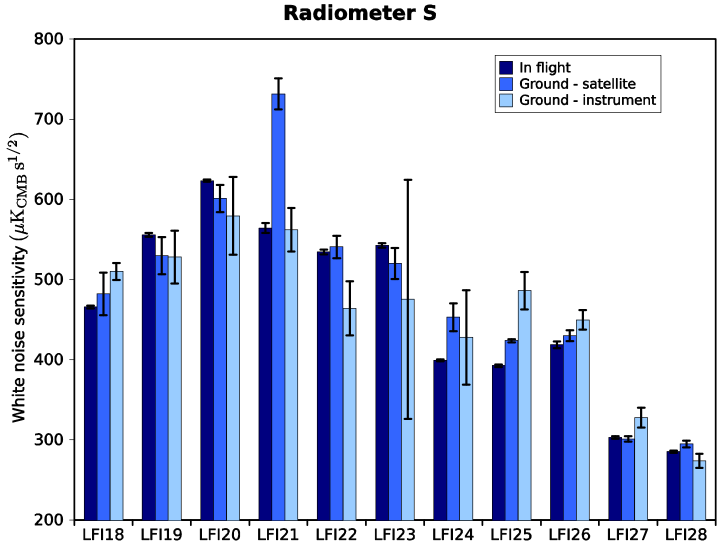

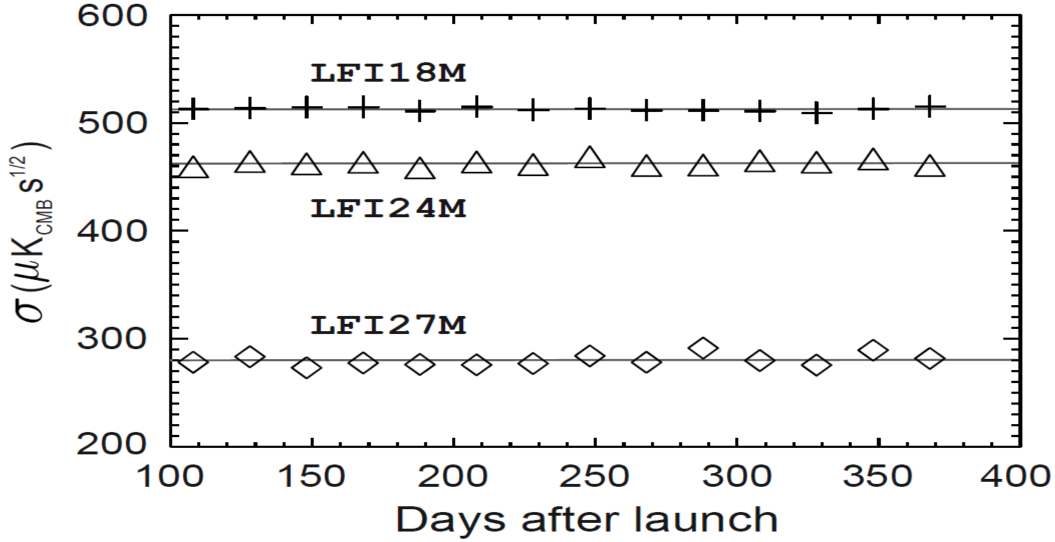

Planck-HFI: Sensitivity

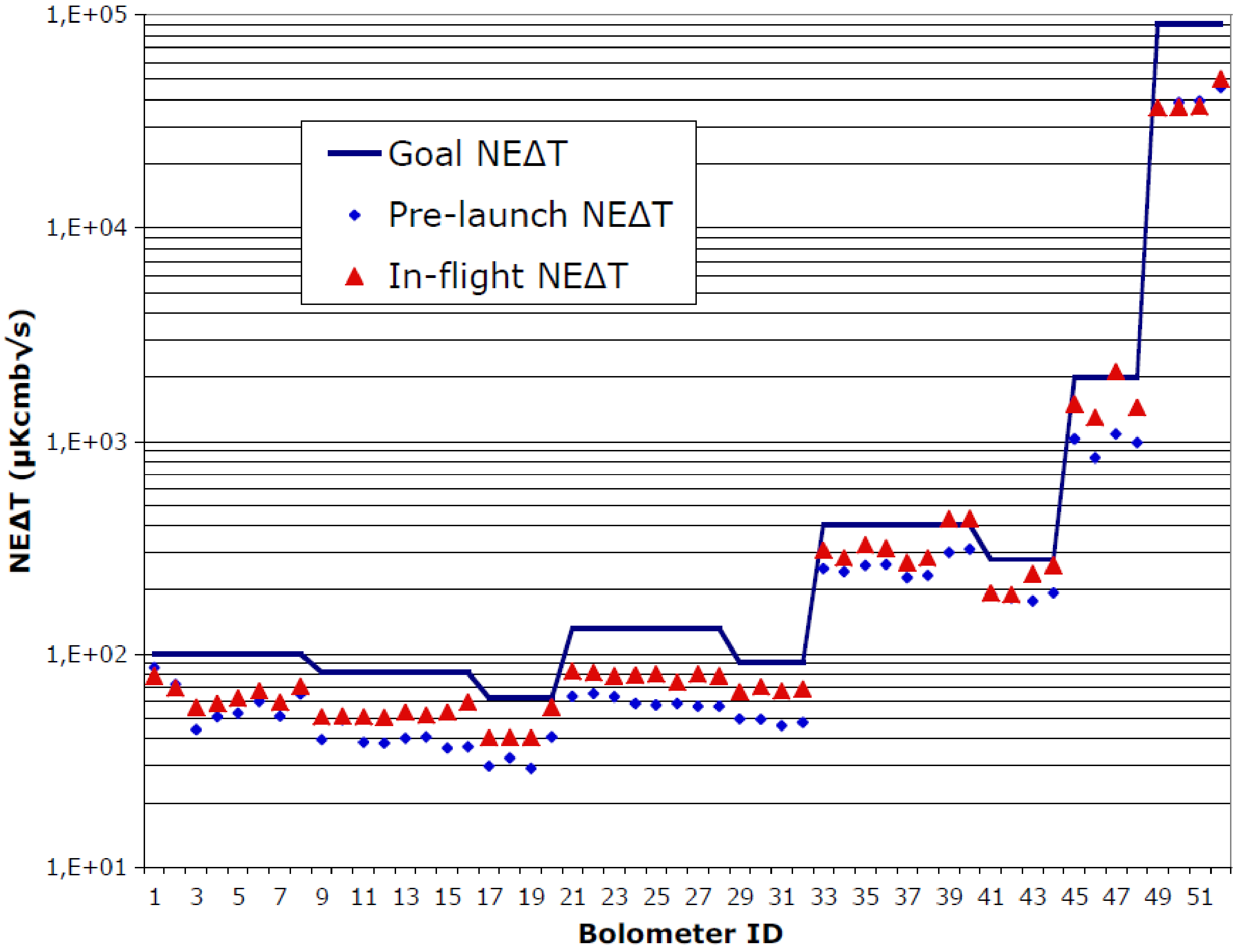

Systematic effects
Thermal effects

(Terenzi et al. 2009, Morgante et al. 2009, Tomasi et al 2009)

Temperature changes are "slow" compared to spin rate: $f_{\mathrm{Thermal}} << f_{\mathrm{Spin}} \simeq 16\ \mathrm{mHz}$

→ Efficiently removed by destriping (Madam)
→ Fast variations damped by thermal mass

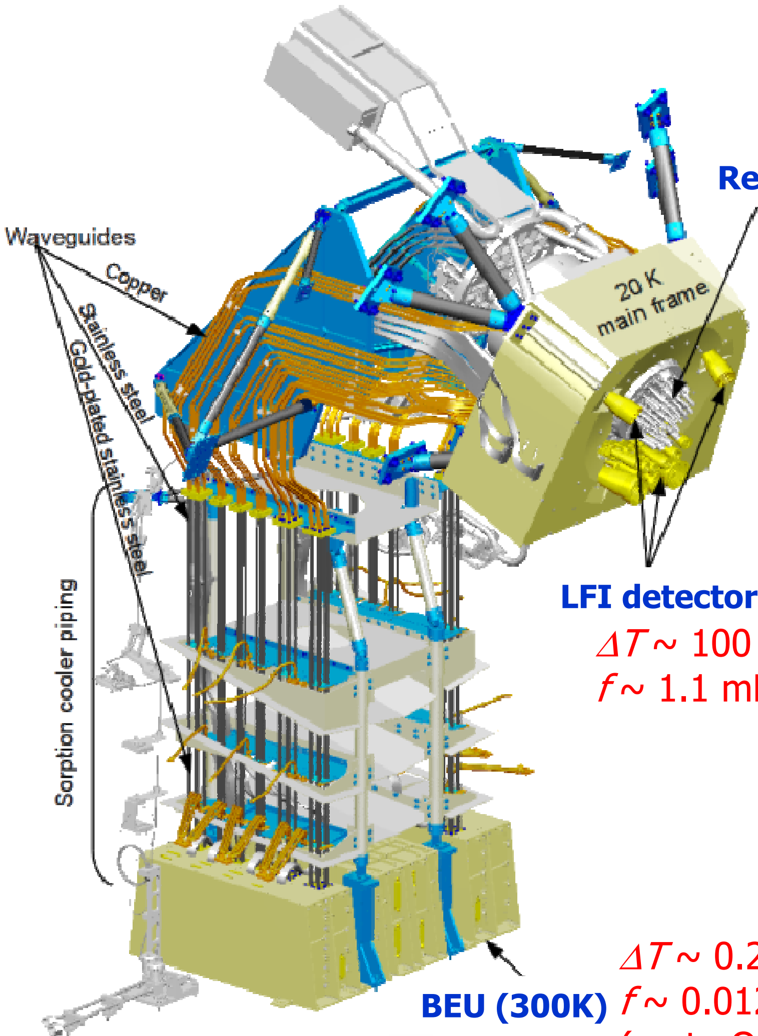

Ref Loads (4K)
$\Delta T \sim$ 0.9 mK
$f \sim$ 1.1 mHz (15min)
$f \sim$ 0.2 mHz (90min)

LFI detectors (20K)
$\Delta T \sim$ 100 mK
$f \sim$ 1.1 mHz (15min)

BEU (300K)
$\Delta T \sim$ 0.2 K
$f \sim$ 0.012 mHz (24h)
(up to OD 258)

Except for 4K loads, fluctuations are common mode
→ Differencing drastically reduces impact

How can we quantify the effect?

- Start with representative Temperature Sensor(s) data streams
- Apply thermal transfer functions (get physical temperature at sensitive component)
- Apply radiometric transfer function (get fluctuation in antenna temperature)
- Re-sample and build differenced time ordered data
- Build destriped maps (with *Madam*)

Thermal systematic effects
Back-end fluctuations (300K)

LFI back-end
Temperature Sensors
(around OD258)

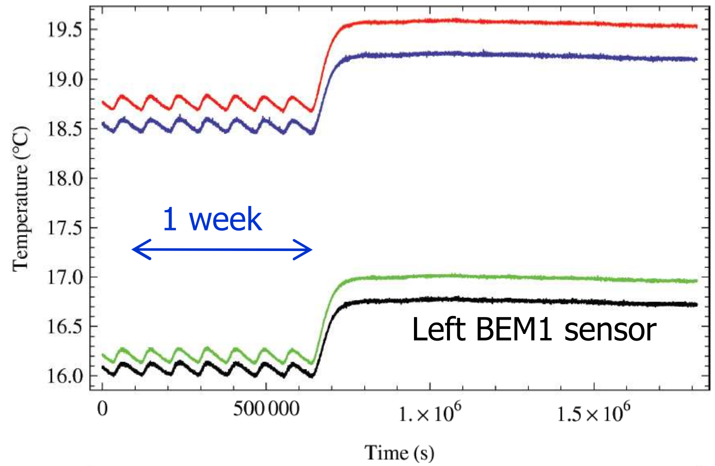

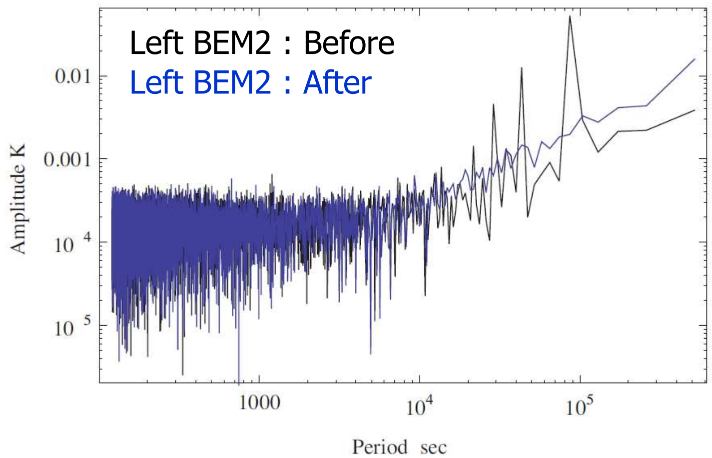

(Planck Collaboration 2011)

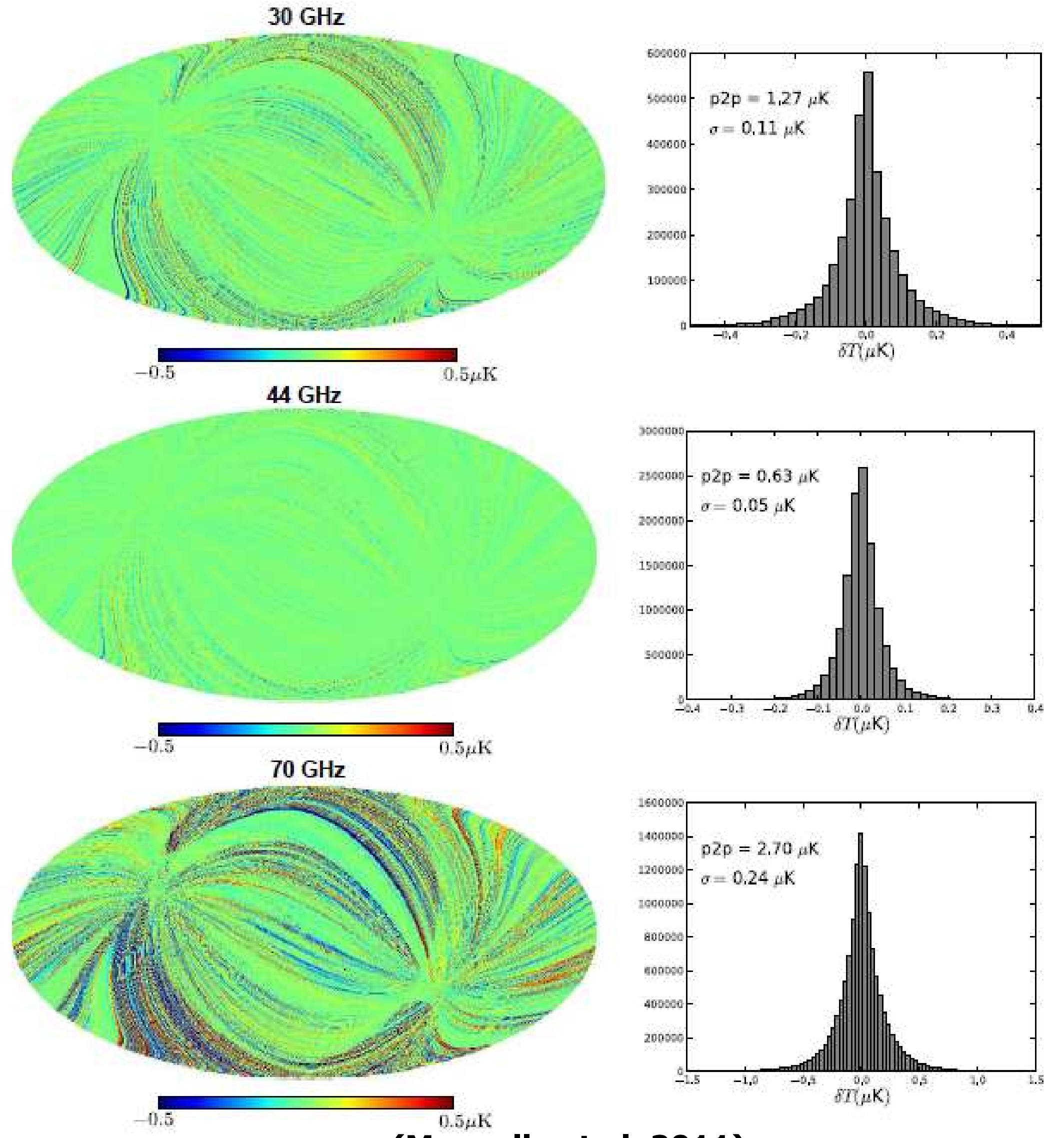

(Mennella et al. 2011)

Thermal systematic effects
Front-end fluctuations (20K)

LFI focal plane
Temperature Sensors
(24h, Oct 09)

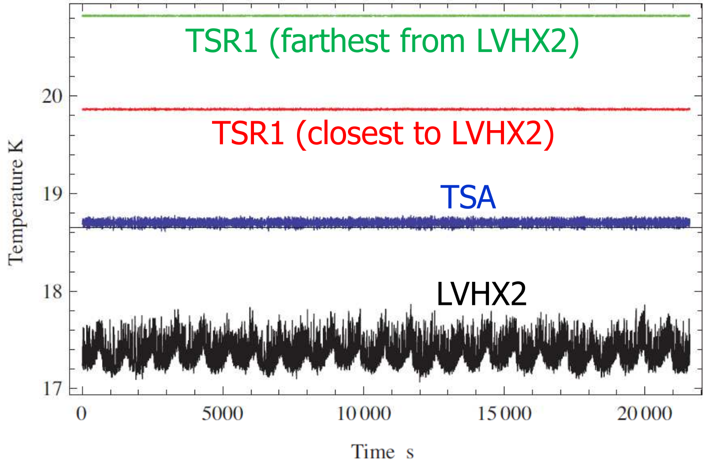

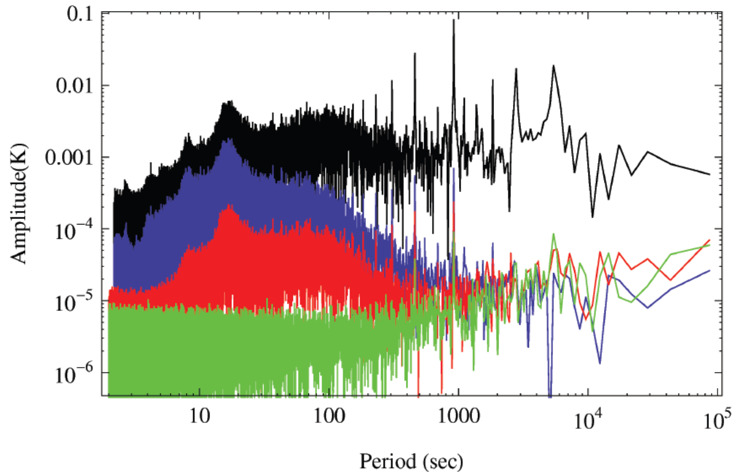

(Planck Collaboration 2011)

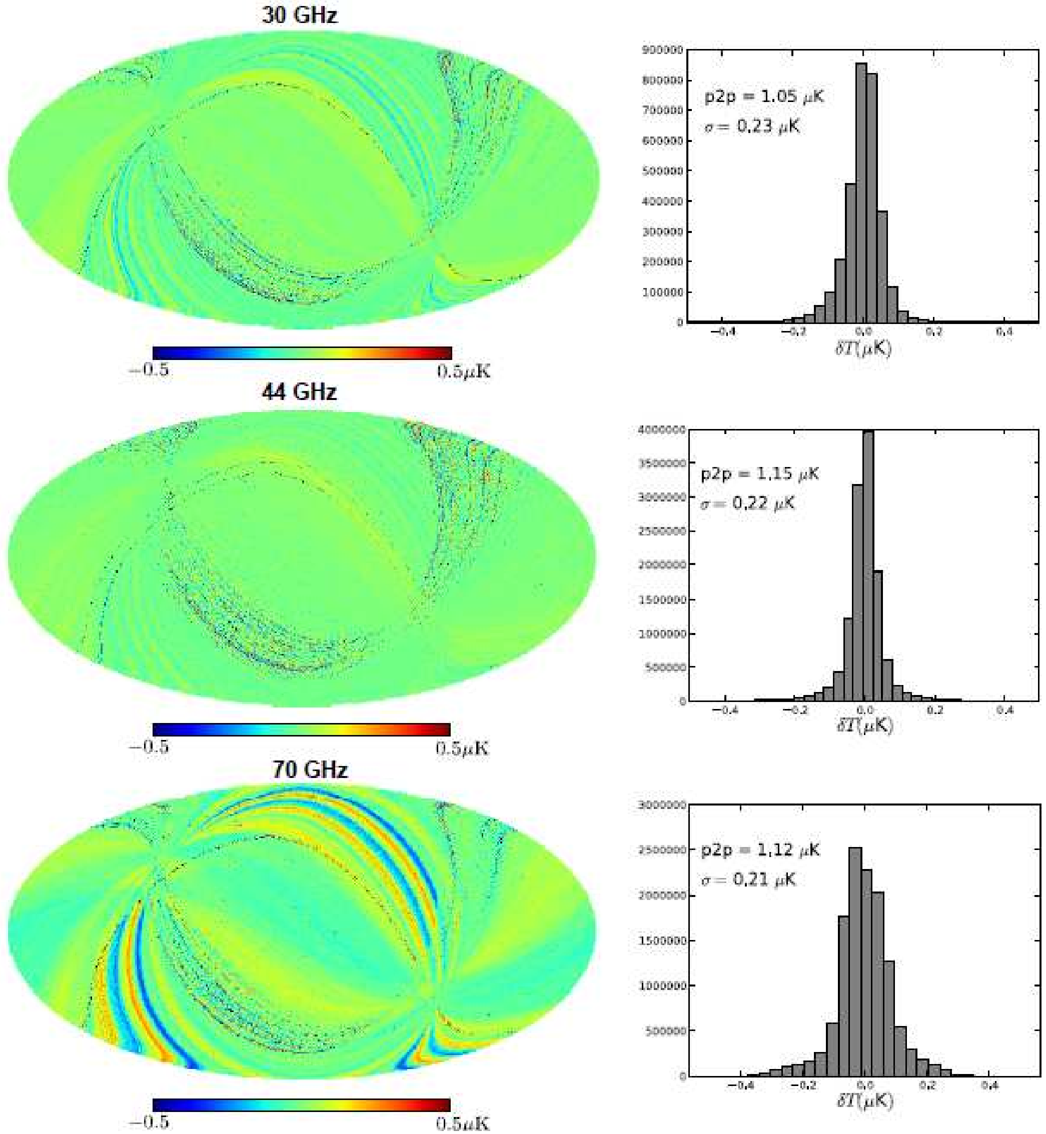

(Mennella et al. 2011)

Thermal systematic effects
Reference Loads fluctuations (4K)

HFI outer shield
Temperature Sensors
(24h, Oct 09)

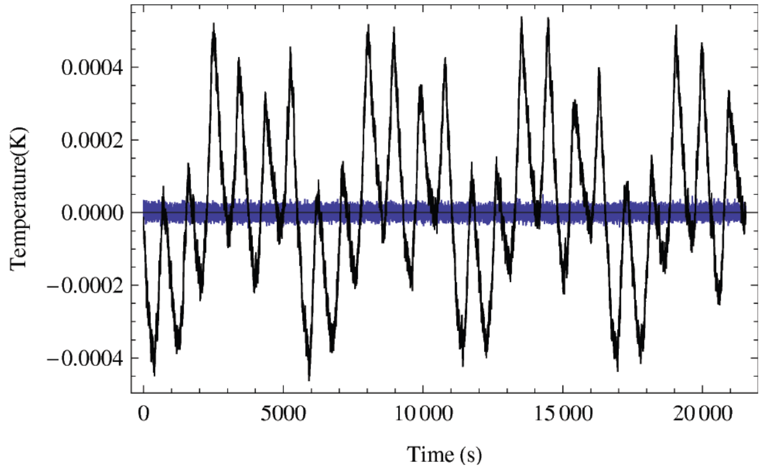

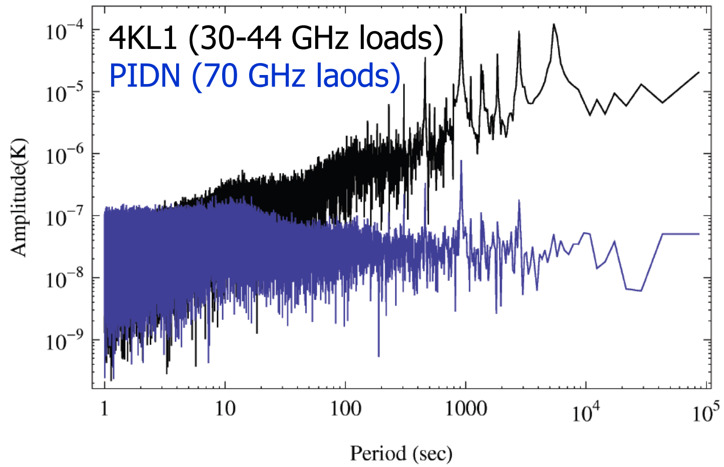

(Planck Collaboration 2011)

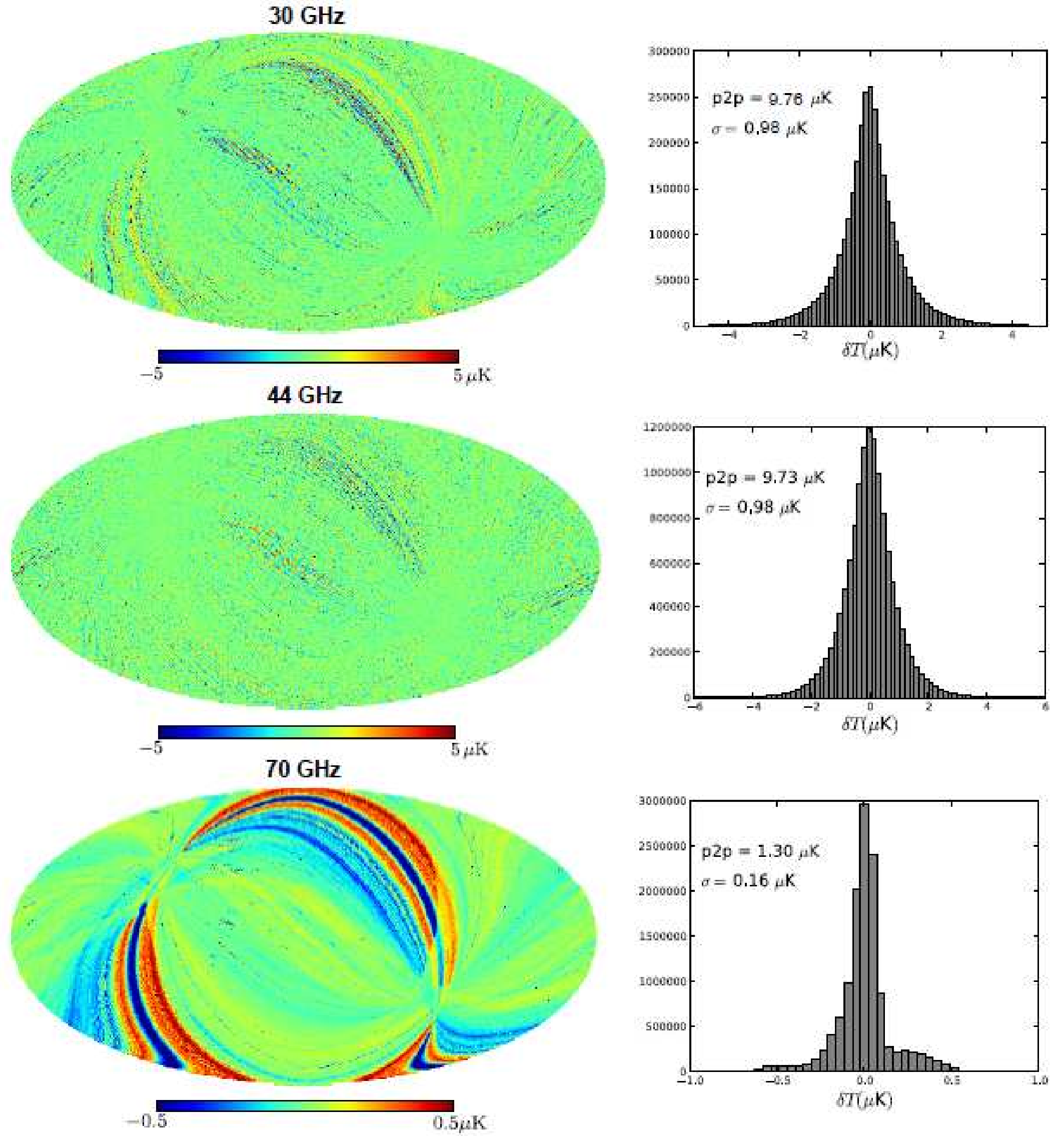

(Mennella et al. 2011)

Systematic effects

Summary

Contribution of LFI systematics to WN power spectrum: $\rho_\ell \equiv C_\ell^{\rm syst} / C_\ell^{\rm noise}$

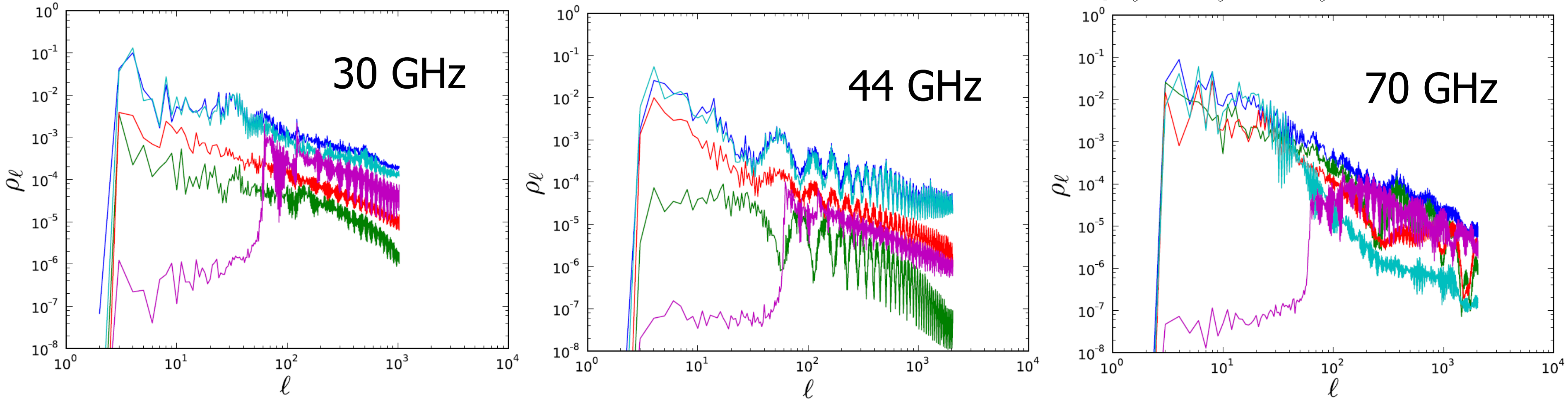

Total systematic effect
Back-end temperature
Front-end temperature
4K temperature
Spikes

	30 GHz		44 GHz		70 GHz	
	p-p	r.m.s.	p-p	r.m.s.	p-p	r.m.s.
1-Hz spikes	4.00	0.45	1.51	0.15	2.56	0.30
BEM T fluct.	1.27	0.11	0.63	0.05	2.70	0.24
FEM T fluct.	1.05	0.23	1.15	0.22	1.12	0.21
4 K T fluct.	9.76	0.98	9.73	0.98	1.30	0.16
Total	10.92	1.10	9.73	0.98	4.28	0.45

NB: per sample (worst case)

- Impact in power spectrum is 1–3 orders of magnitude below WN level (of order ~1μK)
- Only removal in pipeline (to date): 1-Hz spikes at 44GHz
- Dominant effects:
  - → **30 and 44 GHz**: 4K loads fluctuations
  - → **70 GHz**: back-end fluctuations (large scale); frequency spikes (small scales)

Planck Focal Plane

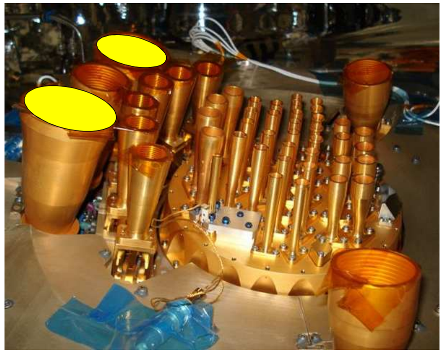

Full sky maps of foreground emission
after 1 year mission

Planck-LFI – 30 GHz Channel

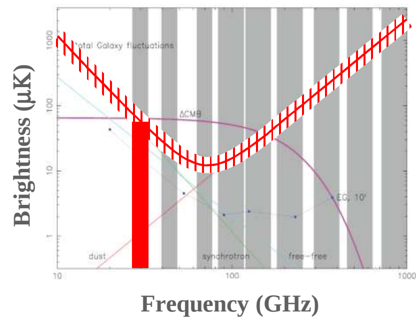

Maps of galactic and extragaactic emission
(CMB removed)

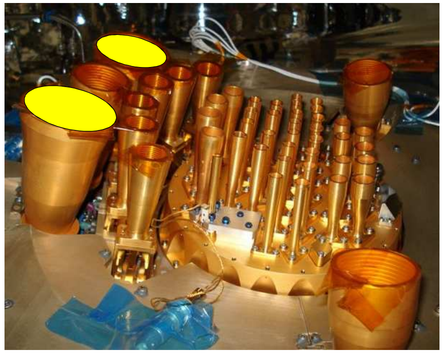

Full sky maps of foreground emission
after 1 year mission

Planck-LFI – 30 GHz Channel

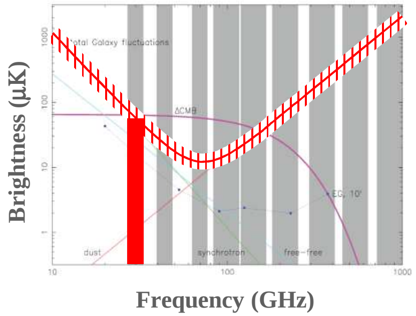

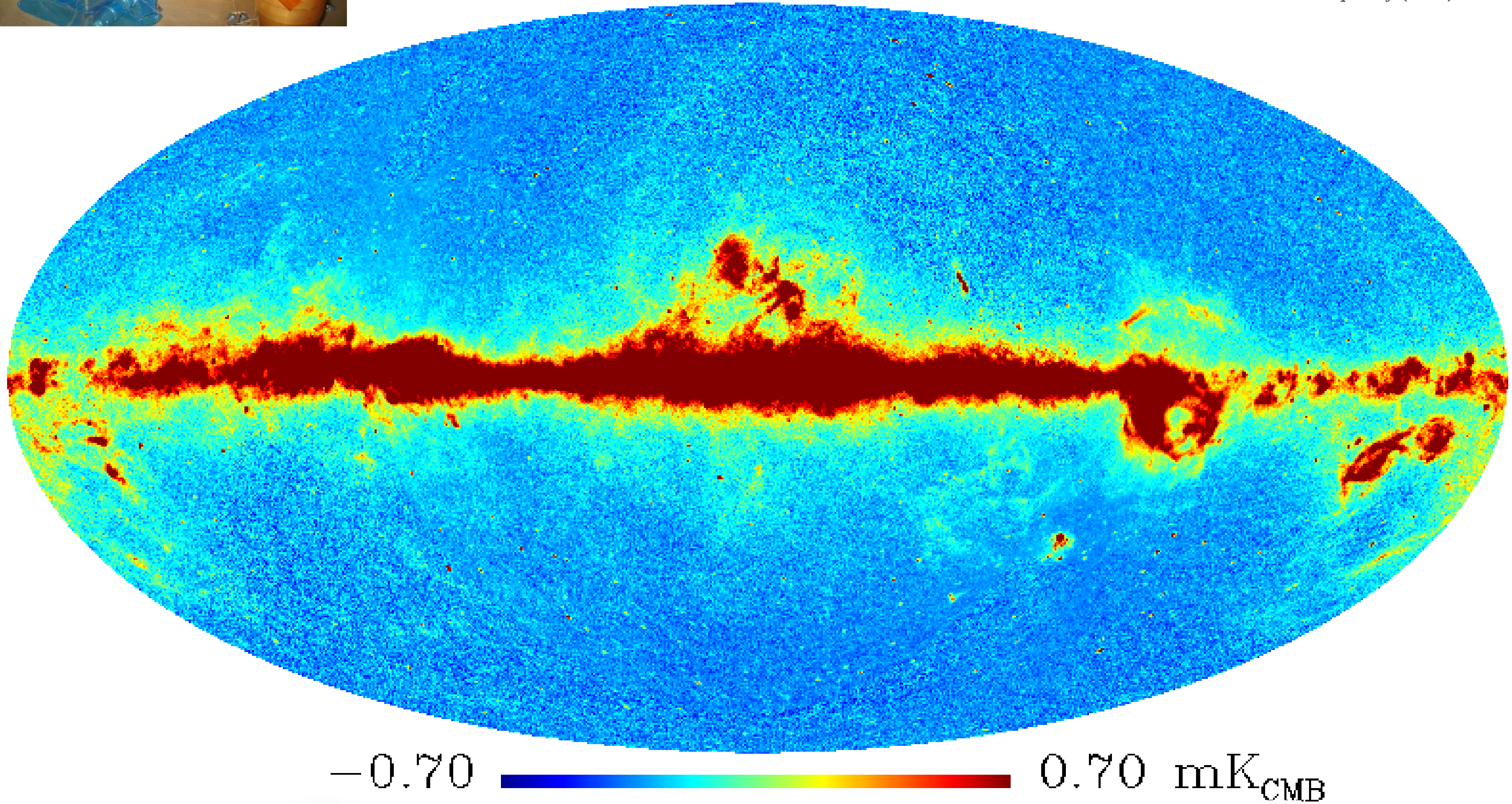

Full sky maps of foreground emission
after 1 year mission

Planck-LFI – 44 GHz Channel

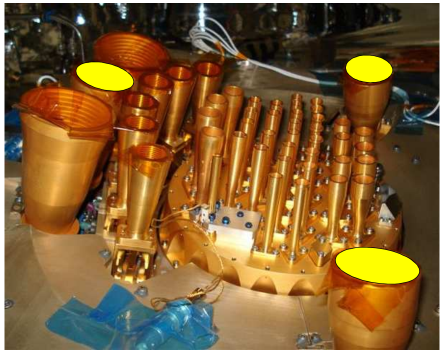

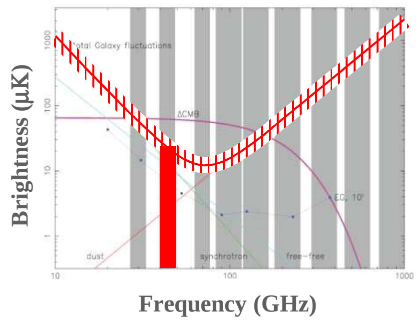

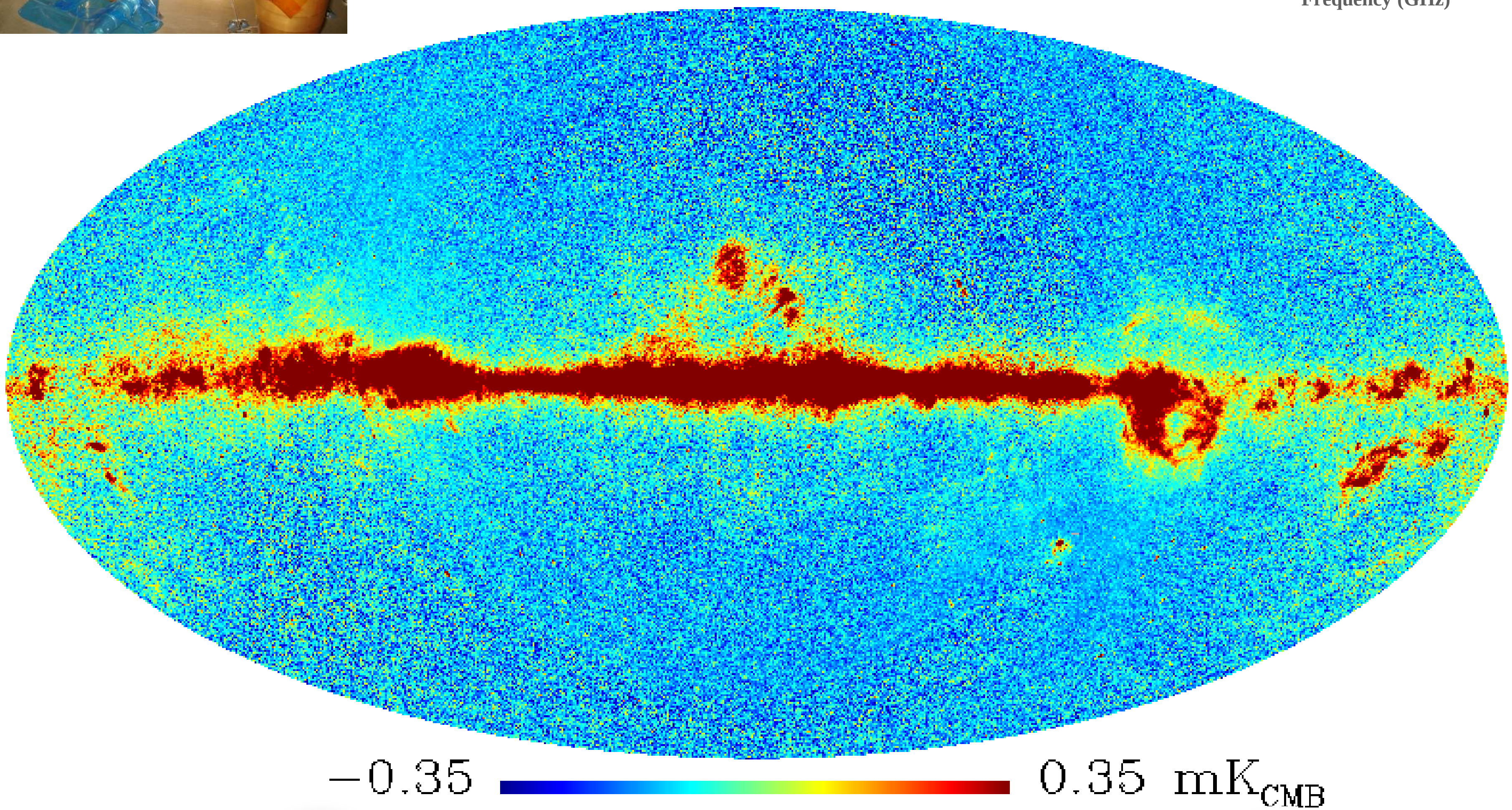

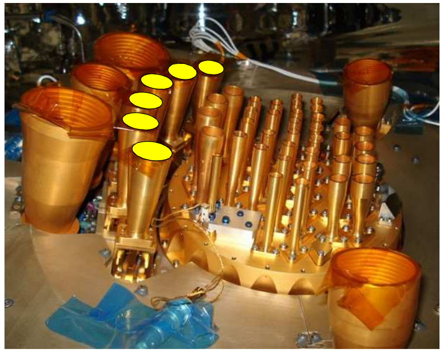

Full sky maps of foreground emission after 1 year mission

Planck-LFI – 70 GHz Channel

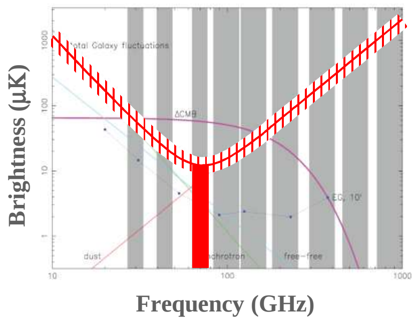

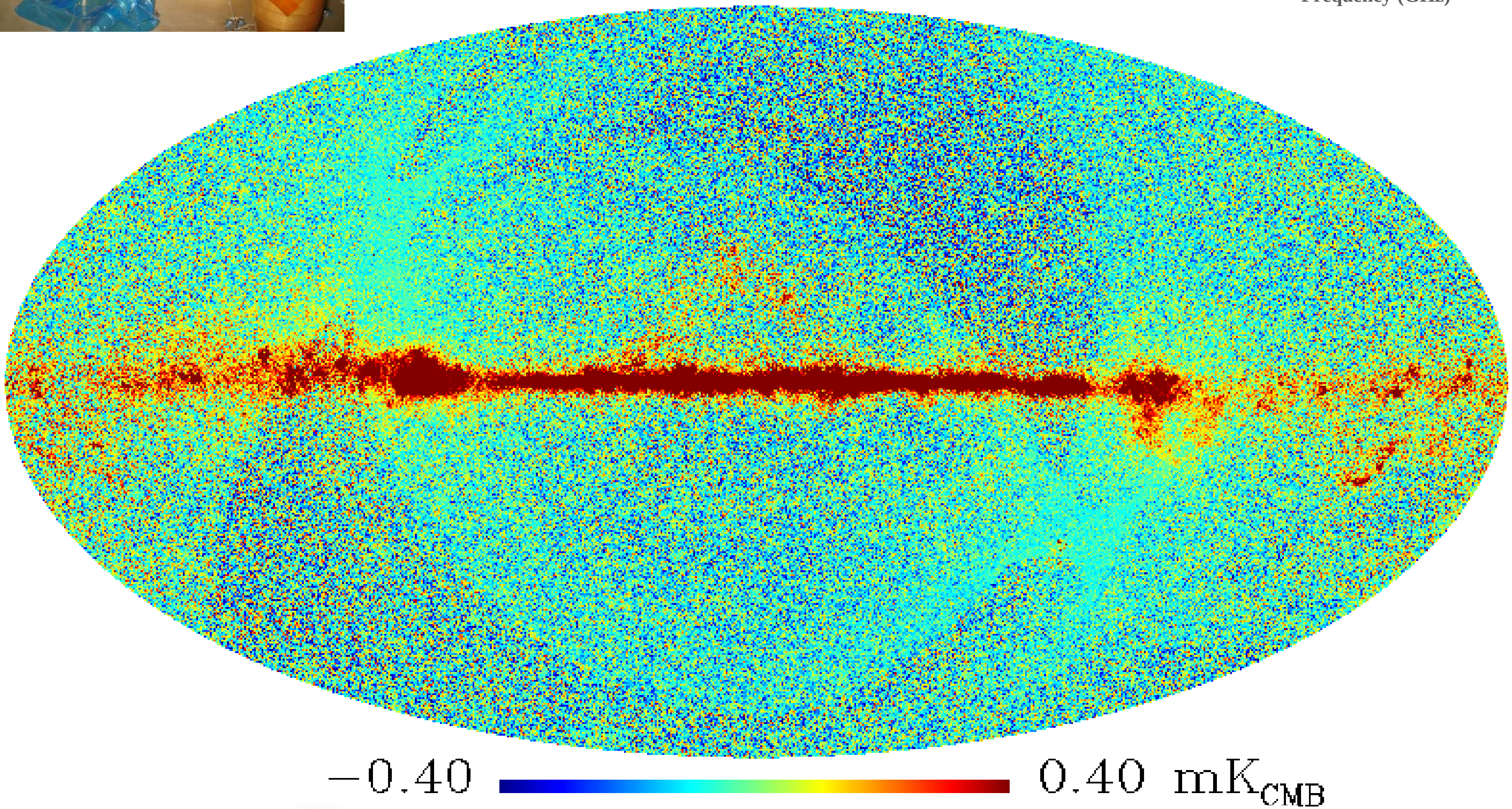

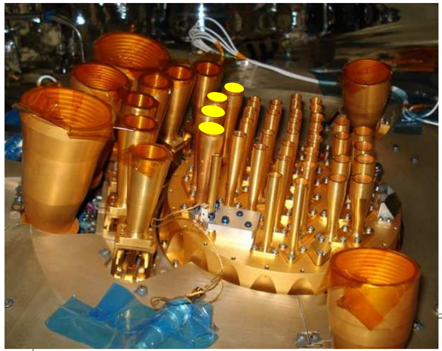

Full sky maps of foreground emission
after 1 year mission

Planck-HFI – 100 GHz Channel

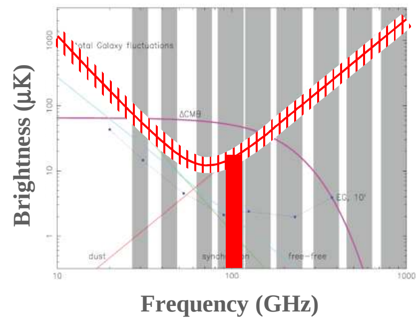

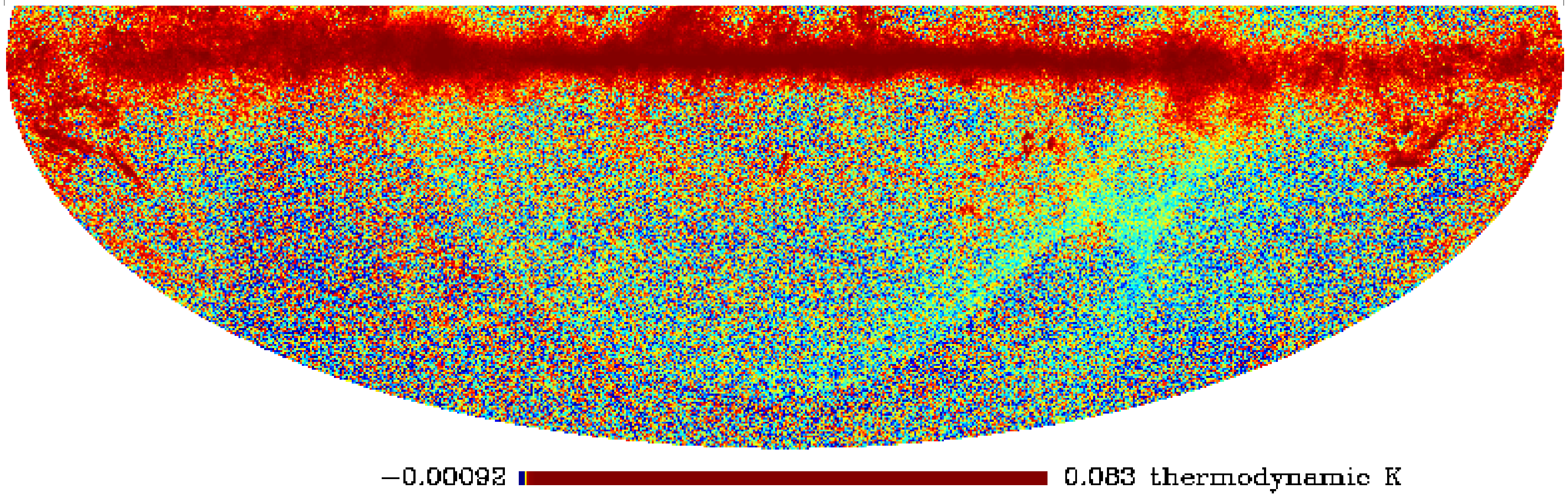

Full sky maps of foreground emission
after 1 year mission

Planck-HFI – 143 GHz Channel

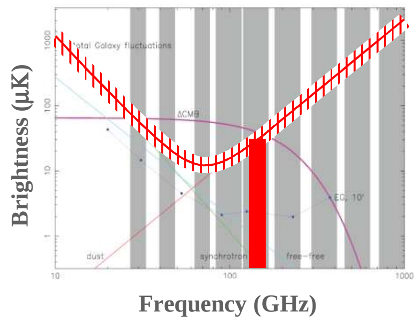

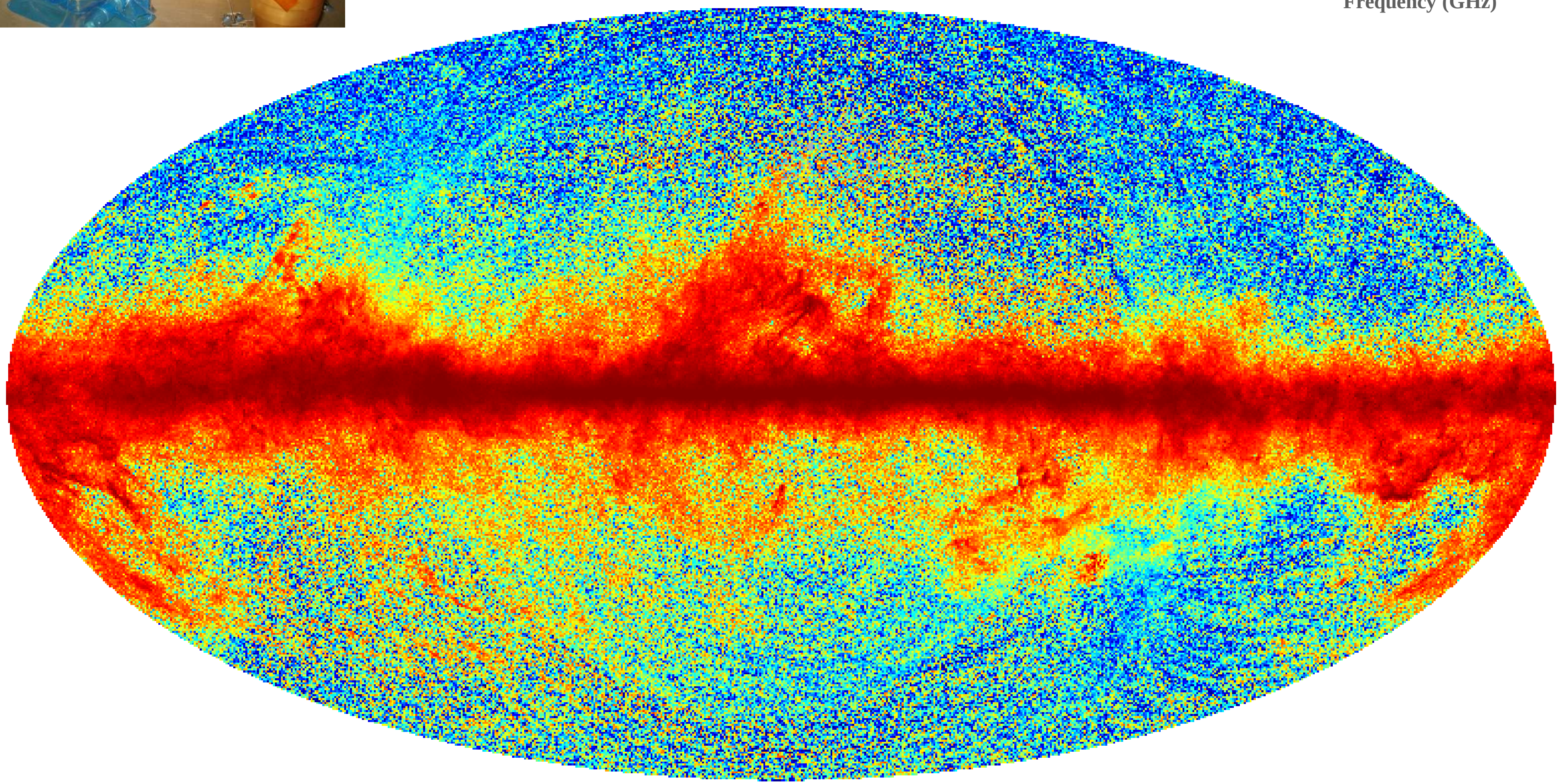

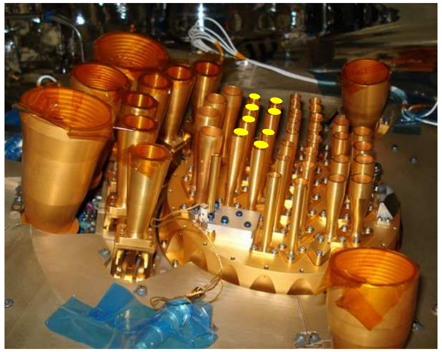

Full sky maps of foreground emission after 1 year mission

Planck-HFI – 217 GHz Channel

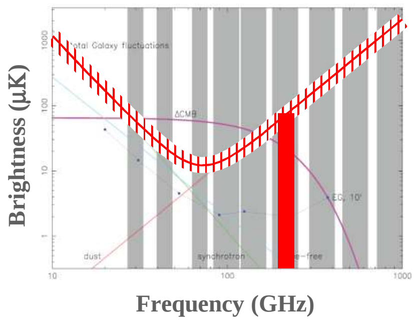

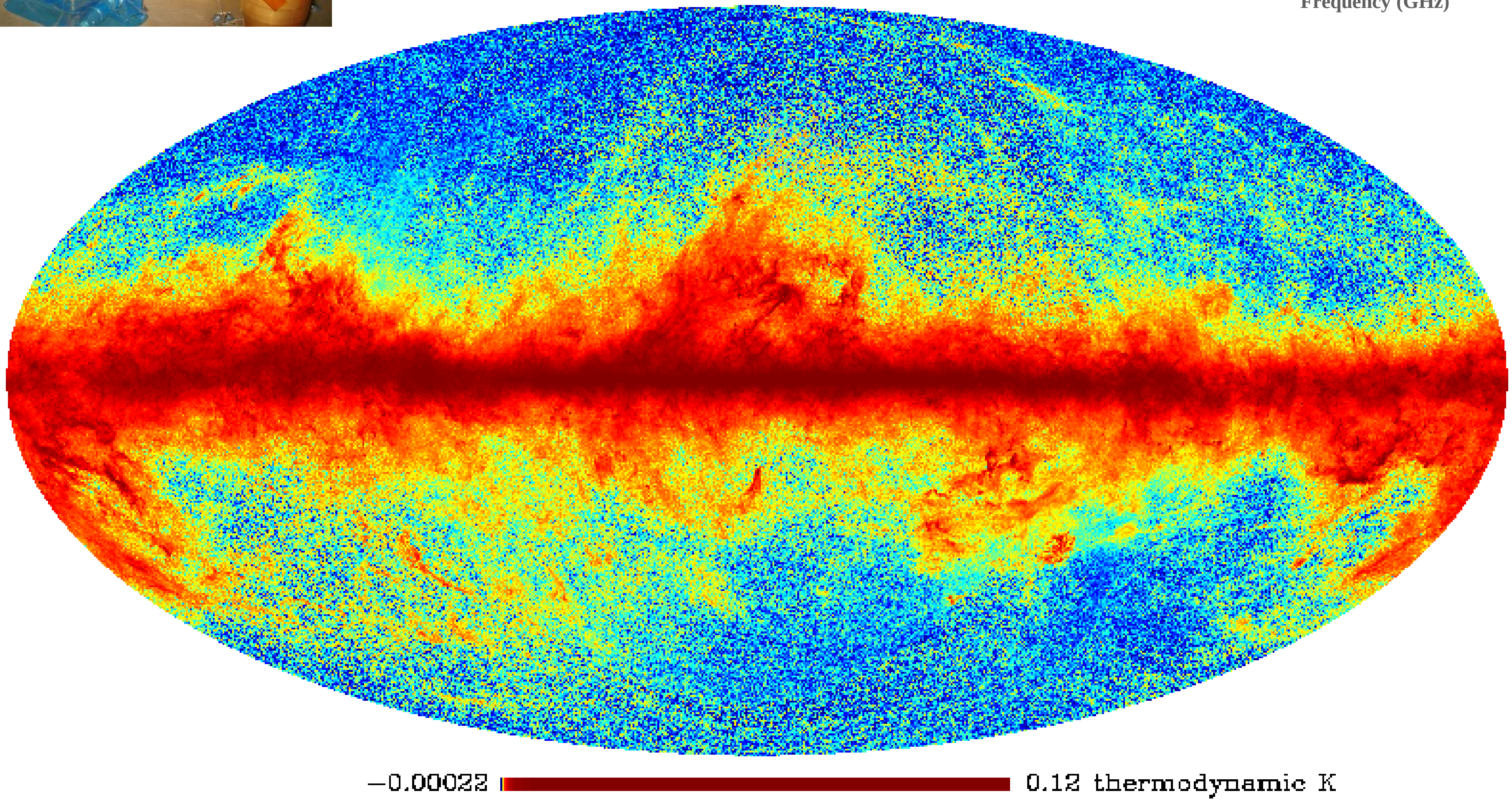

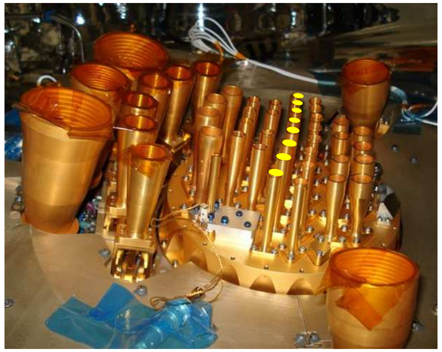

Full sky maps of foreground emission after 1 year mission

Planck-HFI – 353 GHz Channel

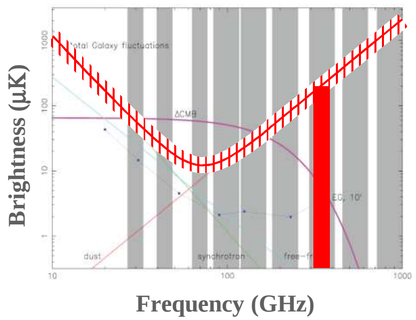

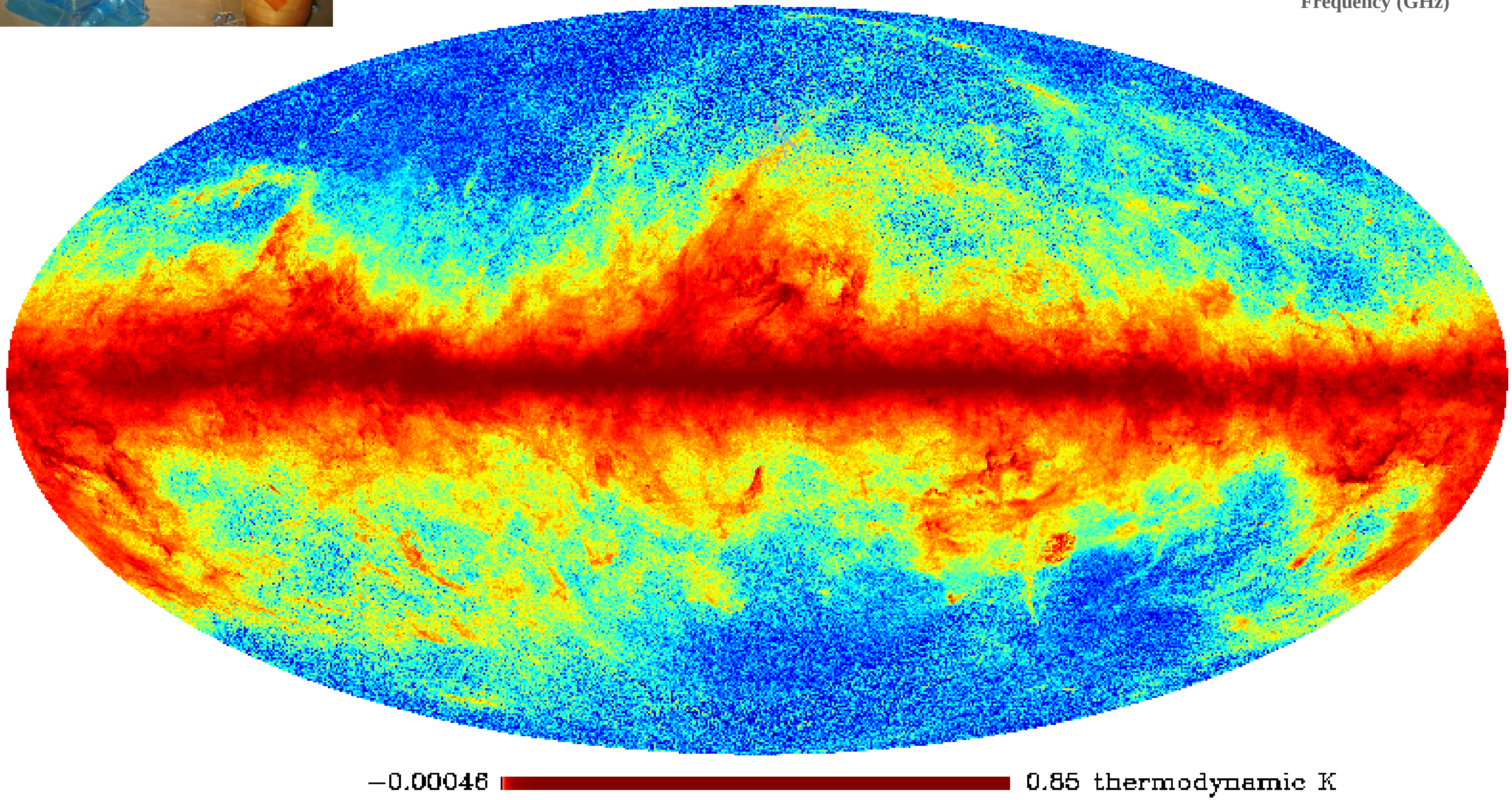

Full sky maps of foreground emission after 1 year mission

Planck-HFI – 545 GHz Channel

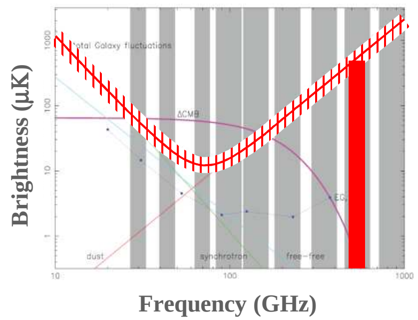

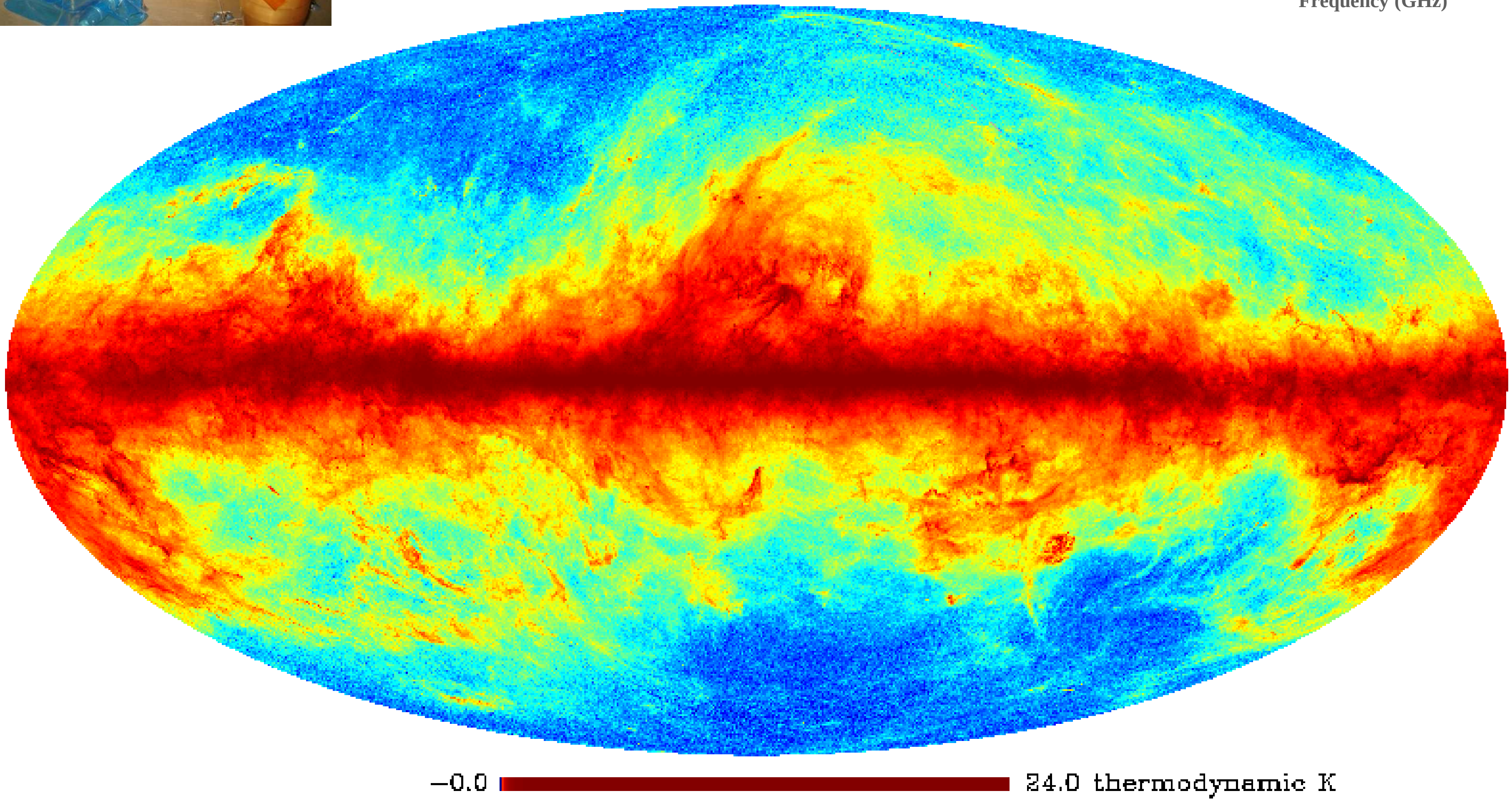

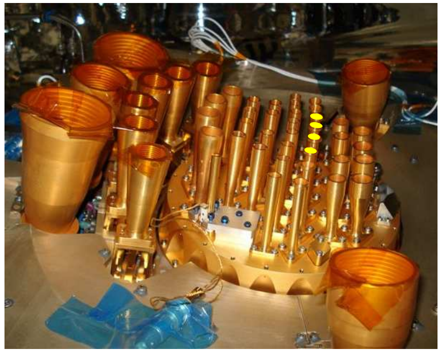

Full sky maps of foreground emission
after 1 year mission

Planck-HFI – 857 GHz Channel

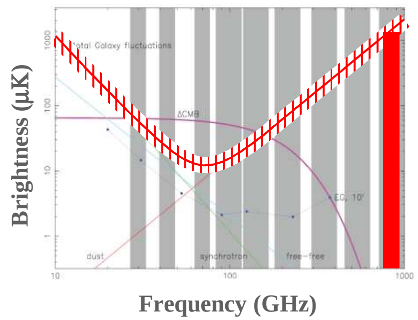

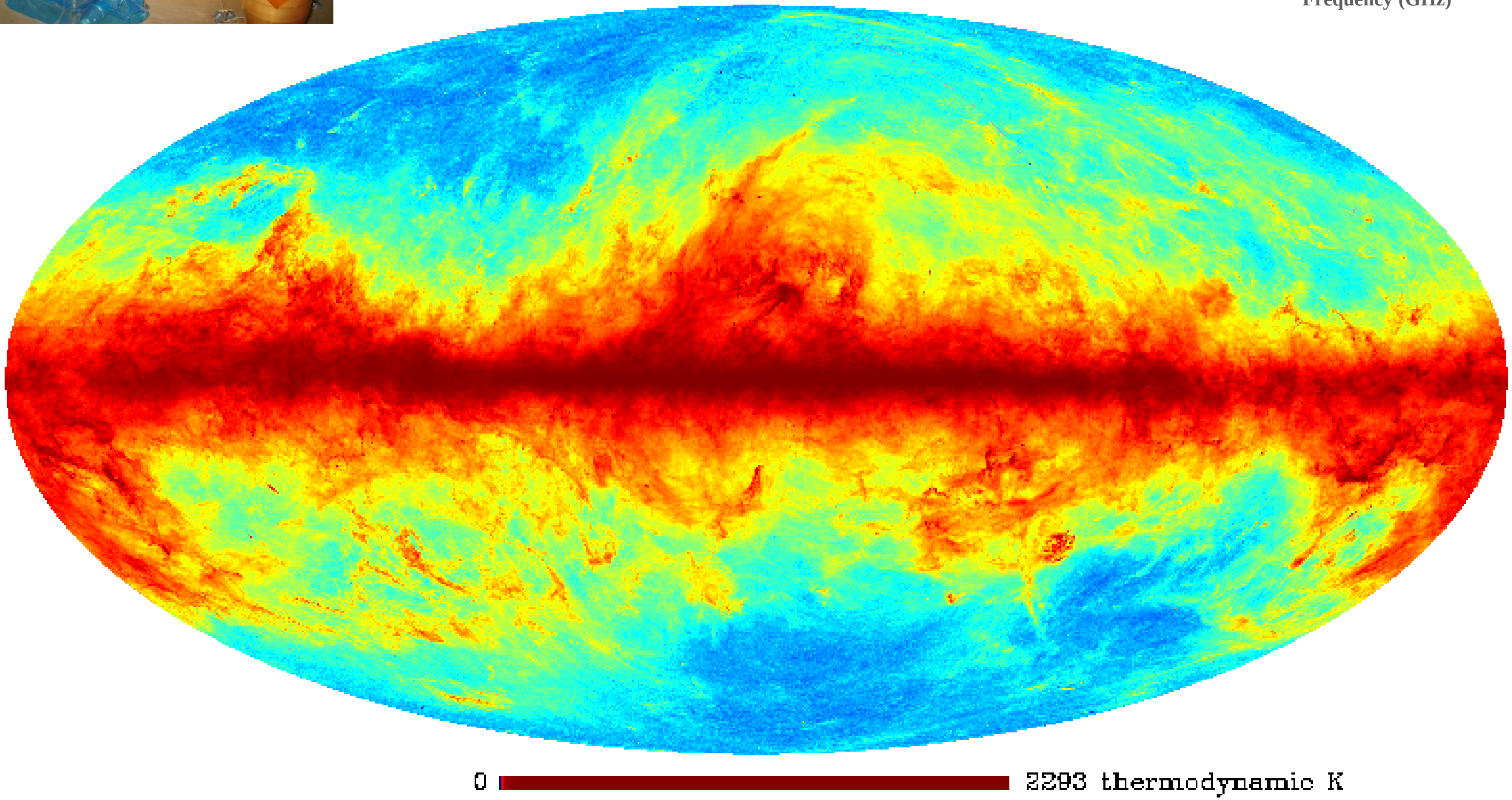

PLANCK

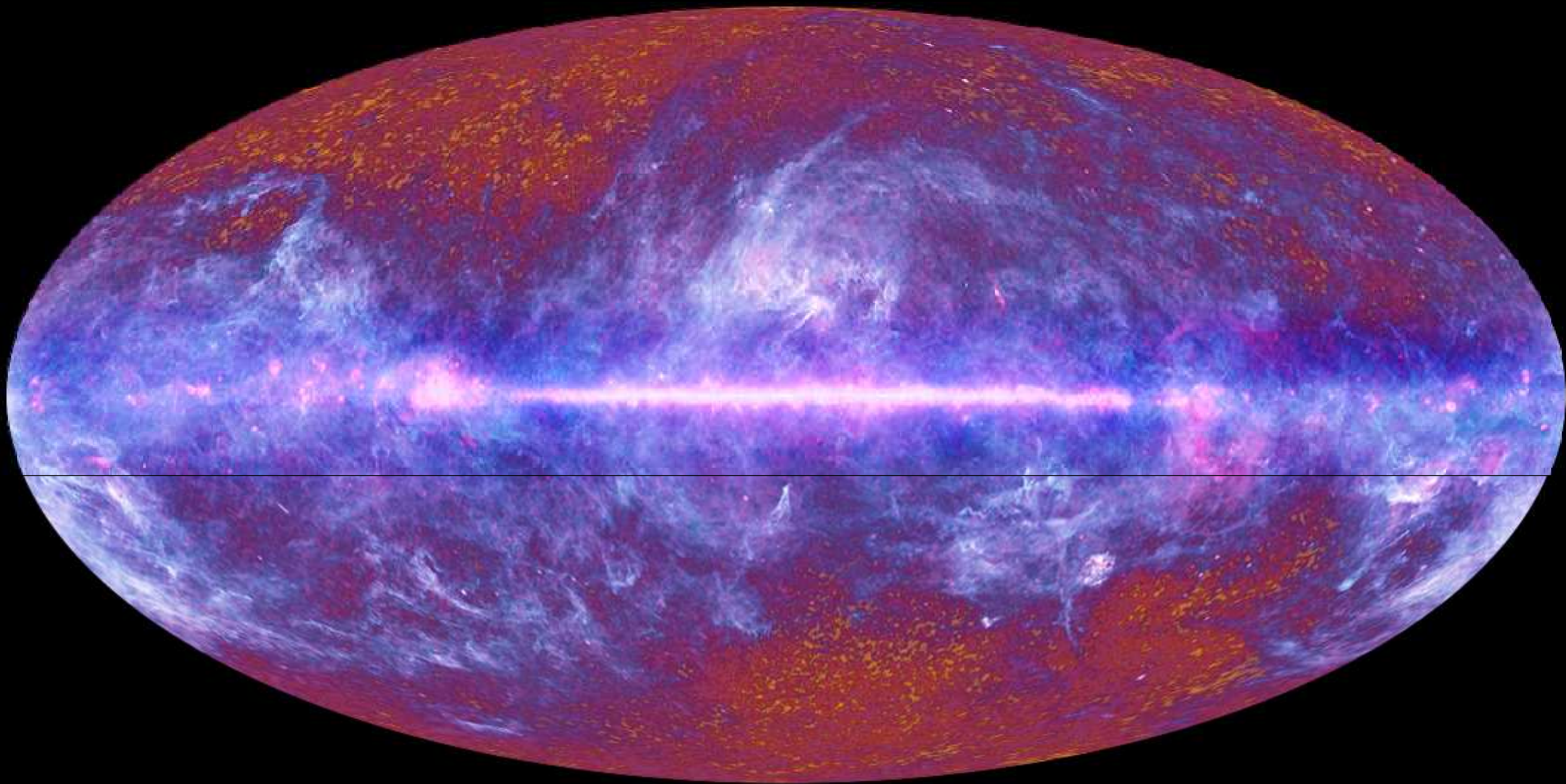

«Those who have reached the stage of no longer being able to marvel at anything simply show that they have lost the art of reasoning and reflection.»

Max Planck

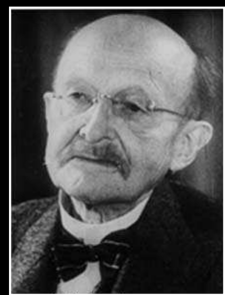

esa PLANCK

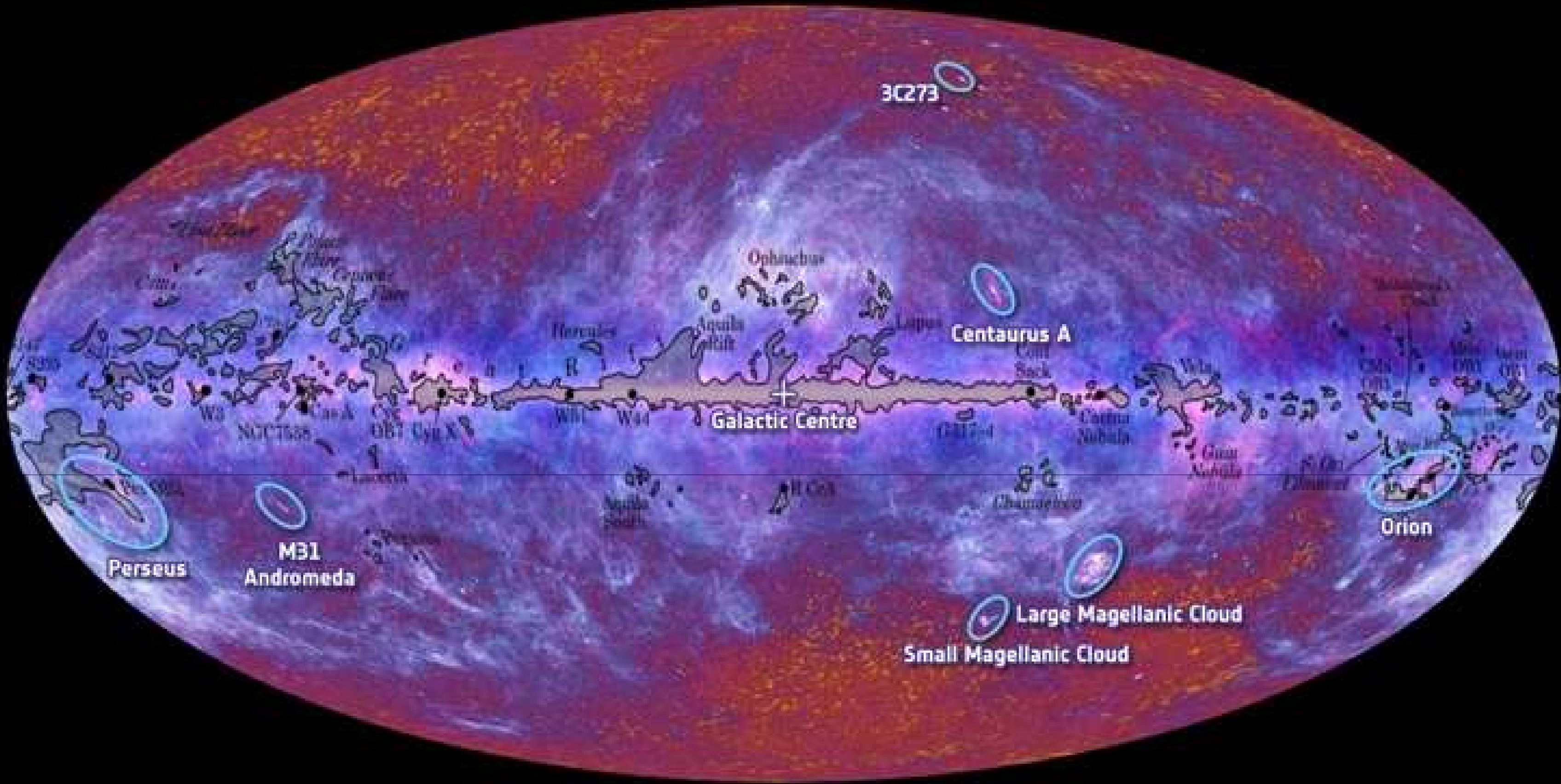

«Those who have reached the stage of no longer being able to marvel at anything simply show that they have lost the art of reasoning and reflection.»
Max Planck

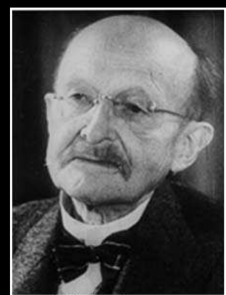

Planck ERCSC

- Widest frequency coverage of any catalogue produced by a single telescope
- More than 15,000 compact sources (both galactic and extra-galactic, radio and infra-red luminous galaxies)
- Includes sample of 189 galaxy clusters (see Mazzotta presentation)
- Early Cold Core Catalogue (915 clouds cooler than 14 kelvin)

15.000 nuove sorgenti, tutte da conoscere

Pictor A - radio galaxy

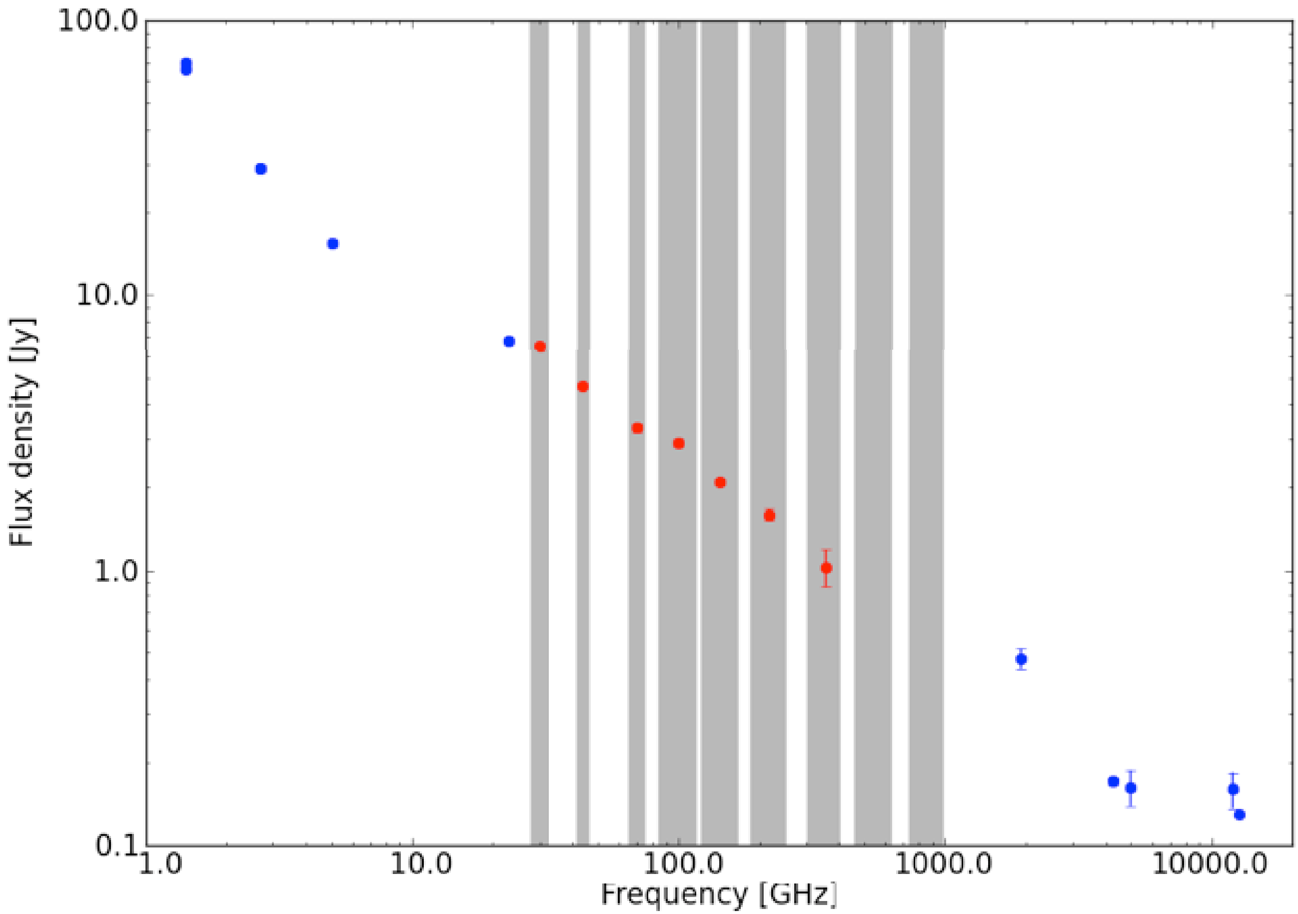

M82 - starburst galaxy

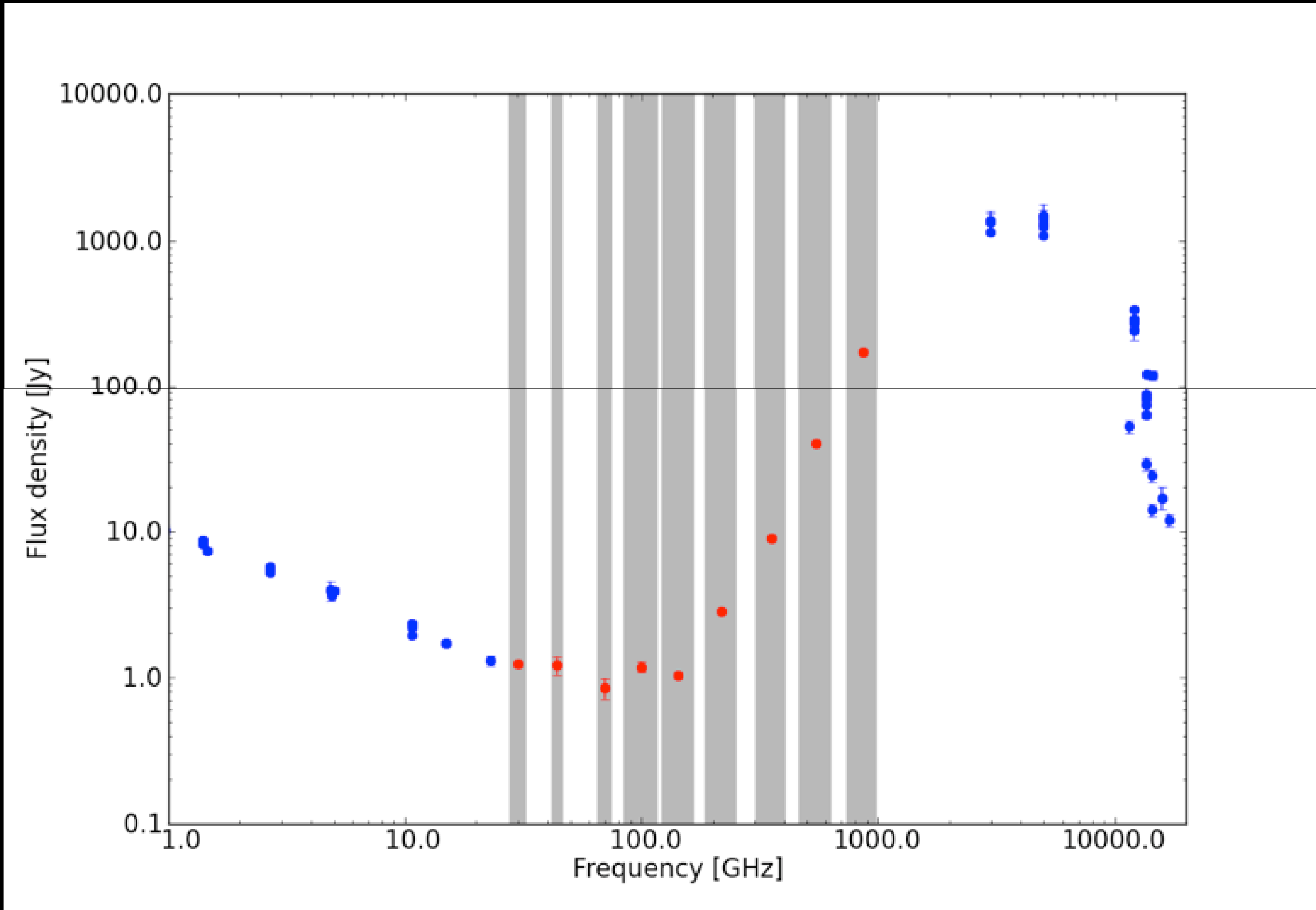

The Cold Cores

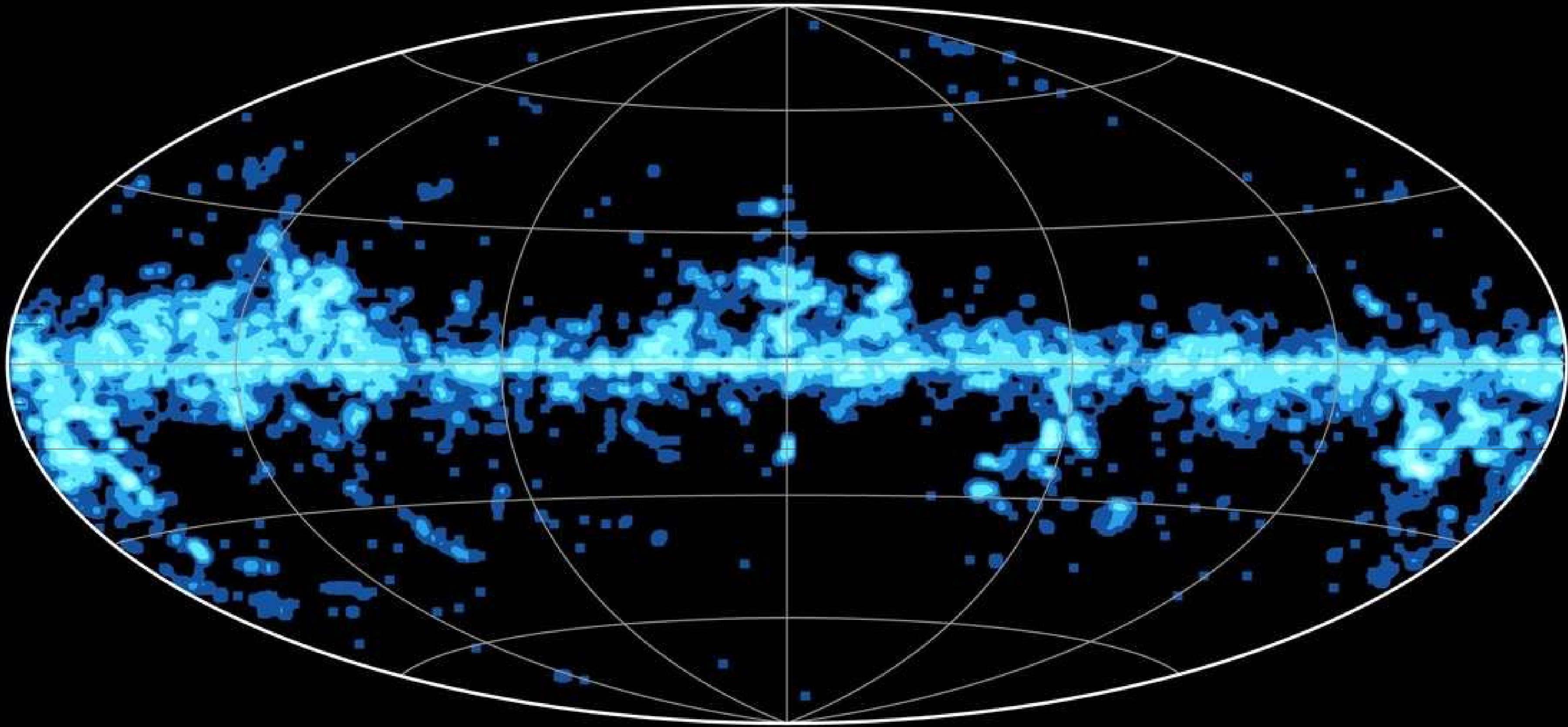

- Coldest spots within molecular clouds (7-16K)
- Hints on early phase of stellar formation
- Most radiation emitted @ sub-mm

The Cold Cores

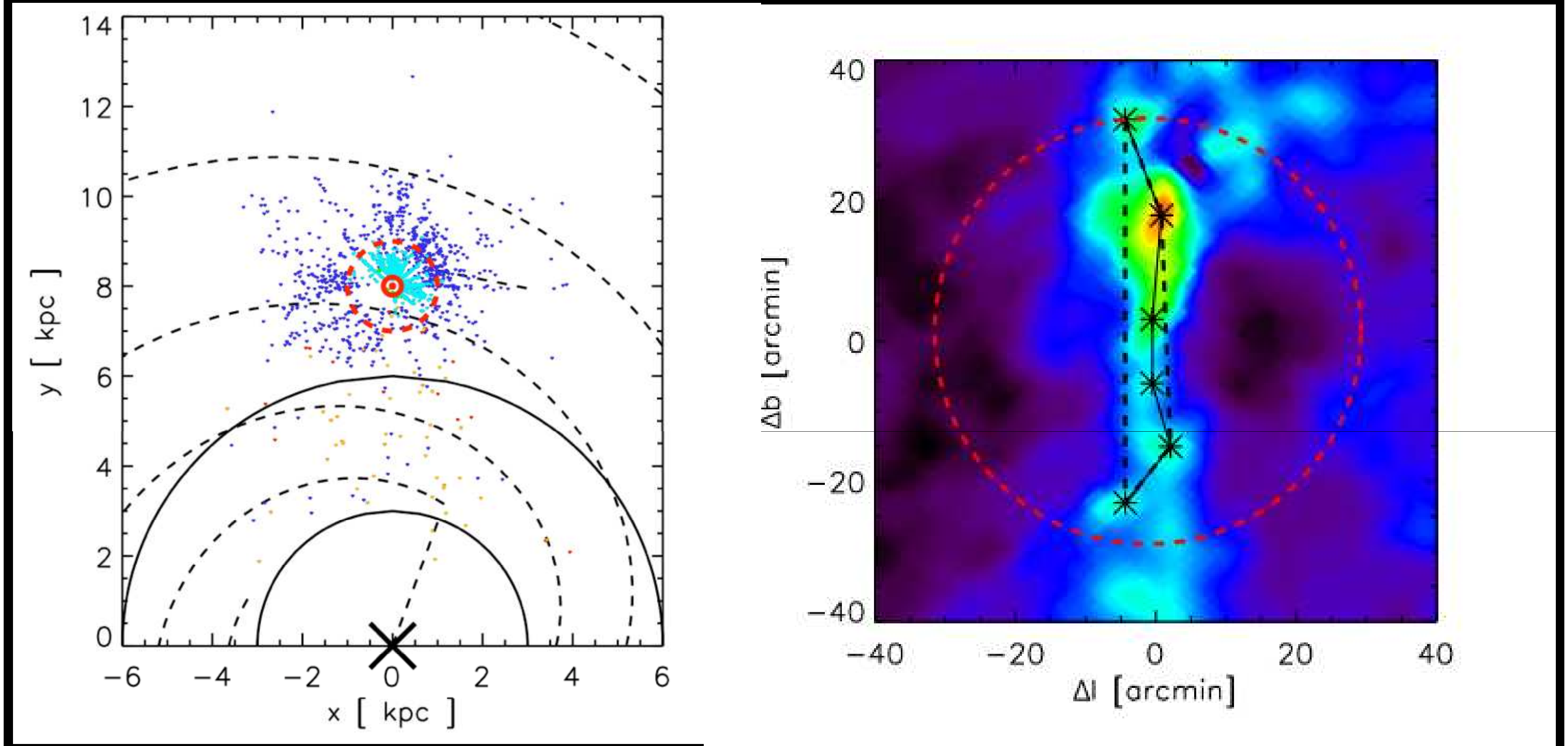

- elongated structures instead of compact cores
- Planck data are well complemented by Herschel data with higher angular resolution

Cosmic Infrared Background

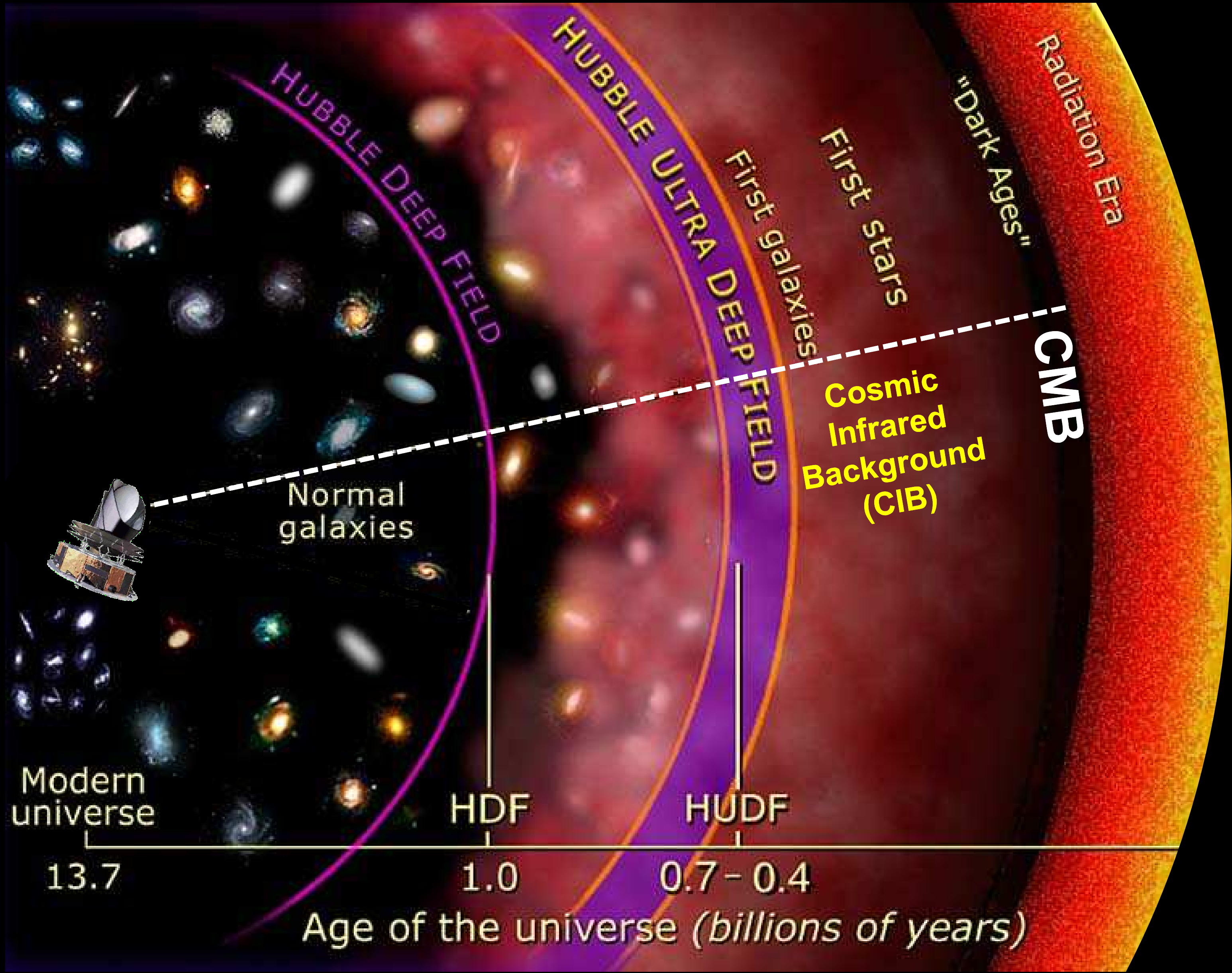

PLANCK

Cosmic Infrared Background

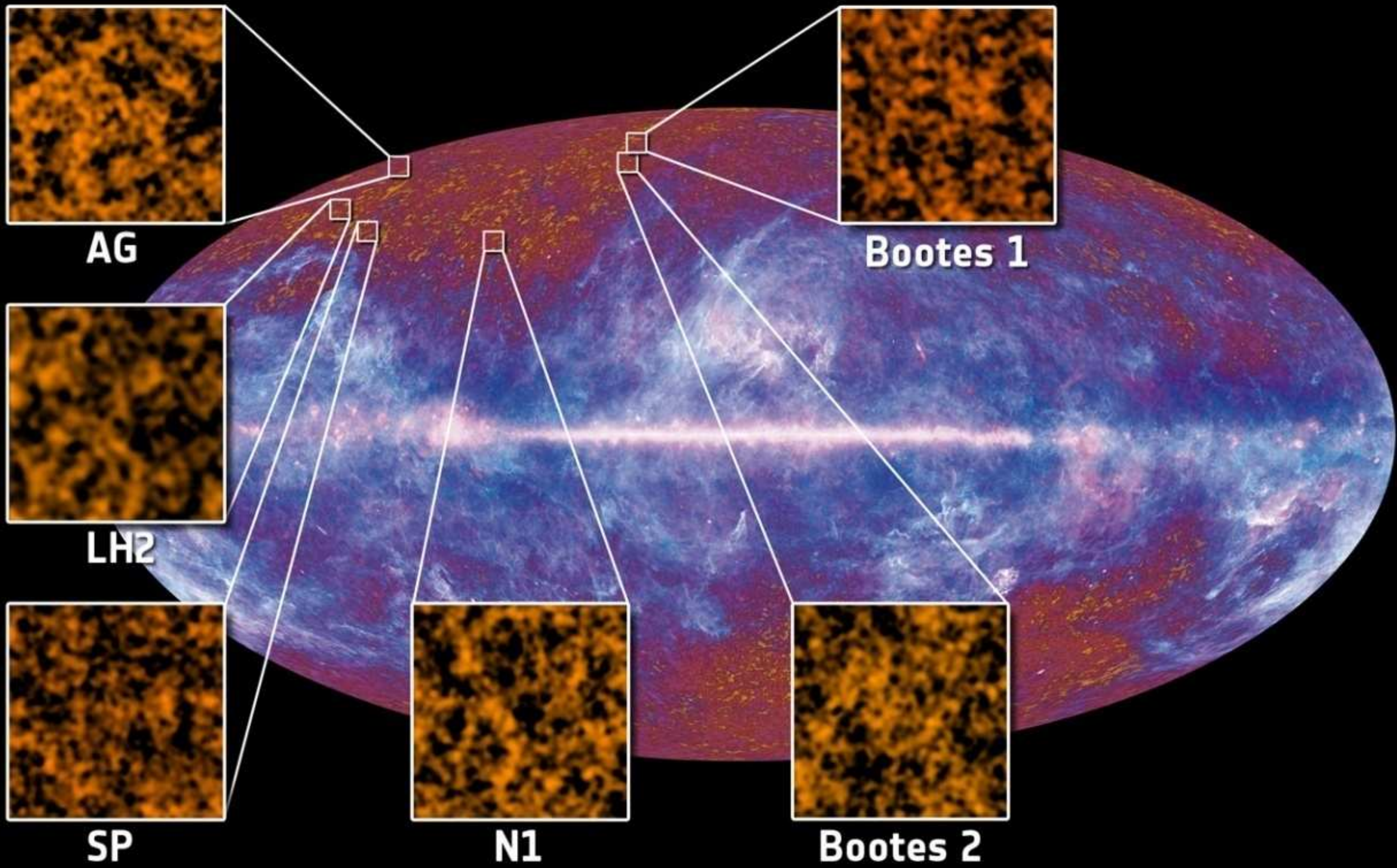

Cosmic Infrared Background

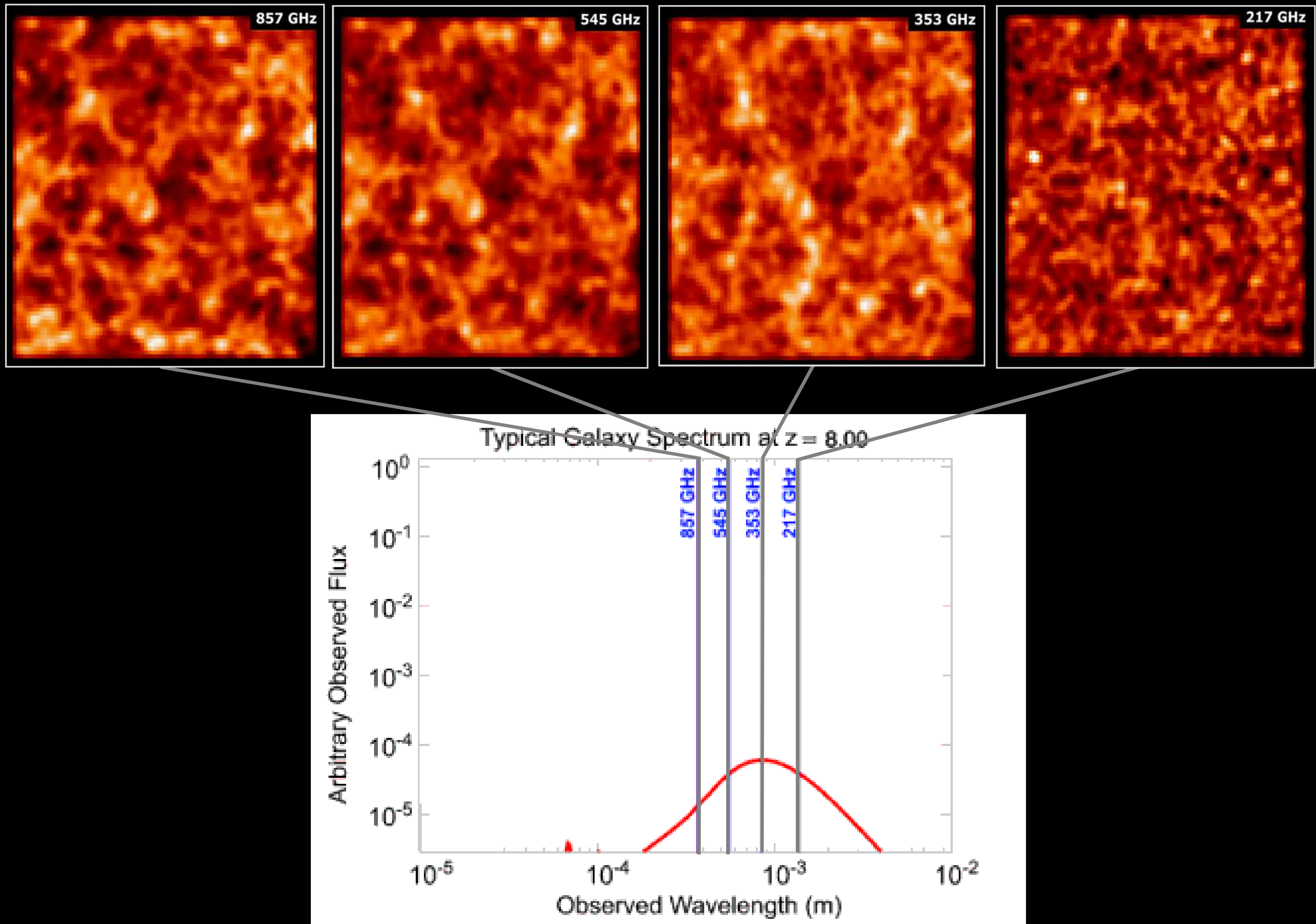

Cosmic Infrared Background

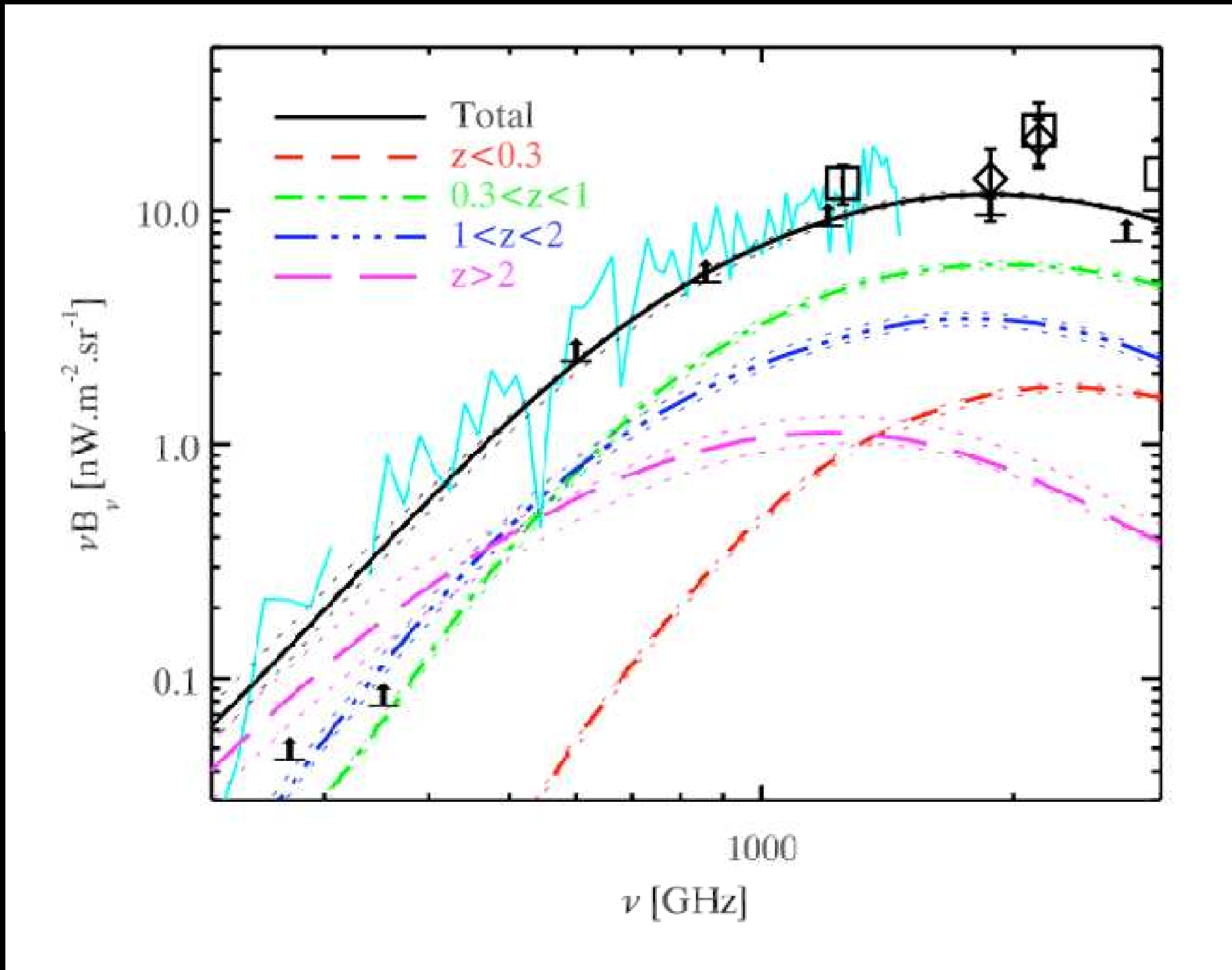

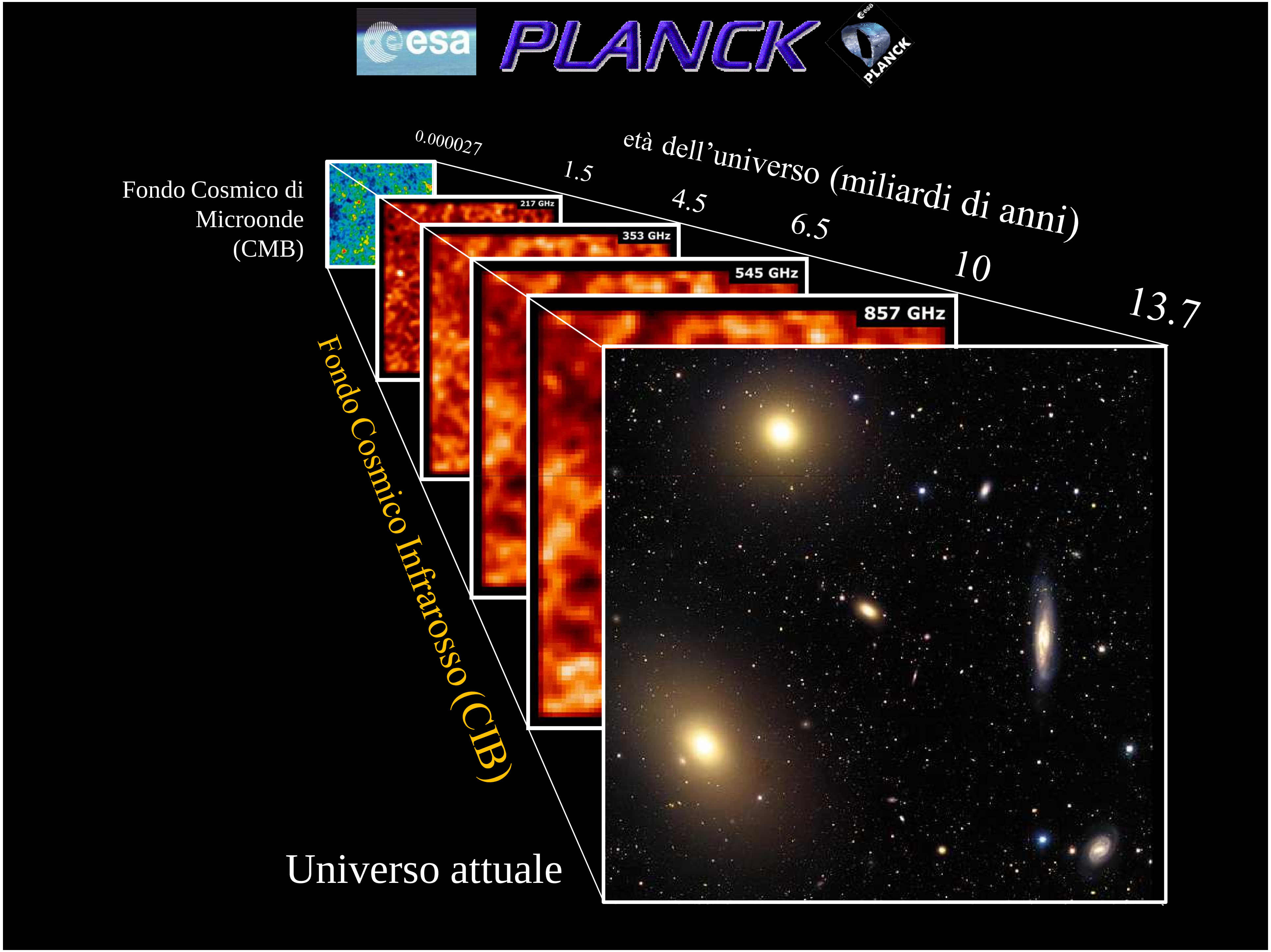
esa
PLANCK
0.000027
1.5
4.5
6.5
10
13.7
età dell'universo (miliardi di anni)
Fondo Cosmico di Microonde (CMB)
217 GHz
353 GHz
545 GHz
857 GHz
Fondo Cosmico Infrarosso (CIB)
Universo attuale

PLANCK

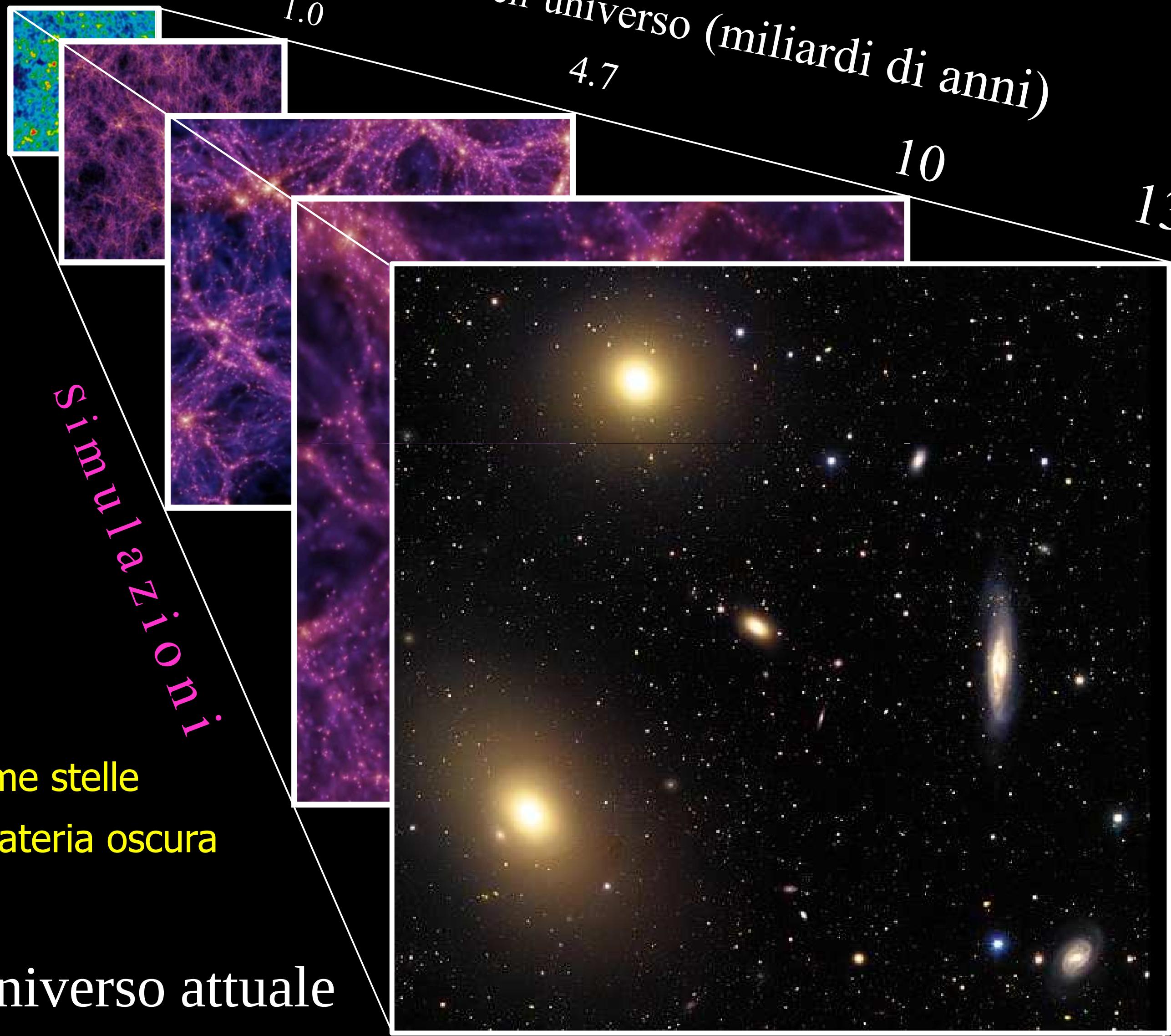

Informazioni su:

- Formazione delle prime stelle
- Distribuzione della materia oscura

Sunyaev-Zel'dovich with Planck

Visible light **X-ray**

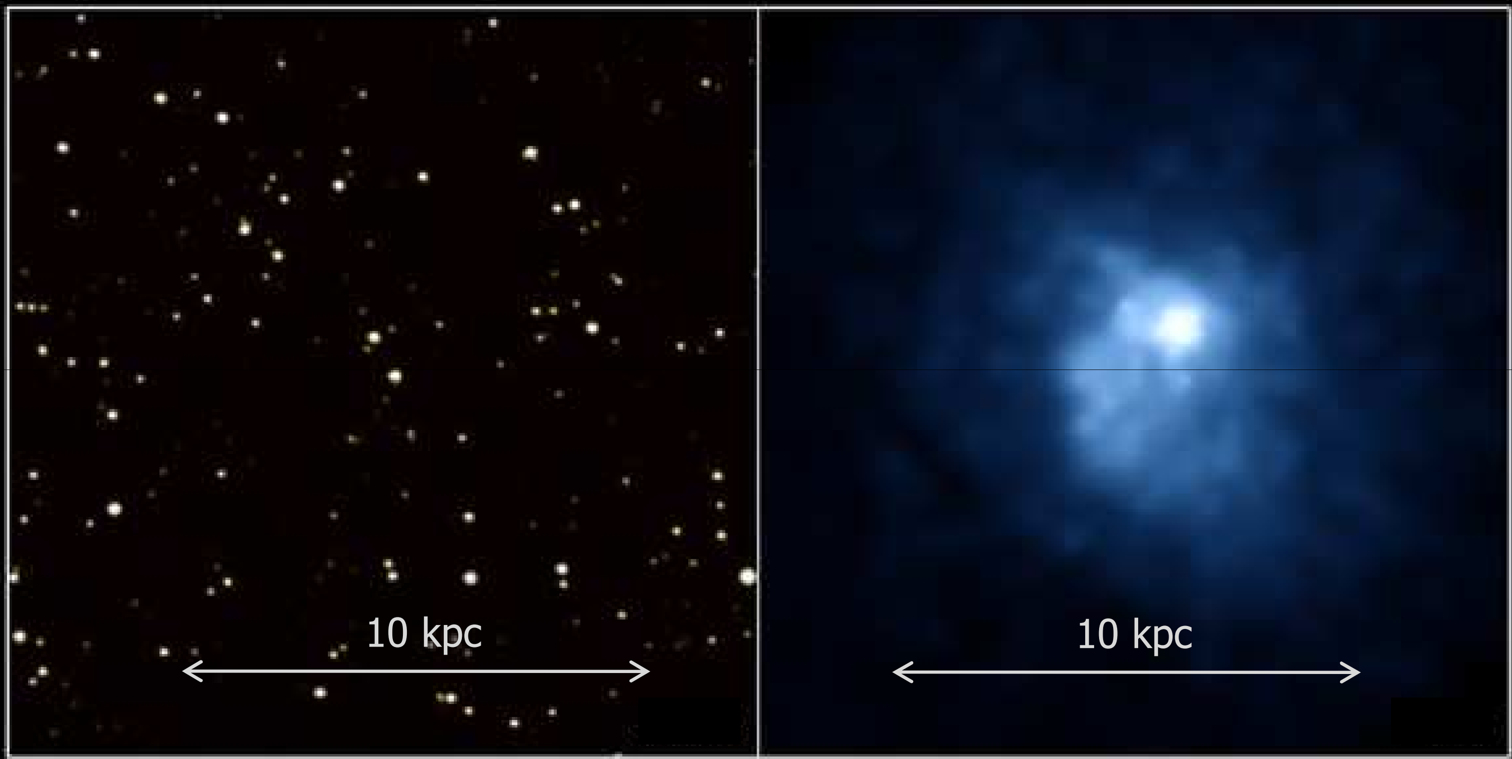

$$m_G \sim 10^{-1} m_{gas}$$

$$m_G \sim 10^{-2} m_{tot}$$

$$T \sim 10^7 - 10^8\,\mathrm{K}$$

$$\rho \sim 10^{-3} - 10^{-4}\,\mathrm{cm}^{-3}$$

Sunyaev-Zel'dovich with Planck

$$y = \frac{kT}{m_e c^2}\sigma_T \int n_e dl = \frac{kT}{m_e c^2}\tau_e$$

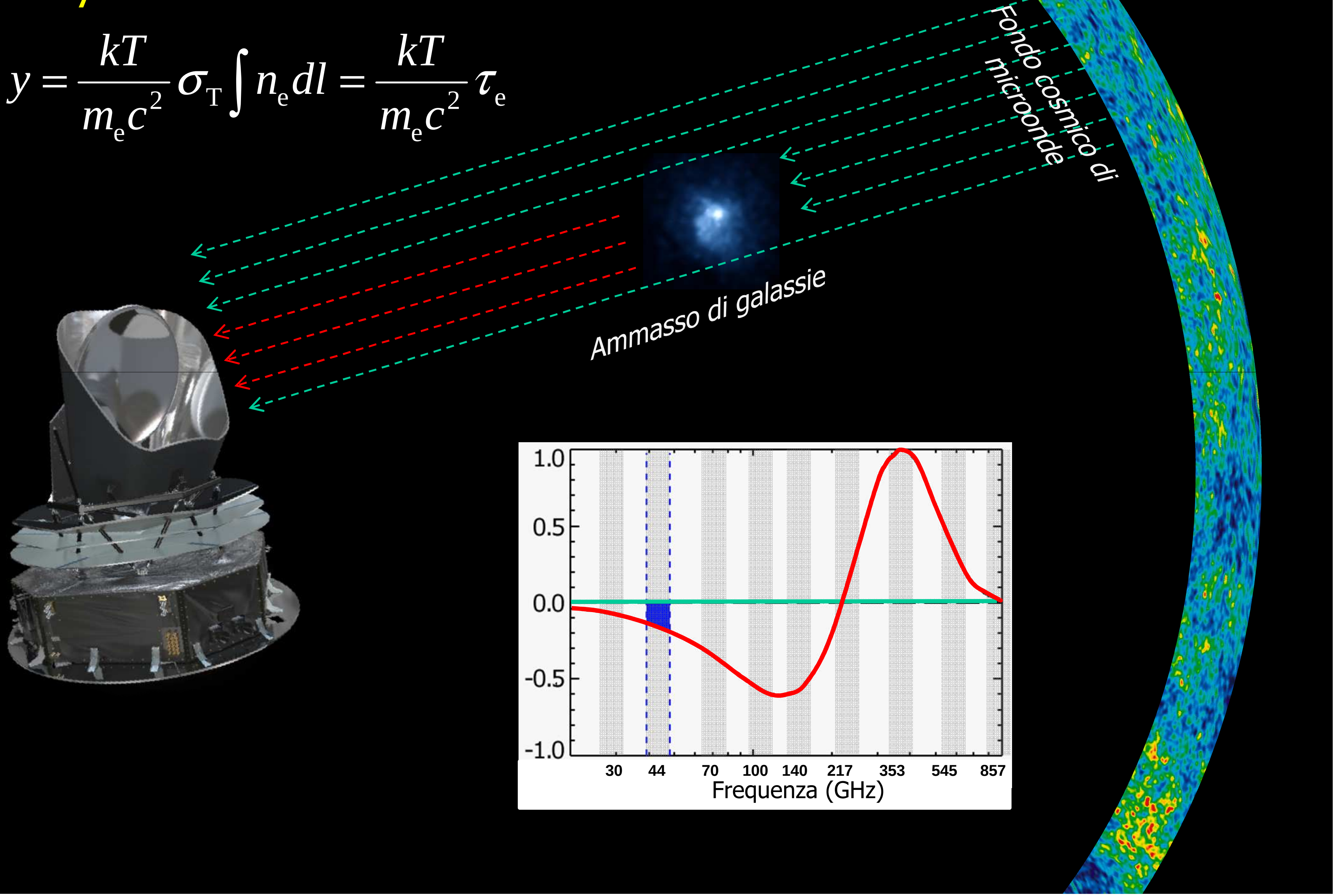

PLANCK

Effetto Sunyaev-Zel'dovich (SZ)

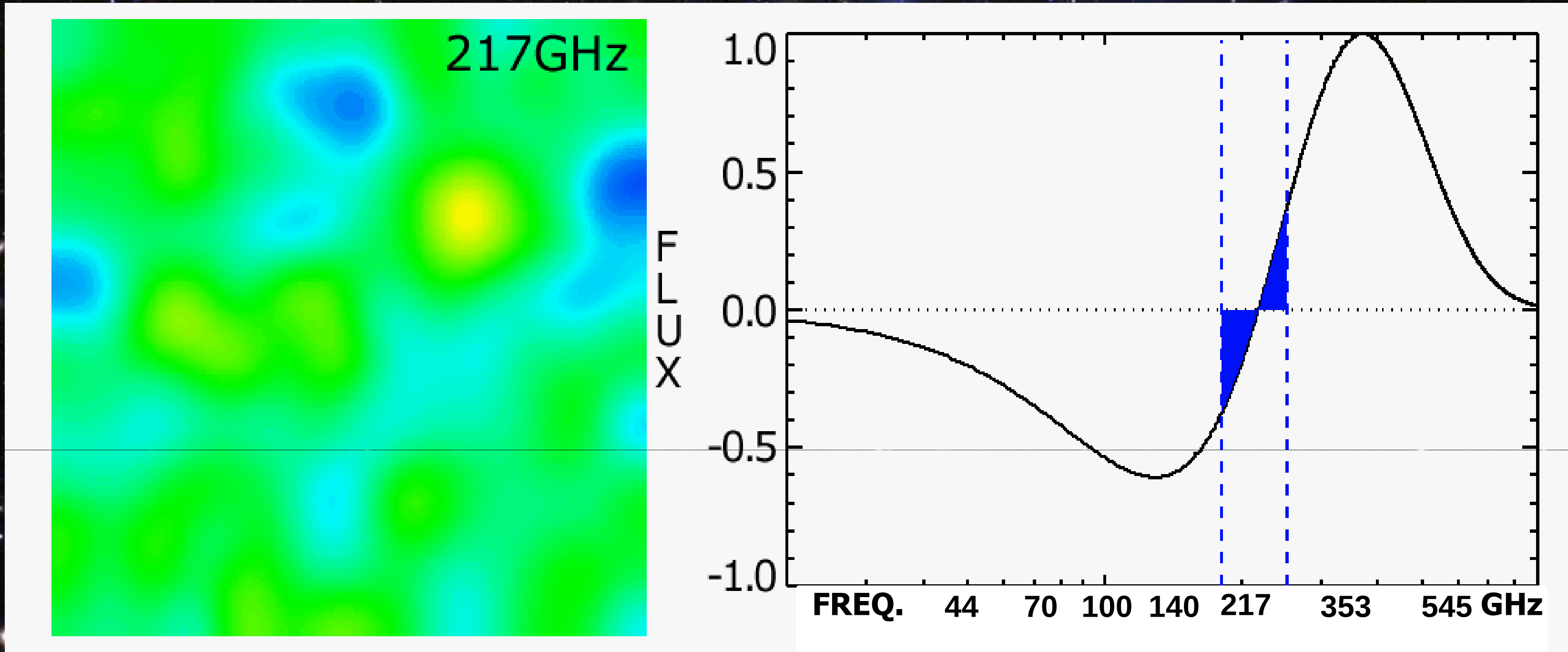

Galaxy Cluster: Abel 2319

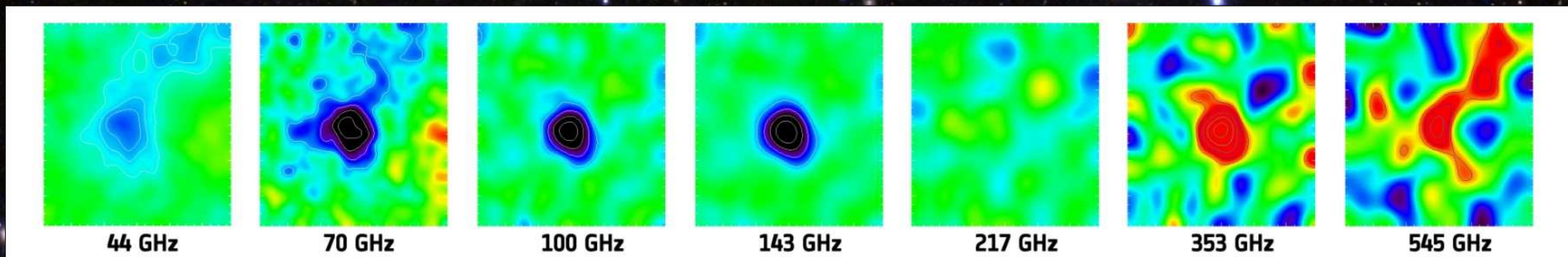

For the first time, Planck has measured the SZ effect on the full sky

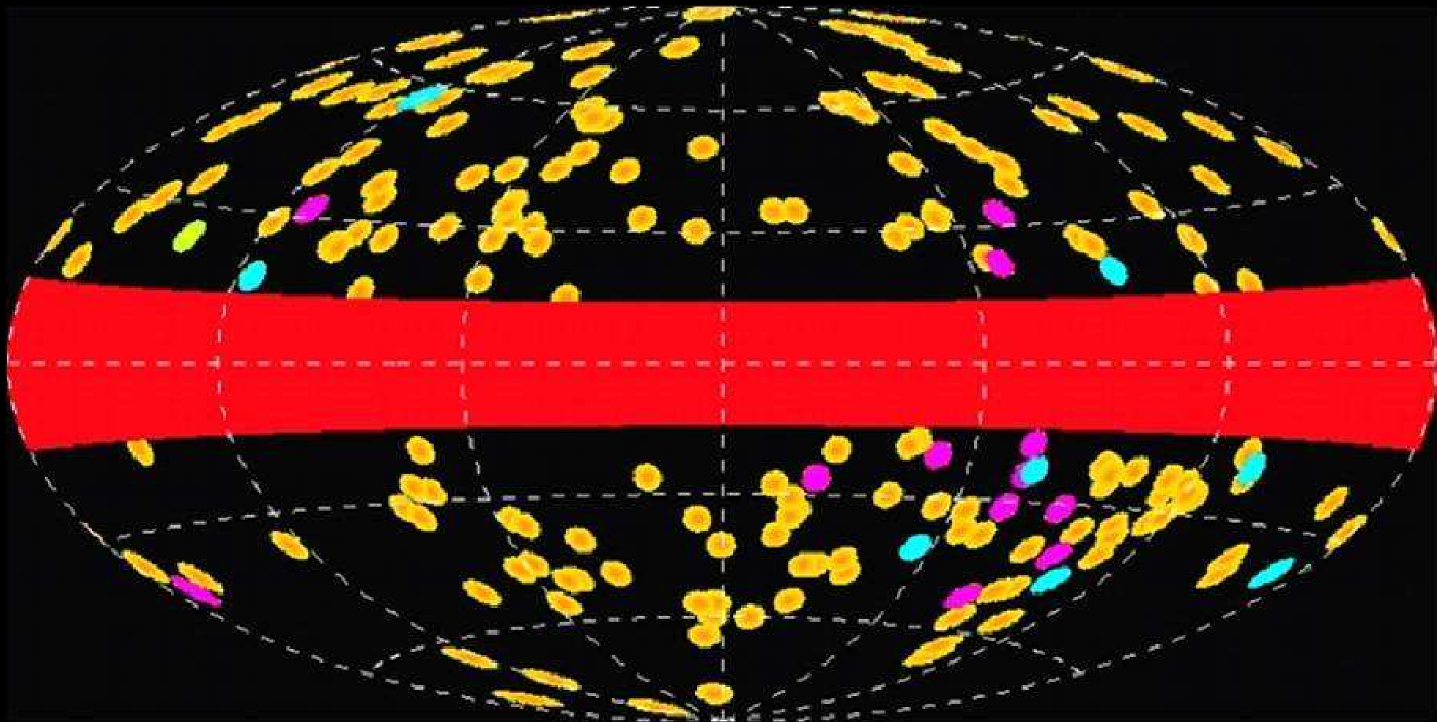

187 galaxy clusters detected
(so far…)

A new "super-cluster" discovered by Planck and confirmed by XMM

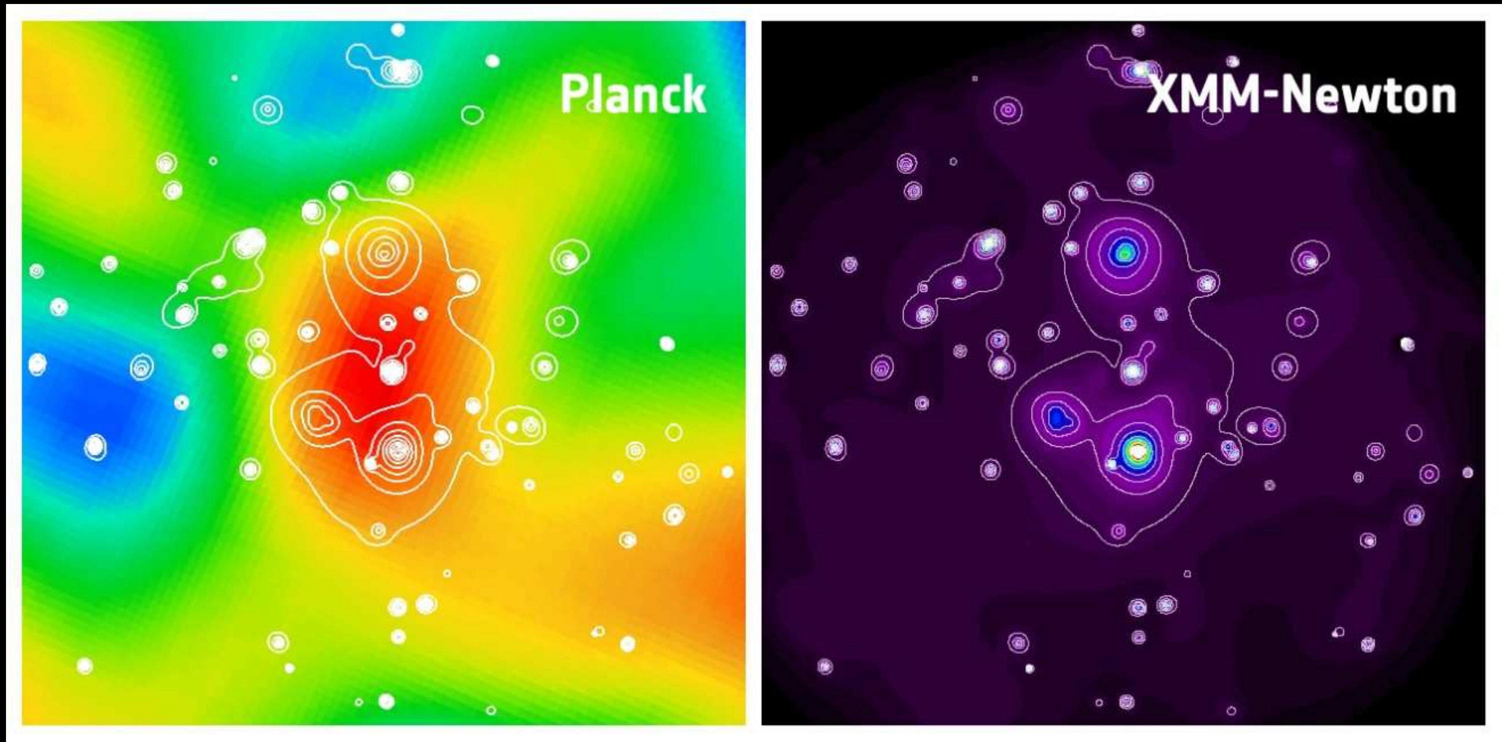

T~1.5 x 10^7K

PLANCK

The deepest view of the early universe

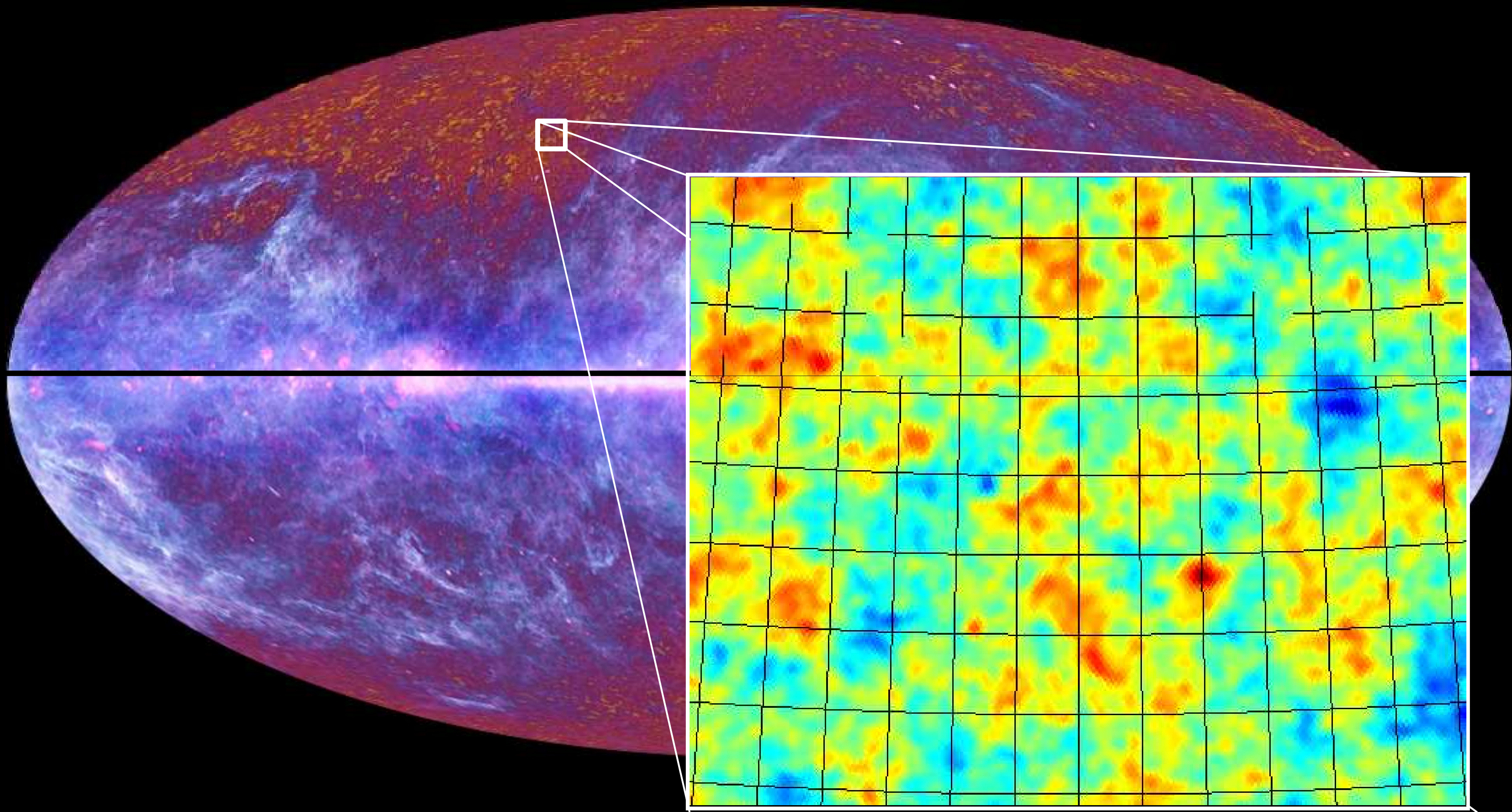

CMB fluctuations – Planck-LFI 70 GHz

Planck CMB results:
Expected in 2013